Physics – Uspekhi **47** (11) 1119 – 1154 (2004)

REVIEWS OF TOPICAL PROBLEMS PACS numbers: **61.46.+w**, **68.43.–h**, 81.07.De

Sorption properties of carbon nanostructures

A V Eletskiĭ

DOI: 10.1070/PU2004v047n11ABEH002017

Contents

Abstract. The current status of research in sorption properties of carbon nanotubes (CNTs) is reviewed. The structural peculiarities of CNTs, determining their sorption characteristics, are considered. The mechanisms of sorption of gaseous and condensed substances by such structures are analyzed. Special attention is paid to the problem of using CNTs for storing hydrogen and other gaseous substances. Methods for filling CNTs with liquid materials, based on capillary phenomena and wetting the graphite surface of the CNT with liquids of various nature, are considered. Properties of 'peapods' formed as a result of filling single-walled CNTs with fullerene molecules are reviewed. Also considered are perspectives on the applied usage of the sorption properties of CNTs in electrochemical and fuel cells, and material storage devices, as well as for producing superminiature metallic conductors.

1. Introduction

The end of the 20th century can be noted by the discovery of new modifications of carbon, which are closed surface structures consisting of hexagons and pentagons with carbon atoms in their vertices. Fullerenes and carbon nanotubes are the most interesting examples of such new carbon structures. The surface of a fullerene has a closed spherical or spheroid form [1 – 3]. The surface structure of fullerenes includes not only regular hexagons, whose number depends on the fullerene size, but also 12 pentagons arranged in a regular manner over the surface. The discovery of fullerenes was awarded with the Nobel Prize in Chemistry 1996 [4 – 6].

A V Eletskiĭ Russian Research Centre 'Kurchatov Institute'
pl. Kurchatova 1, 123182 Moscow, Russian Federation
Tel/Fax (7-095) 196 72 80
E-mail: eletskii@imp.kiae.ru

Received 13 July 2004, revised 27 July 2004
Uspekhi Fizicheskikh Nauk **174** (11) 1191 – 1231 (2004)
Translated by A V Eletskiĭ; edited by A Radzig

Another modification in surface carbon nanostructures is carbon nanotubes discovered by S Iijima in 1991 [7]. These elongated cylindrical structures ranging from one to several dozen nanometers in diameter and reaching up to several micrometers in length consist of one or several graphitic layers scrolled into a tube. A nanotube is usually terminated in a semispherical cap which can be considered half a fullerene molecule.

Nanotubes were first discovered in soot formed in the conditions of an arc discharge with graphite electrodes. Such a discharge is used effectively, in particular, for large-scale production of fullerenes [2].

As was noted wittily by W Krätschmer, shortly after their discovery nanotubes were treated as elongated fullerenes. However, further studies have shown that the variety of their structures and physical and chemical characteristics of carbon nanotubes considerably exceeds that of fullerenes. Therefore, it would seem more properly to treat a fullerene molecule as a limiting case of a carbon nanotube, the two caps of which are joined directly with each other. However, as distinct from fullerenes, which are a molecular modification of carbon, CNTs combine the properties of both molecules and the solid state and may be considered as an intermediate state of the substance (between molecular and condensed states). This feature attracts the continuously rising interest of researchers, addressed to the exploration of basic peculiarities in the behavior of such an exotic object under various conditions [8].

A real boom in investigation aimed at production, exploration of physical and chemical characteristics, and determining ways for more effective practical application of CNTs can be noted in the last few years. Thousands of articles on this subject are published every year. These investigations have resulted in a quick change in our notion about the mechanisms of synthesis of CNTs in various experimental conditions, their structural peculiarities and physical and chemical behavior, as well as possible applications. Some results of the mentioned investigations have been reflected in a large number of review articles and monographs, published

in recent years and devoted to various aspects of carbon nanotube research. Thus, methods for producing nanotubes, as well as some of their physical and chemical properties, have been described in detail in reviews [8 – 10]. Monographs [11, 12] concern mainly the electronic characteristics of these objects. Problems relating to filling CNTs with condensed substances are considered in book [13]. The publications cited contain extensive bibliographies which can help the reader to become orient to the huge literature stream related to nanotube research.

Interest in the investigation of CNTs is inspired by two circumstances. Firstly, CNTs should be treated as a new class of physical objects of nanometer size, which possess extraordinary physical and chemical properties. Exploration of such properties as electronic structure, electrical conduction, chemical activity, mechanical and sorption characteristics, etc. is of basic interest and extends our knowledge of nature. Secondly, the extraordinary physical and chemical properties of CNTs form the basis for a variety of branches concerned with applied usage of these objects. Thus, good conductivity combined with a high aspect ratio make CNTs a unique source of electron field emission, which can be used in highly effective field emission cathodes. Depending on the geometry, an individual CNT can possess the properties of either a metal conductor or a semiconductor with various magnitudes of energy gap and carrier concentration. This permits one to consider a CNT as the most miniature electronic device which can form the basis of future computing machines with an extraordinarily high information capacity.

One more remarkable peculiarity of carbon nanotubes relates to their unique sorption characteristics. Since a CNT constitutes a surface structure, all its mass is contained in the surface of its layers. This gives rise to an abnormally high specific surface for CNTs, which, in turn, determines features of their electrochemical and sorption behavior. The distance between graphite layers in a multiwalled carbon nanotube is close to the corresponding magnitude for crystalline graphite (0.34 nm). This distance is quite large, for some quantity of a substance to be situated inside a CNT. Therefore, CNTs can be treated as a unique capacity for storing gaseous, liquid, or solid-state substances. If the substance is capable of being absorbed on the inner surface of the graphitic layer comprising the nanotube, the density of the absorbed matter can reach that of the condensed state.

High sorption capacity of the graphite surface and the possibility of filling CNTs with various substances permit one, on the one hand, to control their physical and chemical properties and, on the other hand, to design devices for the storage of gaseous and condensed matter. A substance penetrates a nanotube under the action of outer pressure or as the result of the capillary effect, and is confined there due to the sorption forces. The graphitic shell provides therewith quite good protection of the confined matter from outer chemical or mechanical action. This permits one to consider CNTs as a prospective means for the long-term storage of materials. Specifically, intensive studies aimed at developing CNT-based hydrogen storage devices have been performed. These studies, if successful, can result in the creation of a new generation of car engine, which uses hydrogen as a fuel and is noted for being ecologically clean.

The present article contains the review of studies related to sorption characteristics of carbon nanotubes. The interest in the sorption properties of CNTs is inspired by three important issues. Firstly, the carbon nanotube is built of a graphite surface whose high sorption characteristics were known well before the discovery of CNTs. Secondly, the CNT-containing material possesses the high specific surface due to its structure, which makes it an attractive object for performing heterogeneous electrochemical processes. Finally, the third and most important feature distinguishing CNTs from other known materials is the existence of an inner cavity inside the nanotube, the cross section of which usually exceeds the typical size of a molecule. Therefore, this property offers the possibility of creating a new class of objects involving nanotubes filled with a gaseous, liquid, or solid substance [9]. Such objects are distinguished in their properties from both hollow nanotubes and the substances filling them, which permits one to claim a notable expansion of the class of nanomaterials with unique physical and chemical properties. Thus, a nanotube filled with a conducting, semiconducting, or superconducting material can be considered as the most miniature of all known connecting elements of microelectronics.

The opportunity to fill the internal cavity of a CNT with substances of various nature attracted the attention of researchers immediately after the discovery of this unique material. This opportunity was firstly considered, it seems, in Ref. [14] where the problem of an HF molecule being drawn inside a nanotube under the action of the polarization forces was analyzed theoretically. Here, it was supposed that the capillary phenomena resulting in the drawing in of liquids, thus wetting the inner surface of the capillary, retained their nature in going over to tubes of nanometer diameter.

The filling of nanotubes with various substances has been made possible as the result of the development of a method for opening one of the ends of a nanotube through the action of a strong oxidizer [15]. In this case, a fusible liquid metal (e.g., lead) penetrates into an open-ended nanotube due to the capillary effect. The presence of lead inside nanotubes is evidenced through X-ray diffraction and electron energy loss spectroscopy methods. Observations showed that the thinnest lead wire formed inside a nanotube as a result of the capillary drawing-in is 1.5 nm in diameter.

Subsequent efforts by researchers in the area of interest were addressed to a detailed study of the peculiarities of capillary phenomena in carbon nanotubes, which manifest themselves in the filling of nanotubes with substances of various nature. The results of these investigations show an interconnection between the magnitude of the surface tension of a substance and its ability to be drawn in through capillary action inside a carbon nanotube [16, 17]. Particularly, it was stated that liquid substances having a rather high (higher than 200 mN m^{-1}) magnitude of surface tension are not capable of being drawn inside nanotubes due to the capillary effect.

Carbon nanotubes can also be filled with, besides liquids, gaseous substances. The interest of researchers in this opportunity is, along with the purely basic aspect, due to the practically important problem of the development of hydrogen storage devices, targeting their use in the environmentally safe hydrogen fuel car engine. High sorption properties of CNTs and the potential for their large scale production has attracted the interest of researchers to the problem of using nanotubes for hydrogen storage [18]. Solving this problem would not only eliminate the ecologically detrimental action of car transportation on the living conditions on the Earth, but also provide a natural conversion from hydrocarbon to nuclear methods for energy production. In this case, the hydrogen fuel could be used as an intermediate agent

synthesized in nuclear plants. Problems related to filling the CNT-containing materials with hydrogen and other gaseous substances are considered in detail below.

Structures obtained as the result of filling nanotubes with fullerene molecules [19, 20] can serve as remarkable examples of the manifestation of the sorption properties of CNTs. C_{60}, which is the most widespread fullerene molecule, has a diameter of 0.7 nm. Since the equilibrium distance between the neighboring graphitic layers is about 0.34 nm, the inner cavity of nanotubes exceeding 1.3 nm in diameter is sufficient for filling with fullerene C_{60} molecules. The structures formed have a pea pod shape, and therefore have been named peapods. The development of methods for synthesizing and investigating such peapods in various physical and chemical conditions comprises one of the most advanced areas of CNT research. An interesting peapod modification indicating a widening of experimental opportunities in the field is the structures obtained by filling single-walled nanotubes with endohedral fullerenes, i.e., fullerene molecules containing metal atoms inside their cages. Such structures were first produced and studied in detail by the authors of Ref. [21], who filled single-walled nanotubes 1.4 – 1.5 nm in diameter with endohedral fullerene $Gd@C_{82}$ molecules and used the notation $Gd@C_{82}@SWNT$ for the resulting system. An interesting feature of such a structure is the character of the packaging of the $Gd@C_{82}$ molecules inside a nanotube. In accordance with this, fullerene molecules form a 1D crystal with a mean intermolecular distance of 1.10 ± 0.03 nm, which is somewhat lower than the relevant magnitude for the 3D molecular $Sc@C_{82}$ crystal (1.124 nm). A decrease in the intermolecular distance in a 1D crystal encapsulated into the nanotube, compared to a 3D one, can be caused by the transfer of part of the electron charge from the metal atom to the external surface of the nanotube.

2. The structure of carbon nanotubes

Sorption properties of CNTs are determined mainly by their structure. The most important structure peculiarities of CNTs, which govern their sorption properties, are high specific surface area inherent to surface graphitic structures, and the existence of a closed or semiclosed cavity in their structure, whose size is sufficient for holding both single atoms and molecular compounds.

2.1 Single-walled nanotubes

2.1.1 Chirality. An ideal nanotube constitutes a graphite plane rolled into a cylinder, i.e., a surface consisting of regular hexagons, at the vertices of which are located carbon atoms. The result of rolling depends on the orientation angle of the graphitic plane in relation to the nanotube axis. This orientation angle determines the *chirality* of the nanotube, which governs, in particular, its chemical stability and electrical properties. This property of nanotubes is illustrated in Fig. 1a [22, 23] where a part of a graphite plane is shown and possible directions for its rolling are marked.

An ideal nanotube does not form seams in rolling and ends in semispherical caps containing not only regular hexagons but also six regular pentagons. Due to this latter peculiarity a nanotube can be considered as the limiting case of a fullerene molecule whose length considerably exceeds its diameter.

The chirality of a nanotube is denoted by the pair of symbols (m, n) showing the coordinates of the hexagon on the graphite plane, which has to be superimposed on the hexagon at the origin as the result of rolling. Some of these hexagons are shown in Fig. 1a along with related labelling. Another way to specify the chirality consists of indicating the angle α between the direction of nanotube rolling and that of the common site of two adjacent hexagons. However, the diameter of the nanotube should be specified in this case for the full description of its geometry.

The chirality indices (m, n) of a single-walled nanotube uniquely determine its diameter D. This relation is obvious and has the following form

$$D = \sqrt{m^2 + n^2 + mn}\ \frac{\sqrt{3}d_0}{\pi}, \qquad (1)$$

where $d_0 = 0.142$ nm is the distance between neighboring carbon atoms in the graphite plane. The angle α is expressed through the chirality indices (m, n) by the relation

$$\sin\alpha = \frac{\sqrt{3}m}{2\sqrt{(n^2 + m^2 + mn)}}. \qquad (2)$$

Amongst different possible directions of nanotube rolling, those directions are distinguished for which bringing the hexagon (m, n) into coincidence with the origin requires no distortion in its structure. These directions correspond,

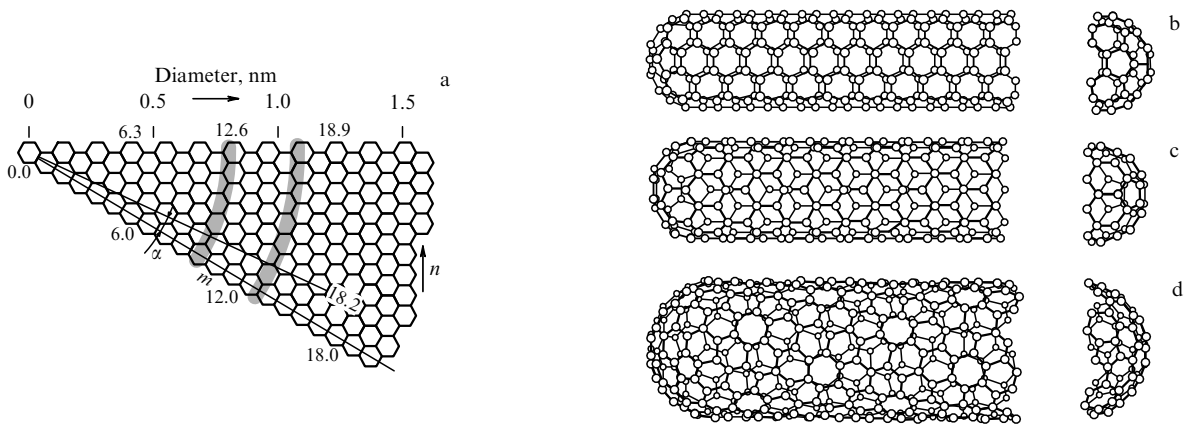

Figure 1. Illustration of the chirality of nanotubes [22, 23]: (a) a part of the graphite surface, the rolling of which into a cylinder results in the formation of a single-walled nanotube; (b) rolling at the angle $\alpha = 0$ gives the *zigzag* structure; (c) rolling at the angle $\alpha = 30°$ corresponds to the *armchair* structure, and (d) a nanotube with chirality indices (10, 5).

particularly, to the angles $\alpha = 0$ (*zigzag* configuration) and $\alpha = 30^\circ$ (*armchair* configuration). Such configurations are specified by the chirality indices $(m, 0)$ and (n, n), respectively. The nanotube structures having *armchair* and *zigzag* configurations are depicted in Figs 1b and 1c. The nanotube structure with the chirality indices (10, 5) is shown in Fig. 1d.

Armchair nanotubes with chirality indices (10, 10) take a special position among single-walled nanotubes. In such nanotubes, two of the C – C bonds incorporated into each of hexagons are oriented parallel with the longitudinal axis of the tube. As follows from calculations [11, 12], nanotubes with such a structure should possess a purely metallic conductivity. Moreover, the thermodynamic calculations [24] show that such tubes are distinguished by an enhanced stability and should prevail over nanotubes of other chirality in the conditions where single-walled nanotubes are predominantly formed. Until recently, such ideal conditions seemed to be unattainable. However, the theoretical predictions have found an experimental verification in the first-rate work [24] where the metal-conductive single-walled nanotubes of 1.36 nm in diameter and up to several hundred microns in length were synthesized on irradiating a graphite surface with two laser pulses in the presence of an Ni-Co catalyst. As follows from electron microscope observations and X-ray diffraction measurements, nanotubes of predominant chirality (10, 10) form bundles 5 – 20 nm in diameter, comprising a 2D ordered structure. Such a structure is shown schematically in Fig. 2 [10]. Moreover, EPR-spectroscopy observations confirmed by direct measurements of conductivity in nanotubes point to the metallic character of electrical transport in these samples.

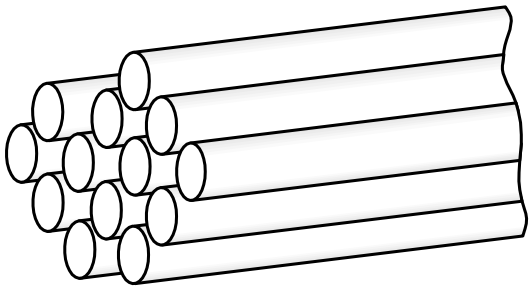

Figure 2. A schematic of a bundle formed by single-walled nanotubes [10].

The experimentally examined structure of single-walled nanotubes differs in many respects from the above-presented ideal picture. First of all, this difference relates to nanotube caps whose structure is far from an ideal hemisphere, as follows from observations.

2.1.2 Methods and results of experimental study of nanotube structure. At the present time, methods of experimental investigation of the structure of single-walled nanotubes have been developed. These methods, being based on conventional approaches to exploration of the structure of nano-sized objects, include X-ray and neutron diffractometry, atomic field microscopy, scanning and high-resolution transmission electron microscopy, as well as optical and Raman spectroscopy. The above-listed methods can be used mainly for the study of a large massif of nanotubes with close structural parameters. The measurements can provide rather averaged structural characteristics of nanotubes but not a detailed analysis of properties of individual objects. Thus, in the first experiments of such a kind [24, 25], bundles containing about a hundred single-walled nanotubes were used as an object of investigation. X-ray diffractometry and high-resolution transmission electron microscopy (TEM) observations have shown that the nanotubes involved in bundles are characterized by an ordering package. This package relates to the 2D triangular lattice with a parameter of 1.70 nm. Supposing the interlayer distance for adjacent nanotubes is close to 0.34 nm, as in crystalline graphite, the authors of papers [24, 25] were led to the conclusion that such a lattice consists of similar nanotubes of about 1.36 nm in diameter. It turned out to be quite tempting to attribute to these nanotubes the chirality (10, 10) corresponding to their metallic behavior.

Nevertheless, further, more detailed, studies demonstrated that the structural parameters of single-walled nanotubes synthesized in real conditions are close, but not similar, to each other. Thus, Raman spectroscopy observations (see, for example, Ref. [26]) clarified that the diameter of nanotubes resided in bundles can range between 1.1 and 1.5 nm. However, direct observations via high resolution (HR) TEM [25, 27] have shown that the distinction in structural parameters of nanotubes involved in a bundle is much less than that for nanotubes belonging to different bundles. Thus, the average diameter of nanotubes relating to different bundles ranges between 1.44 and 1.74 nm. Such a distinction is probably caused by different synthesis conditions occurring in various plasma regions.

In this situation, the necessity to develop methods of investigation providing the distribution of nanotubes over diameter and chirality parameters arises. One such method is based on the use of electron diffraction from a spatial periodic structure which is represented by a bundle consisting of several dozen single-walled nanotubes. Direct measurements of the chirality of nanotubes synthesized by Thess et al. [24] were first reported in one of the subsequent publications by the same group [28]. For this purpose, the authors resorted to an electron diffraction microscope with a very small cross section of the electron beam (about 0.7 nm), quickly scanned over a region of 10 – 20 nm in diameter and filled with a bundle of nanotubes. The diffraction pattern obtained provides conclusions about the structure of the nanotubes composing bundles. 35 bundles were studied with diameters ranging between 3 and 30 nm. All these bundles, except two, contained nanotubes of chirality close to (10, 10). Detailed analysis showed that 44% of CNTs had chirality indices (10, 10), 30% had (11, 9), and 20% had (12, 8).

Further development of the electron diffraction method for detailed exploration of structural characteristics of single-walled nanotubes has manifested itself in combination of electron diffraction with HR TEM observations [29]. Single-walled nanotubes combined into bundles were produced on the surface of a cathode as a result of electrical arc sputtering of graphite in an He atmosphere in the presence of an Ni : Y catalyst. Then the soot which contained the nanotubes was ultrasonicated in ethanol, whereupon it was situated on a grid of a transmission electron microscope. This allowed separation of single rectilinear bundles which were the subject of subsequent electron diffraction studies. As follows from the analysis of experimental data, single-walled nanotubes composing an individual bundle are characterized by practically the same diameter and distinctive (arbitrary) chirality. This statement is in contradiction with the conclusions of works [28, 30] but agrees with work [31].

Use of the scanning tunneling microscope (STM) [32] has enabled passage from the exploration of bundles containing nanotubes to the determination of chirality of individual single-walled nanotubes. Nanotubes were produced utilizing the conventional laser method based on laser irradiation of a graphite surface in the presence of a metal catalyst. The soot produced thereby contained single-walled nanotubes about 1.4 nm in diameter, which were bundled up. In order to untangle the bundles and separate individual nanotubes, the soot was dispersed in dichloroethane and then subjected to ultrasonic treatment. The nanotubes obtained in this fashion were placed onto an Au(111) surface which was used as a substrate in STM observations. These observations were performed at $T = 4$ K. Figure 3 displays representative STM images of two individual nanotubes distinguished from each other in diameter and chirality. One of these nanotubes (I) is a semiconductor having an energy gap width of 0.80 eV, diameter of 1.0 ± 0.1 nm, chirality angle of $26° \pm 1°$, and chirality indices either (12, −1) or (13, −1). The second one (II) possesses metallic conductivity and has a diameter of 1.27 ± 0.09 nm, chirality angle of $21.1° \pm 1°$, and chirality indices (15, 3). Thus, the researchers had at their disposal the possibility of establishing all the structure parameters of a single-walled nanotube, which determine its electronic properties. The example cited illustrates a degree of uncertainty about structural parameters of individual nanotubes, which can be determined through the STM studies.

One more quite informative method for evaluating structural parameters of single-walled nanotubes is based on Raman spectroscopy [33–35]. Typical Raman spectra of single-walled CNTs contain two groups of peaks, one of which (short-wave) is related to so-called tangential vibrations of carbon atoms in a graphitic plane. These peaks, with energies 1590, 1566, and 1551 cm^{-1}, are inherent only to single-walled CNTs and are practically unobservable in the case of multiwalled nanotubes. Thus, the existence of Raman peaks related to tangential modes points unambiguously to the presence of single-walled nanotubes in the sample.

Another group of lines distributed over the energy range of 150–250 cm^{-1} corresponds to the so-called radial breathing modes. These are vibrations of the nanotube diameter in relation to its mean value. The frequency of such vibrations is inversely proportional to the nanotube diameter, and therefore this part of the Raman spectrum contains information about the nanotube diameter distribution. The interconnection between the diameter d (nm) of a single-walled nanotube and the position of the relevant Raman peak ω_d (cm^{-1}) is expressed by the following relation [33, 35]

$$\omega_d = \frac{223.75}{d} . \qquad (3)$$

Figure 4 depicts Raman spectra of a sample containing single-walled nanotubes. These data have been obtained using laser excitation sources of various wavelengths [34]. Analysis of these spectra on the basis of expression (3) leads to the conclusion that the sample analyzed contains, in particular, single-walled nanotubes with the diameters ranging between 1.06 and 1.2 nm. In addition, there are a small number of nanotubes with diameters ranging between 0.83 and 1.36 nm.

Information about structural parameters of single-walled nanotubes is contained not only in Raman spectra, but also in optical absorption spectra of samples [36]. This considerably facilitates the procedure for evaluating nanotube diameter distribution, making it accessible to a much wider circle of researchers. The interdependency between the nanotube diameter and the density of occupied electronic states causes an interconnection between the optical absorption spectrum of a single-walled nanotube and its diameter, as is illustrated, in particular, in Fig. 3c.

2.1.3 Single-walled nanotubes of the smallest diameter. In analyzing structural peculiarities of single-walled nanotubes an interesting question arises. It concerns the smallest possible diameter of a nanotube and the possibility of the

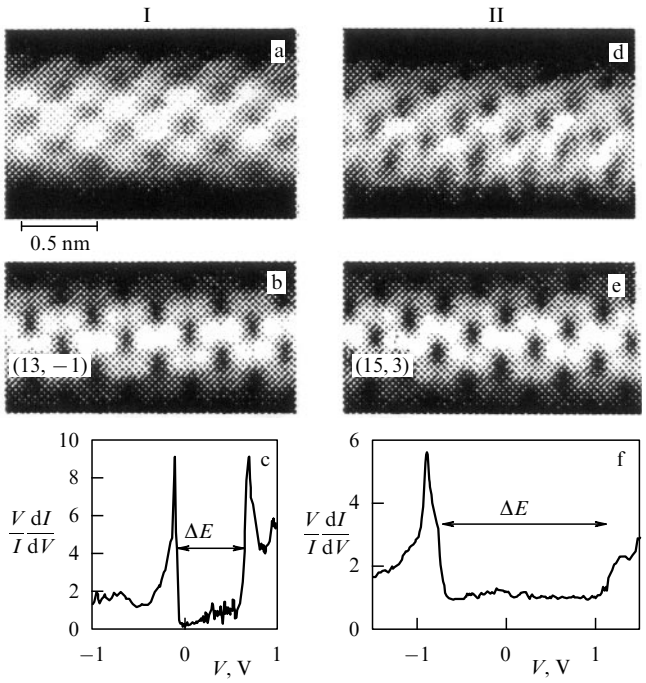

Figure 3. STM images and tunneling electronic spectra of two individual single-walled nanotubes [32]: (a, d) images reconstructed on the basis of STM measurements; (b, e) images calculated for nanotubes with the chirality indices (13, −1) and (15, 3), and (c, f) maps of the density of occupied states, reconstructed on the basis of STM measurements and giving an indication of semiconductor properties of nanotube I, and metallic properties of nanotube II.

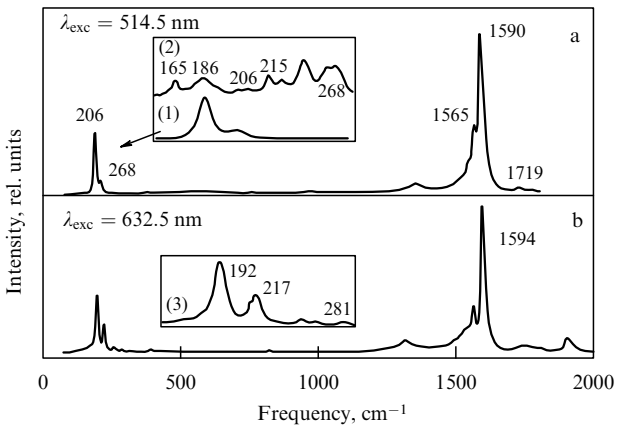

Figure 4. Raman spectra of samples containing single-walled nanotubes [34]: (a) wavelength of the exciting laser is equal to 514.5 nm, and (b) 632.5 nm. Enlarged long-wavelength parts of spectrum, related to the radial breathing modes, are shown separately in the insets.

synthesis and stable existence of nanotubes with such a diameter. This question was first formulated in work [37] shortly after the discovery of nanotubes, the authors of which related the diameter of a nanotube with that of relevant fullerene molecule closing this nanotube. In particular, the diameter of the most abundant nanotube of an *armchair* structure and chirality indices (10, 10) is about 1.36 nm, which is close to that of the fullerene C_{240} molecule having an enhanced stability as well. However, nanotubes of 0.7, 0.47, and 0.39 nm in diameter, which should be closed with quite symmetrical and stable fullerene C_{60}, C_{36}, and C_{20} molecules, were not observed before recently.

The question about the smallest possible nanotube diameter was somewhat clarified recently in the series of publications [38 – 42] reporting on the synthesis of nanotubes with the parameters close to the above-mentioned one. These studies were probably stimulated by work [43], where the smallest possible fullerene C_{20} molecule was first synthesized through a sequence of gas-phase reactions.

The result of work [38], where a single-walled nanotube 0.33 nm in diameter was synthesized and examined, seems to be the most impressive in the field. Such a nanotube with probable chirality indices (4, 0) is incorporated into the heterojunction (11, 11) – (4, 0) – (11, 11), which is the smallest p – n junction produced up to now. The nanotubes were extracted from cloth-like soot produced through the electric arc method. The material was purified using the conventional methods and then studied by means of a high-resolution TEM and Raman spectrometers. The measurement data imply that the sample contains nanotubes with diameters ranging between 0.5 and 1.55 nm. Irradiation of the point of crossing of two (11, 11) nanotubes with the electron beam of a TEM for 10 s results in the appearance of a joining nanotube 0.33 nm in diameter with chirality indices (4, 0).

Single-walled nanotubes with the smallest attainable diameter (0.4 nm) were synthesized in work [42] through the pyrolysis of tripropilamine in pores of monocrystalline $AlPO_4$-5 zeolite. This transparent microporous crystal contains 1D channels 0.73 ± 0.01 nm in diameter, which form a hexagonal matrix. Tripropilamine was inserted into the channels during the crystal growth. The nanotubes are formed inside zeolite channels as a result of thermal treatment of carbon which is a product of the pyrolysis. The nanotubes produced were dissolved in 30% HCl and observed by means of a high resolution TEM. Ultrathin nanotubes 0.42 ± 0.02 nm in diameter can be discriminated in the image. These nanotubes were destroyed in the course of 10 – 15 s under the action of the TEM electron beam. One can imagine three types of single-walled nanotubes with diameters close to 0.4 nm: *zigzag* (5, 0) (0.393 nm in diameter); *armchair* (3, 3) (0.407 nm in diameter), and a nanotube of the chirality (4, 2) (0.414 nm in diameter). *Zigzag* (5, 0) closed with a half of the fullerene C_{20} molecule seems to be the most probable structure.

Single-walled nanotubes situated inside multiwalled cylindrical structures, along with isolated nanotubes of minimum size, were observed in some works. Thus, multiwalled cylindrical structures were obtained in work [40] by the electrical arc method in the hydrogen atmosphere without using a metal catalyst. HR TEM observations show the 18-layer nanotube containing an inner tube 0.4 nm in diameter. Several of these inner nanotubes have the *armchair* structure (3, 3) and end in a fullerene hemisphere that is half of the dodecahedron C_{20}. The angle between two adjacent C – C bonds in such a structure equals 180°, which is close to the relevant angle in the sp^3 configuration of diamond. In work [41], multiwalled nanotubes were obtained as a result of ionic deposition on a substrate, with carbon ions of dozens of eV in energy at a temperature of 150 °C. These nanotubes consisted of 10 – 15 layers separated by 3.4 nm and also contained single-walled nanotubes 0.39 – 0.40 nm in diameter.

2.2 Multiwalled nanotubes

Multiwalled nanotubes are distinguished from single-walled ones by their considerably wider diversity of shapes and configurations. The structural diversity reveals itself in both the longitudinal and transverse directions. Possible modifications of the transverse structure of multiwalled nanotubes are presented in Fig. 5 [10]. The Russian doll structure (Fig. 5a) is an assembly of single-walled cylindrical tubes coaxially stacked one into another. As is seen, the inner space of the ideal Russian doll structure is beyond the reach of penetration by either gaseous or liquid substances.

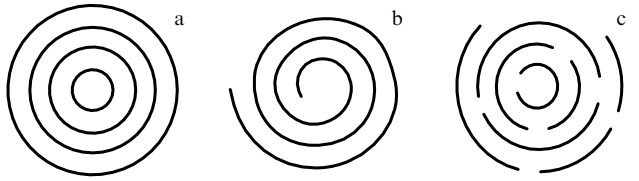

Figure 5. A schematic of the most commonly encountered structures of multiwalled nanotubes [10]: (a) Russian doll; (b) scroll, and (c) papier-mache.

The other version of this structure, shown in Fig. 5b, is a set of coaxial prisms stacked one into another. In this case, the inner volume of a nanotube is found accessible for penetration by liquid or gaseous substances. Finally, the last of the structures presented (Fig. 5c) is a multiwalled cylindrical structure consisting of small graphite fragments, like papier-mache. Such a structure possesses a considerable inner space accessible for penetration by various substances, which is very attractable from the viewpoint of sorption characteristics. For all the structures shown, the magnitude of interlayer spacing is close to 0.34 nm, which is inherent to that in crystal graphite.

The realization of one type of a multiwalled structure or another in a specific experiment depends on the nanotube synthesis conditions. The analysis of available experimental data indicates that the most characteristic structure of multiwalled nanotubes is the Russian doll structure (Fig. 5a) in which tubes of a lesser diameter are inserted successively into those of a larger diameter. Compelling direct evidence of such a structure has been demonstrated in the recent publication [44], the authors of which managed to use a special manipulator to extract the inner layers of the nanotube, keeping the outer ones fixed. By doing so, the nanotube can be extended, taking on a conical form like a telescopic antenna or fishing rod. One end of a multiwalled nanotube 35 nm in diameter was attached to a grounded gold electrode. The other end was connected to another nanotube which was subjected to voltage being varied and played the role of the forming electrode. Supplying a voltage of several volts on this electrode in contact with the nanotube resulted in a current of several hundred mA, followed by a removal of several layers from the nanotube near its vertex and the sharpening of the

nanotube end. This resulted in a decrease in the number of nanotube layers near the end part down to three, and its diameter down to 2.5 nm. Such a sharpened nanotube is, in particular, almost an ideal tip for an atomic field microscope.

Another experiment aimed at establishing the structure of a multiwalled nanotube was described in Refs [45, 46]. In these works, the possibility was first demonstrated of the intercalation of K atoms and $FeCl_3$ molecules inside carbon nanotube bundles to modify their electronic structure. It was found that this possibility is largely dependent on the conditions of the nanotube production.

Multiwalled nanotubes produced in two ways were used as a starting material: in a graphite-electrode arc discharge, and through the chemical vapor deposition with iron and nickel particles as a catalyst, as described by Yudasaka et al. [47]. In the first case, spatially aligned multiwalled nanotubes several dozen nm in outer diameter were produced, being closely packed in bundles which in turn formed thread-like structures up to 3 mm in length and 0.1 mm in diameter. In the second case, the subject of study was a bundle of disordered multiwalled nanotubes several dozen nm in outer diameter applied to a glass substrate. Intercalation was performed in a two-section glass tube. Nanotubes were fitted in one section, whereas an intercalated agent was put into the other one. Either purified K or anhydrous iron chloride ($FeCl_3$) was utilized as an intercalated agent. The tube was pumped out and sealed off. The gas-phase reaction proceeded at a temperature of 300 °C in the case of K, and 280 °C in the case of $FeCl_3$. All the procedures were carried out in a sealed-off chamber in an Ar atmosphere.

It should be noted as the main result of the publications [45, 46] that the intercalation could be performed only in relation to samples produced using the electrical arc method. The intercalation reaction did not change either the dark color or the thread-like structure of the samples, while in the case of $FeCl_3$ some deterioration and disorientation of fibers were observed. The samples were notably increased in weight (15–33% in the case of K, and 110–260% in the case of $FeCl_3$) and size. The intercalation reaction considerably changed the outward appearance of nanotubes viewed under a scanning electron microscope. Straight nanotubes become convex as a result of the reaction, especially in the case of $FeCl_3$. The results of X-ray diffraction investigations showed that the intercalation causes an increase in the interlayer spacing from 0.344 up to 0.53 nm in the case of K, and up to 0.95 nm in the case of $FeCl_3$. This proves that the intercalation affects each tube, but not the intertube region. The intercalated nanotubes are shaped into bead-like or bamboo-like patterns, where the swollen sections alternate with nonintercalated 'necks'. From this it is inferred that the nanotubes produced through the electrical arc method have a scroll structure and are intercalated from the lateral seam but not from the end side. Nanotubes produced through the chemical vapor deposition method are not subjected to intercalation reaction in the conditions described above. Therefore, the authors of the experiment conclude that in this case the structure of the nanotubes is close to the Russian doll one.

One should bear in mind that the perfect transverse structure of nanotubes, where the interlayer spacing is close to 0.34 nm and axially independent, is distorted really due to a perturbing action of adjacent nanotubes. This has been clearly demonstrated in one of the first publications on the subject [48], where the electron microscope observations showed a 2–3% decrease in interlayer spacing in the area of contact between 10-layer and 12-layer adjacent nanotubes. The estimates taking into account van der Waals interaction between atoms confirm this effect quantitatively.

Other deviations from the ideal structure of multiwalled nanotubes were observed in works [49–53] using the electron microscopy and X-ray diffraction methods. Thus, high-resolution electron microscope observations [50, 51] have shown that a considerable portion of multiwalled nanotubes have a polygonized cross section. In such a structure, the plane sections are adjacent to surfaces of high curvature, which contain edges with a high degree of sp^3-hybridization of carbon. These edges confine the surfaces made up of sp^2-hybridized carbon and determine many properties of nanotubes. The impact of sp^3-defects on the ideal structure of the nanotube surface was studied in more detail in works [52, 53]. It was shown, in particular, that the defects cause a distortion in the rectilinear form of the nanotube, shaping it in a pleat-like structure whose wavelength is 2–8 times as large as the six-member ring size.

A great deal of information about the transverse structure of multiwalled nanotubes was provided in work [54] where, in contrast to the conventional approach, the electron beam in diffraction measurements was aligned in parallel to the nanotube axis. Let us consider this work more comprehensively. Nanotube bundles extracted from cathode soot were inserted into an epoxide resin with tweezers. After solidification at 60 °C for 3 days, the plane samples 20–30 nm in thickness were cut from the resin bulk with a diamond knife and examined using a high-resolution electron microscope. It has been found experimentally that one end of the tube is usually connected with a piece of pyrolytic graphite or a polyhedral particle. The other end of the nanotube is closed, while its shape is closer to a cone rather than to a sphere. A wide diversity of tube configurations was observed. Thus, the seven-layer tube 2.04 nm (6×0.34 nm) in inner diameter was seen. The interlayer spacing was always close to 0.34 nm. A 32-layer tube having an inner diameter of 3.4 nm (10×0.34 nm) might also have been seen. A rise in the number of layers results in an increased deviation from the ideal cylindrical shape of a nanotube. In some cases, a polyhedral structure of the outer envelope of the nanotube was evidenced. Sometimes, a nanotube surface was covered with a thin layer of a disordered (amorphous) substance. The ideal closed concentric structure of the cross section was not viewed in any of the diffraction images.

Both the longitudinal and transverse structures of multiwalled nanotubes significantly depend on the production method. As was found in works [55–59] using electron diffraction methods, the widest diversity of longitudinal structures is inherent to multiwalled nanotubes grown on the surface of metal nanoparticles through acetylene catalytic decomposition. Catalytically grown nanotubes usually possess inner and outer diameters of several nm and several dozen nm, respectively, and reach up to several dozen microns in length. About 10% of nanotubes are formed into regular spirals with the radius and pitch varied over wide limits. The tubes curve in an odd manner; they are twisted with themselves and with each other, forming twisted spirals, ropes, loops, and all other sorts of structures.

Observations have shown that the interlayer spacing in multiwalled CNTs produced in an arc discharge can change from the standard value of 0.34 nm to twice the magnitude, 0.68 nm. This implies the existence of defects in nanotube

structures, where one or more of the layers are partly or fully absent.

Another sort of defects quite often observed on the graphite surface of multiwalled nanotubes is a result of the inclusion of a number of pentagons or heptagons into such a surface consisting mainly of regular hexagons. The presence of these defects in the structure of nanotubes causes distortion in their cylindrical shape, so that the inclusion of a pentagon results in a convex bend, whereas a heptagon produces a concave bend of the ideal cylindrical surface of the nanotube. Therefore, such defects result in the appearance of curved and spiral-like nanotubes. The existence of spirals with a constant pitch is indicative of the more or less regular arrangement of defects on the nanotube surface [60].

2.3 Surface and volumetric density of surface carbon nanostructures

The carbon nanostructures of interest to us comprise mainly a graphite surface laid out of regular hexagons with carbon atoms in their vertices. The distance between adjacent atoms in such a structure is roughly 0.14 nm. An ideal crystalline graphite structure contains a large number of such surfaces spaced apart by a distance of about 0.34 nm. The graphitic plane rolled into a cylinder serves as the initial matter for building the carbon nanotube. The specific quantity of an absorbed substance is determined by the magnitude of the surface density of the graphitic layer, which is estimated as follows:

$$\sigma_{\mathrm{C}} = \frac{2m_{\mathrm{C}}}{S} = 0.76 \times 10^{-7}\ (\mathrm{g\ cm^{-2}})\,. \tag{4}$$

Here, $m_{\mathrm{C}} = 2 \times 10^{-23}$ g is the mass of the carbon atom, and $S = 5.24 \times 10^{-16}$ cm^2 is the area of the regular hexagon with a side of 1.42×10^{-8} cm, which is an elementary cell of the graphitic plane. This corresponds to the specific surface $S_{\mathrm{C}} = 1/\sigma_{\mathrm{C}} \approx 1300$ m^2 g^{-1} of an individual CNT. If both outer and inner graphite surfaces of a nanotube are accessible for sorption, this magnitude is doubled. Therefore, the magnitude of the specific surface $S_{\mathrm{C}} \approx 2600$ m^2 g^{-1} can be considered the maximum reachable value for carbon-based materials. The roughly similar estimation of the maximum specific surface is obtained using the reference magnitude of the density of graphite, $\rho = 2.267$ g cm^{-3}, and the distance between hexagonal planes in graphite crystal, $d = 3.355 \times 10^{-8}$ cm. This results in

$$S_{\mathrm{C}} = (\rho d)^{-1} = 1315\ (\mathrm{m^2\ g^{-1}})\,. \tag{4a}$$

The coincidence between the magnitudes of the specific graphite surface, evaluated using the ideal crystal structure of graphite, and the experimental value of its density indicates that the real crystal structure of graphite only slightly differs from the ideal one.

The density of a single-walled carbon nanotube with diameter D is determined by the following relation

$$\rho_{\mathrm{t}} = \frac{4\sigma_{\mathrm{C}}}{D} = \frac{30.4}{D}\ (\mathrm{g\,cm^{-3}})\,, \tag{5}$$

where D is the diameter of the nanotube in units of 10^{-8} cm. The single-walled nanotubes synthesized through the electrical arc or laser ablation method usually form a regular quasi-crystal of trigonal structure in its cross section with the minimum distance between the surfaces of adjacent nanotubes being about $d = 0.335$ nm, like that in crystal graphite. The density of such a structure is determined by the following expression

$$\rho_{\mathrm{mt}} = \sigma_{\mathrm{C}}\,\frac{\pi D}{0.866(d+D)^2} = 27.6 \times 10^{-8}\ \frac{D}{(d+D)^2}\ (\mathrm{g\ cm^{-3}})\,, \tag{6}$$

the maximum of which is reached at $D = d$ and accounts for about 2 g cm^{-3}.

Now let us consider an n-layer nanotube ($n \gg 1$) in which, in accordance with the numerous measurement results, the interlayer distance $d = 0.34$ nm. The diameter of such a tube is $D = D_0 + 2d(n-1)$, where D_0 is the diameter of the smallest inner nanotube. The density of such a tube is given by the relation

$$\rho_{\mathrm{C}} = \frac{4n\sigma_{\mathrm{C}}\left[D_0 + d(n-1)\right]}{\left[D_0 + 2(n-1)\,d\right]^2}\,. \tag{7}$$

As the number of layers $n \gg 1$ rises, this quantity approaches (from above) the density $\rho = \sigma_{\mathrm{C}}/d \approx 2.3$ g cm^{-3} of an ideal crystal structure of graphite.

The measured magnitude of the specific surface of CNTs and other carbon surface structures is usually considerably lower than the above-given model estimates [61]. Thus, the measured magnitude of the specific surface of single-walled CNTs does not exceed 180 m^2 g^{-1} [62], which is about an order of magnitude lower than the maximum reachable value of 2600 m^2 g^{-1} estimated above. The nanotubes were obtained as a result of the catalytic decomposition of CO, purified through nitric acid treatment, and opened through oxidation in air. This rather low magnitude of the measured specific surface of CNTs is obviously caused by a close packing of the nanotubes into bundles, which hinders the penetration of the gas inside the bulk of the matter. This is also the reason for a high sensitivity of the results of measuring the specific surface of CNTs to the conditions of sample preparation. Thus, the measured specific surface of a sample of single-walled nanotubes obtained through the electrical arc method and purified using HCl acid comprised 483 m^2 g^{-1} [63]. The measured specific surface of a sample containing both single-walled and double-walled nanotubes was 790 m^2 g^{-1} [64].

Measurement data imply that the highest specific surface is inherent to single-walled nanotubes obtained as a result of thermocatalytic decomposition of CO at a high pressure (HiPC). This process proceeds effectively on the surface of an Fe catalyst, the particles of which, in turn, form on a substrate as a result of thermal decomposition of pentacarbonyl iron $Fe(CO)_5$ [65, 66]. Therefore, pentacarbonyl iron is an initial material for both catalyst production (iron particles) and nanotube formation (CO). The specific surface of nanotubes obtained in this way was measured as 861 m^2 g^{-1} [67].

An even higher magnitude of this parameter (1587 m^2 g^{-1}) was measured by the authors of work [68], who paid special attention to the procedure of purification and loosening of samples in order to increase the surface accessible for sorption. At the first stage of this procedure, the sample containing 100 mg of single-walled nanotubes 0.93 – 1.35 nm in diameter was inserted into a mixture of dimethylformamide (200 ml) and ethylenediamide (100 μl). The nanotubes were produced through the HiPCO method. The suspension obtained was stirred for 18 hours, which was followed by

ultrasonication for 6.5 h, centrifugation, and filtration. This sequence of operations was repeated twice. At the second stage of sample preparation, the nanotubes were inserted into 250 ml of a 37% aqueous solution of HCl, where they were subjected to ultrasonication for 15 min, followed by thermal treatment at a temperature of 45 °C for 2 h. Thereafter, the solution was twice dissolved by distilled water and subjected to centrifugation and repeated filtration, followed by blowing with moist air at a temperature of 225 °C for 18 h. Such a treatment promotes the removal of metal catalyst particles, as well as amorphous carbon, from the sample. The second stage of the purification procedure was also repeated several times, varying the moist air temperature and duration of treatment. The samples of single-walled nanotubes obtained through the above-described procedure were analyzed using a high-resolution transmission electron microscope, Raman spectrometer, and thermogravimetric analyzer (TGA). The specific surface of samples was measured through standard methods based on the adsorption of molecular nitrogen at a temperature of $T = 77$ K [69].

The electron microscope observations [68] and TGA measurements have shown that the above-described purification procedure resulted in lowering the iron content in the sample from 22 down to 0.4 wt.%. The purified material with low metal content possessed a notably higher chemical stability. A considerable influence of the purification procedure on the measured specific surface of the sample has been found. Thus, the initial nonpurified sample of CNTs was characterized by a magnitude of measured specific surface of 577 $m^2\ g^{-1}$. The purification of the sample using only the second stage of the above-described procedure increased the magnitude of this parameter up to 968 $m^2\ g^{-1}$. Finally, the complete purification procedure has resulted in an increase in this magnitude up to 1587 $m^2\ g^{-1}$, which is a record achievement at the present time. The high sensitivity of the measured specific surface of CNTs to the sample purification procedure is obviously related to an increase in the surface accessible for sorption of nitrogen molecules.

3. Filling CNTs with condensed substances

3.1 Capillary phenomena in CNTs

As already shown in the Introduction, capillary phenomena in CNTs became a subject of intense investigation immediately after the discovery of nanotubes [15]. Comprehensive exploration of the capillary phenomena has been made possible since the development of methods for opening nanotubes, based on the action of strong oxidizers, which allows the penetration of liquid and gaseous substances into their inner cavity. In this case, a fusible liquid metal (lead) penetrates an open-ended nanotube due to the effect of capillary drawing in. In this experiment [15], an electrical arc at a voltage of 30 V and 180–200 A current, designed for nanotube synthesis, was ignited between graphite electrodes 0.8 cm in diameter and 15 cm in length. As a result of the thermal decomposition of the anode surface, a material forming a layer 3–4 cm in thickness was deposited onto the cathode surface. This substance contained nanotubes with diameters ranging between 0.8 and 10 nm, having seamless structure and caps of regular shape. The deposit was extracted from the chamber and conditioned under flowing carbon dioxide at $T = 850$ °C for 5 h. This procedure resulted in a sample mass loss of about 10% and promoted the partial removal of amorphous carbon particles and the opening of nanotubes present in the deposit. The interior of the nanotube-containing deposit was immersed in ethanol and ultrasonicated in order to separate the nanotubes from each other and provide a liquid material with easy access to their opened caps. The TEM observations revealed that the oxidation resulted in damage to the caps of about 10% of the nanotubes and in partial stripping of the layers around the caps. The nanotube-containing sample designate for examination was filled in a vacuum with molten lead droplets produced by irradiating a metal surface with an electron beam. Lead droplets ranging from 1 to 15 nm in size were observed on the outer surfaces of the nanotubes which were annealed in air at $T = 400$ °C (higher than the melting point of lead) for 30 min. As shown by the transmission electron microscope observations, a portion of the nanotubes was found to be filled with a solid material after annealing. A similar tube filling effect was observed upon irradiating the sample with a powerful electron beam. Sufficiently strong irradiation resulted in the melting of material located near the open end of a tube and its penetration into the interior of the tube. The occurrence of lead inside the tubes was indicated by X-ray diffraction and electron spectroscopy methods. The thinnest lead wire was 1.5 nm in diameter.

The results of subsequent detailed investigations of the peculiarities of the capillary filling of CNTs with liquid substances of various nature point to an interconnection between the magnitude of the surface tension of a substance and its capacity to be capillary drawn inward a carbon nanotube. Some of these data are summarized in Table 1 [16, 17], where the experimentally established capacity of various liquid substances to be capillary drawn inside carbon nanotubes is correlated with the magnitude of their surface tension. As can be seen, the capillary properties of nanotubes show themselves only in relation to materials having a rather low (less than 200 mN m^{-1}) magnitude of surface tension in the liquid state. This conclusion is in agreement with a qualitative analysis of the phenomenon, performed by Ebbesen [16, 17].

In analyzing the problem of capillary filling of nanotubes with a liquid substance, one should note that such macroscopic characteristics as surface tension, wetting, etc. are, generally speaking, inapplicable to objects of a nanometer size. A more comprehensive approach to this problem must employ notions based on the interaction potential of an individual molecule with a surface. However, one should

Table 1. Wetting properties of nanotubes (the substance temperature is close to the melting point; the lead and bismuth oxide stoichiometry is uncertain) [16, 17].

Substance	Surface tension, mN m^{-1}	Capillarity
HNO_3	43	Yes
S	61	Yes
Cs	67	Yes
Rb	77	Yes
V_2O_3	80	Yes
Se	97	Yes
Tin oxides	$PbO \sim 132$	Yes
Bismuth oxides	$Bi_2O_3 \sim 200$	Yes
Te	190	No
Pb	470	No
Hg	490	No
Ga	710	No

take into account the fact that the carbon nanotube is a unique object for which it is possible to establish experimentally the minimum size starting from which the macroscopic description of surface phenomena becomes adequate. The experimentally established interrelation between the magnitude of the surface tension of a liquid and the possibility of capillary filling of the nanotube with that liquid can serve as compelling evidence of at least the qualitative validity of macroscopic notions for describing the set of phenomena under consideration.

When analyzing experiments related to the investigation of capillary phenomena in nanotubes, attention should be paid to the role of oxygen whose presence can essentially modify experimental results. Thus, experiments aimed at nanotube filling with lead and bismuth in a vacuum have failed, whereas similar experiments performed in the presence of atmospheric air have resulted in the occurrence of the capillary effect. This observation is quite explicable from the viewpoint of the above-expounded consideration of the correlation between capillary phenomena and the magnitude of the surface tension of the melt. The surface tension of molten lead and bismuth oxides is much less than that for pure molten metals; therefore, the presence of oxygen giving rise to oxides promotes the occurrence of capillary phenomena.

As noted first by Ebbesen [70] in the matter of filling CNTs with liquids, the surface tension of which exceeds the magnitude of $\sigma_0 \sim 200$ mN m^{-1}, an outer force should be applied. The value of this force depends on the difference between the surface tension of the filling substance and the above-indicated value σ_0. In this case, filling CNTs with nonwetting liquids is attended by the expenditure of energy which is proportional to the inner surface of the CNTs. Therefore, the material containing the CNTs can be used as an accumulator of mechanical energy whose specific density W is proportional to the internal specific surface S_i of the CNTs multiplied by the excess in the surface tension coefficient σ over the value of $\sigma_0 \sim 200$ mN m^{-1}:

$$W = (\sigma - \sigma_0)\, S_i\,. \tag{8}$$

Using the results of the above estimations of the internal specific surface $S_i \sim 1000$ m^2 g^{-1} of single-walled nanotubes and the data related to the surface tension coefficients of metals, presented in Table 1, one can conclude that the material containing CNTs can be used as an accumulator of mechanical energy with a specific energy storage W on the level of several hundred J g^{-1}. This quantity is dozens of times lower than the relevant parameter in such traditional chemical-energy storage materials as gunpowders and hydrocarbon fuels, but is comparable to the corresponding characteristics of electrochemical capacitors. The considered method of mechanical energy storage combines the practical convenience of use with a high degree of reversibility, which makes CNT-based mechanical energy storage devices comparable to electrochemical capacitors and fuel cells.

Another method for inserting materials into the inner cavity of a nanotube is based on using solvents having a low surface tension and therefore capable of penetrating into nanotubes due to the capillary effect [71, 72]. The authors used concentrated nitric acid, which is characterized by a rather low magnitude of surface tension (about 43 mN m^{-1}), quite effectively as a solvent. Soot containing nanotubes was produced by electrical arc graphite sputtering. The productivity of the facility was about 15 g h^{-1} of cathode deposit containing up to 25% nanotubes, along with carbon nanoparticles. 2 g of the deposit was inserted into a nitric acid of 68% concentration and conditioned at a temperature of 240 °C for 4.5 h. After drying, the insoluble powder was ultrasonicated in chloroform and dried again in a vacuum. The tunnel electron microscope images of the resulting material show about 89% of the nanotubes to be open. Treatment with the nitric acid for a longer time resulted in the opening of almost all the nanotubes.

For filling nanotubes with a metal dissolved in nitric acid, a suspension containing 0.4 g of closed nanotubes and 20 g of nitric acid solution involving 1 g of hydrated nickel nitrate was prepared. The suspension was conditioned at a temperature of 140 °C for 4.5 h. After filtration and drying, the sample was heated up to $T = 450$ °C with flowing He and annealed at the same temperature for 5 h. According to observations, this promoted the opening of 80% of the nanotubes, 60 – 70% of which contained nickel oxide (NiO) crystals up to 30 nm in length and 3 – 6 nm in diameter. The small crystals were usually situated rather far from the open ends of the nanotubes. A similar material was also evidenced on the outer surface of the nanotubes and nanoparticles.

The above-described method was employed for filling CNTs with iron and cobalt oxides, in addition to nickel oxide. The subsequent treatment of samples containing Ni, Co, and Fe oxides with hydrogen at a temperature of $T = 400$ °C for 4 h seemingly caused a reduction in metal crystals from the oxides. In doing so, the possibility of filling CNTs with metals that have a melting temperature on the same order of magnitude or higher than that of nanotube decomposition has been demonstrated. In addition, the treatment of closed nanotubes with a uranyl nitrate solution made it possible to obtain nanotubes filled with a uranium-containing material consisting of uranium oxide to the extent of 70%. The processing of nanotubes filled with uranium oxides with an aqueous solution of nitric acid resulted in the dissolution of most of the uranium-containing crystals and their escaping from the nanotubes. Thus, the possibility of the reversible filling of nanotubes with refractory metals has been demonstrated. As may be seen, nitric acid plays a twofold role in this operation. On the one hand, the action of the acid upon the nanotube promotes its opening, and, on the other hand, nitric acid well dissolves metals and has a rather low magnitude of surface tension, so it quite easily penetrates inside nanotubes and is capable of bringing dissolved substances there.

The interest in the problem of filling CNTs with metals and other substances is related to the possibility of a directional action on the electronic characteristics of a nanotube as a result of doping. Thus, a metal atom intercalated inside the internal cavity of a nanotube displays a tendency towards the transfer of some part of the valence electron to the outer surface of the nanotube, where nonoccupied electronic states exist. As a result of such a transfer there arises an additional mechanism of electrical conduction, related to the travel of an electron about those states. As reported by Rao et al. [73], filling nanotubes with potassium or Br_2 resulted in an increase in the room temperature electro-conductivity as high as 20 – 30 times. Furthermore, doping nanotubes changes their electronic band structure, as well as the Fermi level position. Therefore, filling CNTs with various substances provides an effective means of controlling their electronic characteristics.

Filling nanotubes with metals through the capillary effect permits one to form an elongated homogeneous metal wire a nanometer in diameter inside the inner cavity of a nanotube. Such a wire can be considered a prototype of future elements of nanoelectronic circuits. Work [74] can be cited as an example, where single-walled nanotubes obtained by the electrical arc method using a catalyst were filled with the molten salt mixture $KCl-UCl_4$ or $AgCl-AgBr$ through the capillary effect. Samples containing nanotubes were powdered together with the salt mixture and sealed off in a quartz ampoule in a vacuum. Then, the ampoule was slowly (at 3 cm per minute) inserted into an oven 30 cm in length, the maximum temperature of which was 100 K higher than the melting point of the mixture. Thereafter, the ampoule was cooled for 3 h down to room temperature. Samples of nanotubes filled in such a manner were studied using a high-resolution tunnel electron microscope and an X-ray spectrometer. Observations indicate quite a high degree of filling the single-walled nanotubes, having chirality indices (10, 10), with molten $KCl-UCl_4$ in the molar ratio of 3 : 1. The filling level of nanotubes with molten $AgCl-AgBr$ varies between 20 and 50%. With an increase in nanotube diameter, $AgCl-AgBr$ salts tend to decompose under the action of the electron beam of the microscope. This results in the predominance of pure silver in nanotubes of large diameter. Thus, a nanotube 3.8 nm in diameter having chirality indices (28, 28) was filled with 17 layers of silver. The measured average interatomic distance 0.204 ± 0.005 nm is practically the same as in the silver monocrystal (200). Therefore, the possibility of filling nanotubes with metal crystal structures, the parameters of which do not practically differ from those of monocrystal structures, was demonstrated.

Further development of work on the formation and study of metal crystal structures inside nanotubes has resulted in a notable expansion of the list of elements comprising the basis of nanowires. Thus, the problem of encapsulation of crystal structures inside the inner cavity of a nanotube was reviewed at length by Sloan et al. [75]. In particular, the monocrystal Sb_2O_3 encapsulated inside a single-walled nanotube 1.5 nm in diameter was described. The experimentally established interconnection between the structure of such crystals and the chirality of nanotubes was noted. A regular KI crystal 2×2 in size was grown inside a single-walled nanotube 1.4 nm in diameter [76]. The electron microscope image of this crystal is presented in Fig. 6. There was observed some enlargement (from 0.35 to 0.4 nm) in the lattice parameter of the KI nanocrystal in the direction perpendicular to the nanotube axis, compared to that in a macrocrystal. A similar conclusion was also reached by the authors of Ref. [77], who managed to grow a KI crystal 3×3 in size inside the cavity of a single-walled CNT 1.6 nm in diameter. Electron microscope observations also indicate slight distortions in the crystal structure (the K^+ ion is displaced 0.13 nm in the direction of the expansion of the lattice, whereas the I^- ion is displaced 0.22 nm in the direction of compression).

In nanotubes filled with a crystalline material, chemical transformations resulting in a change in the composition of a filling substance are possible. Thus, irradiation of single-walled CNTs filled with $ZnCl_4$ crystal with a 300-keV electron beam results in the detachment of the Cl_2 molecule and the partial reduction in Zn. Thereafter, the clusterization of the rest of the $ZnCl_x$ structure ($x < 4$) occurs, which is followed by the spatial separation of clusters [78]. Ideal images of structures observed through a high resolution

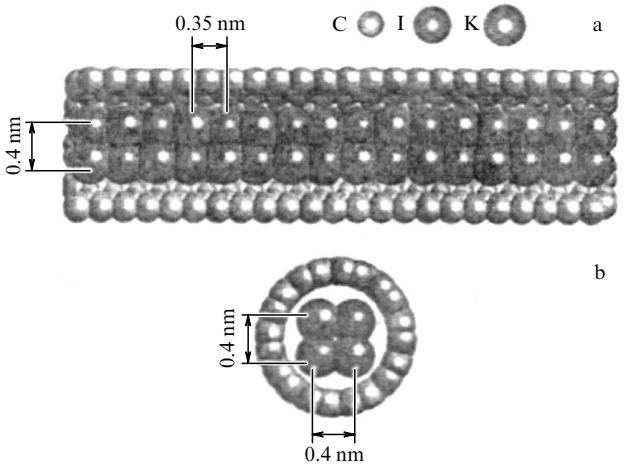

Figure 6. High-resolution electron microscope image of the KI crystal structure encapsulated inside a single-walled carbon nanotube 1.4 nm in diameter [76]: (a) side view, and (b) end view.

electron microscope at various points in time are shown in Fig. 7. The above-described procedure results in the formation of Zn monocrystals that have properties of quantum dots and can be considered superminiature elements of nanoelectronic devices.

The enhanced sorption capacity of CNTs in relation to wetting liquids leads one to consider these structures to be nanosponges that can soak up the liquid in which they are immersed. This effect was studied in detail in work [79], where single-walled nanotubes obtained by the laser ablation of graphite and bound into bundles were used as samples. A sample containing about 36 μg of CNTs was plated onto a gold substrate 1.3 cm^2 in area, covered with a graphite layer 3–5 nm thick, from a dimethylformamide suspension, followed by evaporation of the suspension. Before performing the experiment on molecular sorption, the nanotubes were heated in a vacuum to 1073 K, which promoted the removal of function groups from their surfaces and the opening of their inner cavities. Experiments on filling the sample with CCl_4 were carried out at $T = 97$ K and a flux of 8.7×10^{12} $cm^{-2}\,s^{-1}$ of CCl_4 onto the substrate surface. After terminating the filling procedure, the sample was heated at a rate of 2 K s^{-1} in order that the CCl_4 molecules having been desorbed could reach a mass spectrometer. Measurements show that when the substrate does not contain CNTs, the effective desorption of CCl_4 occurs at $T = 175$ K. The presence of nanotubes on the substrate surface causes a notable depression of the desorption phenomenon at the above-indicated temperature and an increase in the characteristic desorption temperature up to about 260 K. Hence, it follows that the characteristic sorption energy of the CCl_4 molecules on a nanotube surface notably exceeds that for the substrate surface. Processing the measured temperature dependences of the desorption rate made it possible to elucidate the behavior of CCl_4 molecules on a substrate surface containing CNTs. At a relatively low temperature, when the characteristic desorption time of a CCl_4 molecule from a surface exceeds that necessary for the molecule to reach the surface, the molecule undergoes random walking over the substrate surface until it reaches a nanotube surface. The characteristic time for a molecular desorption from a nanotube surface exceeds considerably that for a substrate

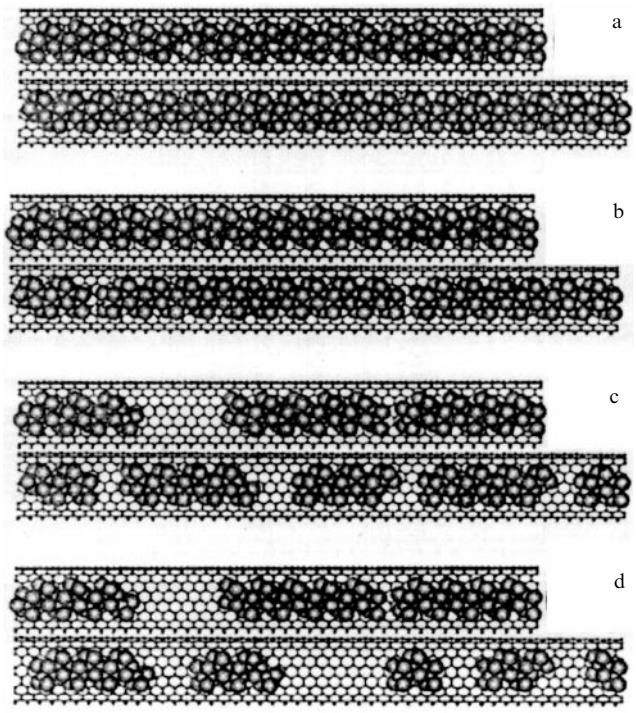

Figure 7. High-resolution electron microscope ideal images of structures formed at various points in time as a result of high-energy electron beam irradiation of a single-walled nanotube filled with a $ZnCl_4$ crystal [78]: (a) nonirradiated nanotube; (b) a modest dose of irradiation resulting in a partial destruction of the crystal structure and emission of gaseous Cl_2; (c) further irradiation causing the formation of small clusters of $ZnCl_x$ ($x < 4$), and (d) subsequent irradiation leading to the eventual separation of clusters and the formation of quantum dots consisting of Zn nanocrystals.

surface, therefore a nanotube constitutes an effective device for removing CCl_4 molecules from a surface, operating like a sponge. Due to the extraordinary high specific surface of CNTs, such a device can be used as a tool for collecting toxic or highly valuable molecules.

3.2 Filling CNTs with metal vapor

In parallel with approaches based on capillary drawing-in phenomena, other methods are used for filling CNTs with metals. Thus, in work [80], targeted at establishing the influence of filling single-walled nanotubes with potassium on their electronic properties, a specimen containing nanotubes was conditioned in K vapor. Single-walled CNTs 1 nm in average diameter were produced as a result of the thermocatalytic decomposition of CO. Three kinds of samples were studied: an initial sample of nanotubes bound into bundles, nanotubes with closed caps, and nanotubes with caps opened through a thermal treatment in air at a temperature of 693 K. Incorporation of K inside the nanotubes was achieved by conditioning the samples with a small quantity of K in a sealed-off cell for 25 h. This resulted in potassium filling the intertube space in two samples and the inner cavity of the open-cap nanotubes. The nanotube samples intercalated with K and the initial samples were studied by photoemission spectroscopy methods. Before performing the measurements, the samples doped with K were treated in water for 1 min, followed by vacuum thermal processing at a temperature of 873 K for 30 min. This treatment promoted the removal of K from the intertube space and from the surface of the samples. Measurements show an enhanced density of electronic states near the Fermi level for open-cap nanotubes doped with K, which indicates the metallic character of the conductivity of the samples. In contrast, the energy spectrum of doped closed-cap nanotubes is characterized by a rather low density of electronic states near the Fermi level and practically coincides with that of the initial nonintercalated nanotubes. The analysis of photoemission spectroscopic data indicates that the degree of filling of open single-walled nanotubes with K atoms reaches $K/C \sim 0.14$. It was found that filling the nanotubes with K atoms results in a displacement of the photoelectron spectrum by about 1.4 eV, which can be interpreted as the corresponding lowering of the electron work function from 4.7 to 3.3 eV. This last result is of great practical importance because it offers the possibility to improve emission characteristics of single-walled CNTs by their doping with alkali metal atoms.

Structural changes in CNTs due to the filling of their inner cavity with metal vapor can be determined through the use of Raman spectroscopy. This approach was applied, in particular, in work [81] where single-walled nanotubes with a minimum possible diameter of 0.4 nm, filled with lithium vapor, were studied. These nanotubes were synthesized inside pores formed in a zeolite ($AlPO_4$) structure. The filling of the samples with lithium vapor was performed in a sealed-off chamber at $T = 500$ K for 5 h. Raman spectra were measured using He – Ne laser radiation focused on a spot 2 μm in diameter. The Raman spectrum of specimens that were not treated with Li contained the 510 and 550 cm^{-1} lines of the radial breathing mode. These lines were assigned to nanotubes of about 0.4 nm in diameter and chirality indices (5, 0) and (4, 2), respectively. As the nanotubes are filled with lithium, the intensity of the radial breathing vibrations is lowered, while the frequency of lines is enhanced, which is caused by an increase in the degree of hardness of the nanotubes with respect to the radial vibrations.

In parallel with capillary drawing-in and saturating with heated vapor, electrochemical methods based on passing the electrical current through an electrolyte containing dissolved metal atoms are also used for filling nanotubes with metals. To do so, a metal electrode is used as an anode, while a sample containing CNTs serves as a cathode. In the case of the reversible filling of a sample containing nanotubes with a metal, one can consider a new type of electrochemical cell that is capable of accumulating and releasing electrical energy. As an example of such an approach, work [82] can be cited where multilayer nanotubes were utilized. These nanotubes were produced through the thermocatalytic decomposition of acetylene at a temperature of 600 °C in the presence of a Co catalyst at a content of 2.5 wt.% and a zeolite substrate with an NaY admixture. The nanotubes obtained had an entangled and twisted structure, ranging from 15 to 25 nm in diameter and reaching 10 μm in length. The purity of the samples was estimated at the level of 90%. Electrochemical doping of the samples with lithium was performed in a cell containing Li – electrolyte – CNTs and placed into a glove box. Nanotubes doped with 5% polytetrafluorethylene, which served as a binding material, and 5% carbon black were used as the cathode, while a lithium foil was employed as the anode. As an electrolyte, 1M $LiPF_6$ solution in a carbonate mixture was utilized. The cell charging/discharging procedure was performed at a 10 mA g^{-1} current of carbon. The open-circuit voltage of cells before the experiment was 2.7 V. The specific reversible capacity of the

specimens was estimated at about 300 A h kg^{-1}, which is close to that for graphite. After the charging/discharging cycle, the magnitude of this parameter was smoothly lowered, reaching the value of 260 A h kg^{-1} after 20 cycles. Tunneling electron microscope observations and Raman spectroscopy measurements show that lithium accumulates on the outer surface of CNTs but not within the interlayer space. As can be seen, further enhancement of the cell capacity can be achieved by filling the inner cavity of the nanotubes with lithium as well.

The degree to which the inner cavity of a CNT is filled up with a metal depends considerably on the nanotube length. This relates to the extraordinarily low magnitude of the diffusion coefficient of the metal inside the nanotube, due to which the inner cavity of a nanotube is filled very slowly. Therefore, the degree of filling of a nanotube rises as its length decreases. Thus, it was shown by Shimoda et al. [83] that decreasing the mean length of single-walled CNTs about 10-fold results in an increase of their specific capacity with respect to absorption of Li from LiC_6 up to LiC_3. Single-walled nanotubes bound into bundles were produced by the laser evaporation method using isotopically enriched graphite containing about 10% ^{13}C isotope. The samples were purified up to 90% in a flowing H_2O_2 solution, followed by filtration. The bundles over 10 μm in length and 30 – 50 nm in diameter mainly contained nanotubes of about 1.4 nm in diameter. The purified bundles were ultrasonicated in a mixture (3 : 1) of H_2SO_4 and HNO_3 for 10 – 24 h in order to decrease the length of the nanotubes, whereupon they were annealed for an hour in a vacuum at 500 °C. TEM observations showed a decrease in the mean length of a bundle from 10 to 4 μm (10 h of treatment) and down to 0.5 μm (24 h). Electrochemical filling of samples of single-walled CNTs with lithium was performed in a two-electrode stainless steel cell, where the samples containing single-walled nanotubes were used as electrodes. The quantity of lithium intercalated was determined by integration of the current over time. Three types of specimens were studied: nontreated (A), and treated for 10 h (B) and 24 h (C). As a result of the reversible intercalation, the specific content of Li in specimen A reached LiC_6, which corresponds to the results of earlier publications.

One more effective approach to the problem of filling CNTs with metal atoms is based on irradiation of a sample containing nanotubes with an ion beam. This approach was first applied by the authors of work [84], who used as a target single-walled nanotubes produced by the electrical arc method with either an Fe/Ni or Se catalyst. A cloth-like specimen containing single-walled nanotubes, which were purified by the standard method, was dispersed through ultrasonication in ethanol, whereupon droplets of the suspension were deposited onto a stainless steel substrate and dried. The samples produced were irradiated with a Cs-ion beam up to 100 eV in energy, obtained from a gas discharge plasma source subjected to an outer magnetic field. The ion number density in the beam was estimated at 10^{10} cm^{-3}. Scanning tunneling electron microscope observations showed the occurrence of nanotubes partially filled with cesium atoms. The boundary between the filled and nonfilled regions of a nanotube is clearly discriminable. The existence of such a boundary means that the nanotube is filled with cesium atoms through the open cap but not through defects in its cylindrical surface. One should note that, since the existence of cesium atoms inside the inner cavity of the nanotube considerably changes its electronic characteristics, the nanotube partially filled with cesium can be considered a superminiature p – n junction, appropriate for use as an element of nanoelectronic information devices.

3.3 Synthesis of filled nanotubes

The most natural way for producing nanotubes filled with metals and their compounds is based on the method of catalytic synthesis of nanotubes using the metals as catalysts. In doing so, the nanotubes are already filled with metals in the course of synthesis, which permits one to avoid the above-mentioned limitations related to the surface tension of a metal. This approach usually results in the production of multiwalled nanotubes partially or fully filled with small crystals of metals, their oxides, or carbides. The list of substances that have been successfully inserted into nanotubes by this means includes such metals as Rh, Pd, Pt, Mn, Co, Fe, Ni, Sc, La, V, Ce, Gd, Zr, Y, Ti, etc., as well as compounds of these elements. In so doing, one should note a wide variety of crystalline forms and chemical states of encapsulated metals. Thus, in one of the first publications on the subject [85], where metals of the iron group (Fe, Co, Ni) were utilized as catalysts for producing nanotubes, both metal particles (bcc-Fe, fcc-Co, and fcc-Ni) and metal carbides X_3C (X is the metal atom) were found inside the nanotubes.

Special attention should be paid to Ref. [86], where carbon nanotubes filled with a superconductive material TaC were synthesized. The success of this experiment has opened the possibility of using carbon nanotubes in superconductor technology. To produce TaC crystals encapsulated in the inner cavity of nanotubes, powdered Ta of 99.9% purity and finely ground graphite were mixed in the weight ratio of about 6 : 10 and pressed into a hollow graphite rod (8 mm in length, 3 mm in inner diameter, and 6 mm in outer diameter) served as an anode. A fixed graphite disk 17 mm in diameter was used as a cathode. An arc was burnt in an He atmosphere at a pressure of 100 – 300 Torr, a voltage of 30 V, a current of 30 A, and an interelectrode gap of 2 – 3 mm. The temperature of the end cathode surface was estimated at 1500 °C. Under the action of the discharge, a carbon deposit with an admixture of TaC particles was formed on the cathode surface; the particles were found both on the surface and in the bulk of the deposit. For extracting the nanotubes filled with TaC particles, the deposit samples (100 mg) were placed into a 70% solution of sulfuric acid and held at a temperature of 80 °C for two weeks. As a result of this treatment, the nonencapsulated particles were fully dissolved in acid. The rest of the material was repeatedly washed with distilled water, dried, and dispersed using ultrasonication in ethanol. Afterwards, one to two drops of the suspension were placed with a dropper onto a carbon-coated copper grid for making electron microscopic observations. It has been found experimentally that the cathode deposit contains a large quantity of nanotubes filled with TaC crystals and a handful of such crystals encapsulated in elongated or compact polyhedrals. In the substance taken from the partly sputtered anode surface, by contrast, a large quantity of particles enclosed in polyhedral cells and a small quantity of short multiwalled nanotubes were found.

Multiwalled nanotubes filled with TaC particles and extracted from a cathode surface are characterized by an interlayer distance of 0.3481 nm, which is 3.9% higher than that of pure graphite. TaC particles range from 2 to 20 nm in size with a maximum in the distribution function at 6 nm. The crystal structure of the nanotube-encapsulated TaC was

studied using the X-ray diffraction method. Measurements show that this structure does not practically differ from the conventional crystal structure of TaC (NaCl structure type) with a lattice constant $a_0 = 0.4455$ nm. Superconducting transition was observed at $T = 10$ K through magnetic susceptibility measurements. The distinctive feature of a TaC crystal is its extraordinarily high melting point (3985 °C), which is the highest among all carbides and is well over the melting point of pyrolytic graphite (2500 – 3500 °C). This leads us to believe that a carbon nanotube enclosing a thallium carbide particle is formed after the carbide crystallization.

One more interesting method for producing nanotubes filled with a metal was demonstrated in Ref. [87], where the gaseous iron pentacarbonyl $Fe(CO)_5$ was utilized as a metal-containing agent. A graphite-electrode arc was burnt at an electrode voltage of 20 V and a current of 100 A in a mixture of He (50 mbar) and $Fe(CO)_5$ (50 – 200 mbar). At a high temperature, iron pentacarbonyl dissociates, releasing Fe. The iron content in plasma was varied by changing the temperature of the reservoir with liquid $Fe(CO)_5$, which determined the partial pressure of the carrier gas. The soot produced in the gaseous phase as a result of the discharge was dispersed in alcohol and then mounted on a copper grid for making electron microscope observations. In the soot collected from the chamber walls, fullerenes were observed, along with carbon particles containing particles of iron and iron carbides. Chemical analysis of the soot showed the iron concentration ranging from 1.8 to 12 wt.%. The soot contained iron nanoparticles incorporated into a graphite envelope and a large amount of multilayer carbon nanotubes, partly filled with iron. The diameter of the nanotubes ranged between 20 and 65 nm, and their length reached 2.5 μm. The shape of the tubes was far from rectilinear; they were only partly filled with metal, and not over their entire length. Nevertheless, the interlayer spacing was always equal to 0.34 nm. The metal enclosed in the nanotubes had either a single-crystal or a polycrystalline structure. In some cases, inclusions of FeC and Fe_3C (cementite) particles were observed.

The most detailed study of the peculiarities of filling carbon nanotubes with various metals was reported in Ref. [88], whose author performed experiments resulting in the encapsulation of 17 various metals inside nanotubes. The experimental facility was described in detail in a preceding work of the same author and his colleagues [89]. Graphite rods 9 mm in diameter and 42 and 72 mm in length were used, respectively, as an anode and a cathode. A hole 6 mm in diameter and 38 mm in depth, drilled in the anode, was filled with a mixture of graphite and metal powders. The arc burnt for 30 – 60 min at an interelectrode separation of several mm, a current of 100 – 110 A, an electrode voltage of 20 – 30 V, and an He pressure of 450 Torr. The experimental data are given in Table 2. Two modes of nanotube filling with metals may be distinguished. The first is observed in the event of Cr, Ni, Dy, Yb, and Gd. In this case, the nanotubes are uniformly filled lengthwise with a metal, forming a wire of constant diameter, which is aligned strictly in parallel with the axis of the tube. These are true metal wires ranging from 100 nm to over 1 μm in length, surrounded with a graphite envelope. The second type of filling is observed in the event of Pd, Fe, Co, and Ni. In this case, the nanotubes are filled incompletely along their full length with a metal which may be found as encapsulated particles located from place to place along the length of the nanotube and near its cap. Nanotubes nonuniformly filled with a metal over their length are variable in diameter, although the graphite layers remain aligned along the tube axis. In all instances but Co and Cu, where the nanotubes are filled with a pure metal forming a face-centered crystal structure, a metal is present in the form of a carbide. Thus, the carbides Fe_3C (cementite), Ni_3C, and TiC have been identified.

Table 2. Experimental data related to filling nanotubes with metals [88, 89].

Element	Size of the metal grain, μm	Boiling point, K	Filling of nanotubes	Unfilled shells	Length of the filled section of a tube, nm	Number of holes
Ti	10	3562	–	–	–	0
Cr	5	2945	+	+	3000	7
Fe	1	3135	+	+	200	5
Co	2	3201	+	+	200	3
Ni	10	3187	–	+	1000	2
Cu	40	2836	–	–	–	0
Zn	10	1180	–	–	–	0
Mo	10	4912		–	–	
Pd	1	3237	–	–	1000	2
Sn	20	2876	+	+	3000	0
Ta	40	5731	+	+	200	0
W	5	5828	+	+	200	0
Gd	400	3539	+	+	1200	7
Dy	400	2835	–	–	600	5
Yb	400	1467	–	–	200	1
Sm	–	–	+	+	10	9

The experimental data presented in Table 2 show that the formation of metal nanowires inside carbon nanotubes does not depend on the boiling point of the metal. It follows, thence, that in the first stage of nanotube synthesis the arc temperature in the vaporization region exceeds the boiling points of the metal and graphite. The observed correlation between the formation of nanowires and the existence of unfilled electron shells in metal atoms points to the fact that the metal ions in the process of nanotube filling are found in the most stable oxidation state. As is seen from the table, the more vacancies in the unfilled electron shells, the greater the length and higher the quality of nanowires. Thus, Cr and Gd are the best metals for nanowire production, having the maximum number of vacancies in the unfilled electron shells and forming the longest wires.

The experiments performed show that filling CNTs with metals during their growth usually has the character of a catalytic reaction. This follows, specifically, from detailed studies of the crystal structure and chemical composition of nanowires enclosed in a graphite envelope, which were carried out in Ref. [90] through TEM and electron energy loss spectroscopy (EELS). In the work cited, CNTs were filled with metals in the course of electrical arc synthesis of the nanotubes using a graphite anode with the addition of a metal powder. Cylinders 9 mm in diameter, manufactured from graphite of 99.4% purity, were used as electrodes. A hole 6 mm in diameter was drilled in the anode, which was filled with a mixture of graphite and metal powders. A dc arc was burnt for 30 – 60 min at a current of 100 – 110 A, an electrode voltage of 20 – 30 V, and an He pressure of 0.6 atm. A cathode deposit containing filled nanotubes and nanoparticles enclosed in a graphite envelope was grounded and

ultrasonicated in ethanol. A drop of the suspension was applied to a graphite grid for making TEM observations. Depending on the powder content in the anode hole, CNTs filled with metals such as Cr, Ni, Dy, Yb, Ge, and Se have been observed. The length of the nanotubes ranged from several hundred nm to several μm. The degree of filling of the CNTs with metals was usually close to unity, except in the cases of Co and Fe, which show a partial filling. Both single-crystal and polycrystalline structures of the metals filling the CNTs were observed. The chemical composition of the filled CNTs was determined through EEL spectroscopy. In addition to the metal contained in the anode hole, a notable quantity of sulphur, which along with iron (0.3 wt.%) is involved as an admixture (about 0.25 wt.%) in the composition of graphite, was found inside the CNTs. For example, the content of sulphur in CNTs filled with chromium is close to that of chromium itself. As distinct from chromium filling, the content of sulphur varies along the length of the nanotube in the cases of Ni and Co filling. When an anode hole was filled with sulphur, nanotubes filled with iron sulphides were observed. In order to establish in detail the decisive role of the presence of metal and sulphur in the nanotube growth mechanism, experiments with electrodes manufactured from pure graphite (purity 99.997%) filled in sequence with pure materials Cr (purity 99.95%), Ni (99.9%), Co (99.9985%), Dy (99.9%), and S were performed, but no filled nanotubes were observed. In filling the anode hole with Ni and Co, single-walled nanotubes were produced, in agreement with experiments by other authors. In the cases of Cr, Dy, and S, only a bare handful multiwalled nanotubes was observed. When filling the pure graphite anode with a mixture of Cr and S with an atomic ratio of S/C = 0.04%, Cr/C = 8%, and S/Cr = 0.5%, a large quantity of multiwalled CNTs filled with either chromium or its sulphides and carbides was observed. The authors assumed that the presence of sulphur enhances the catalytic activity of a metal in relation to the graphitization of carbon, and promotes the further penetration of the metal filling the nanotube in the course of its growth, the metal being remained in the liquid state.

Due to the high conductivity of copper, the question of manufacturing copper nanowires enclosed in the graphite envelope of a nanotube is of great practical interest. Such nanowires can be used in the future as the basis for developing nanoelectronic devices. One of the approaches to solving this issue was demonstrated in Ref. [91], where the nanotubes filled with copper were produced through the MPCVD (microwave plasma-assisted CVD) method. According to this method, two copper electrodes 13.5 cm in length and 2.5 mm in diameter, connected by a tungsten filament, were utilized as a source of copper. Each of the electrodes was inserted into a ceramic tube 10 cm in length that can be moved along the electrode. The electrodes were held 5 mm over a silicon substrate heated up to 700 °C in the course of nanotube growth. A mixture of H_2 and CH_4 in the ratio of 1 : 1 at a total pressure of 18 Torr flowed through the reaction chamber. The microwave discharge input power reached 800 W, the filament temperature was fixed at the level of 1150 °C, and the reaction time comprised 30 min. Microwave discharge caused the sputtering of copper clusters from the naked surface of the copper electrodes, which resulted in the growth of CNTs between 40 and 80 nm in diameter, filled with copper. The quantity of such nanotubes is mainly determined by the length of the naked copper electrodes located above the substrate. The optimal magnitude of this parameter is 5 mm. TEM observations show that the length of copper wires inside CNTs reaches several dozen μm, while the optimal degree of nanotube filling exceeds 10%. Most of the nanotubes are not fully filled, and the structure of the outer graphite layers is rather imperfect. Ramified dendrite-like structures of nanotubes were observed. Similar experiments were performed in Refs [92, 93], where nanowires from platinum and a Pt–Si alloy, enclosed in a graphite shell, were produced using the MPCVD method.

When a nanotube is filled with a metal, a mutual influence of the structures of the matrix (carbon nanotube) and the metal substance filling it shows up. Unusual structures that can be obtained only by combining nanotube and filling metal are then observed. As an example of such a situation, work [94] concerning the synthesis and study of nanotubes filled with metallic chromium can be mentioned. The nanotubes were produced by the field anode activation method, in accordance with which CNTs are grown in the medium of gaseous hydrocarbons on the surface of an anode that is the source of the field ion emission. In the work cited, a mixture of naphthalene ($C_{10}H_8$) vapors and chromium carbonyl $Cr(CO)_6$ was used as a gaseous medium. A ground tungsten filament 10 μm in diameter, spaced 5 mm from a disk cathode, was used as an anode. The anode temperature determined by the anode current was controlled with an optical pyrometer. The optimal growth rate of chromium filaments occurs in the temperature range between 1100 and 1200 °C. To enhance the electrical field amplification factor in the anode vicinity, a graphite powder was deposited onto its surface. The total gas pressure in the chamber reached 0.06 Torr at a naphthalene-to-carbonyl content ratio equal to 3 : 1. The discharge in the chamber was performed at an electrode voltage of 4–6 kV and promoted growth of filaments on the anode surface. TEM observations show that the thread-like crystals formed at the anode were about 10 nm in diameter and up to 0.5 μm in length. These crystals contained chromium with a small admixture of chromium carbide and were enclosed in a graphite envelope which is a CNT consisting of about 7 layers. Only the bottom part of the nanotube was filled with the metal filament. The multiwalled structure of an unfilled region of a nanotube is obviously less perfect than for a filled one. X-ray diffraction pattern implies an extraordinary crystal structure of chromium nanocrystals that has not been described before. Seemingly, the occurrence of such a structure is caused by the effect of an adjacent graphite surface on the character of crystal growth. Moreover, an inverse catalytic influence of chromium on the character of the nanotube growth is noticeable.

3.4 Nanotubes filled with fullerenes (peapods)

3.4.1 A peapod as the 1D fullerite crystal. The characteristic magnitude of the diameter of a single-walled nanotube amounts to 1–1.5 nm. This is sufficient for filling a nanotube not only with atoms or molecules of various substances but also with more complex high-molecular compounds. Specifically, one of the most interesting objects, formed as a result of filling CNTs with a condensed substance, is called a 'peapod' and can be obtained by filling nanotubes with fullerene molecules. The fullerene C_{60} molecule has a diameter of about 0.7 nm. In addition, the equilibrium distance between adjacent graphite layers is approximately 0.34 nm. Therefore, filling a single-walled nanotube with fullerene C_{60} molecules becomes possible if its diameter is on the order of or higher than 1.38 nm. One should note that just such a diameter is

inherent in nanotubes having the *armchair* structure with chirality indices (10, 10) (see Section 2.1.1). Nanotubes of or close to that structure are formed in a notable quantity using plasma synthesis methods [8, 24]. In an analogous manner to endohedral fullerenes (fullerene C_n molecule containing k encapsulated atoms), which are designated as $M_k@C_n$, peapods are sometimes designated as C_n@SWNT, where SWNT is a single-walled carbon nanotube.

The procedure for the production and identification of peapods was first described by Smith et al. [19]. A sample of the soot obtained by the laser sputtering of a graphite surface and containing, along with single-walled nanotubes, fullerene C_{60} molecules was subjected to a thermal treatment at $T = 1100^\circ$ C for 14 h. 1–2 mg of this sample was inserted into 4 ml of a (3 : 1)-mixture of 90% sulphuric acid and 70% nitric acid, whereupon the suspension produced was conditioned at $T = 90\,^\circ$C for 10 min. The material obtained after repeated washing and drying was observed with a high-resolution transmission electron microscope. The material was inserted into toluene for taking the optical transmission spectra. The measurements showed that the material under investigation contained single-walled nanotubes about 1.4 nm in diameter, partly filled with chains of C_{60} molecules. The distance between the centers of adjacent molecules was about 1 nm, which coincides with the relevant magnitude in the fullerite crystal. The degree of nanotube filling with fullerene molecules reached 5.4%.

The above-cited work [19] has been further developed in subsequent publications by various authors (see, e.g., Refs [21, 95–111]). Thus, samples of single-walled nanotubes were synthesized in Ref. [96] by the laser ablation method using Ni/Co catalyst, purified for 12 h in a flowing aqueous solution (2.6 M) of HNO_3, and extracted with toluene. Two types of samples were used in the experiment. In producing the type A samples, the suspension obtained was filtered using polytetrafluorethylene, which resulted in the formation of a cloth-like material that was subjected to annealing in a vacuum at a temperature of 225 °C for 15 h. Then, each of the samples of several mg, after careful weighing to the nearest 0.006 mg, was inserted into an ampoule containing C_{60} in an amount sufficient for fully filling all the nanotubes resided in the sample. The filling of the samples with fullerenes was performed at temperatures of 350, 450, and 550 °C for 64.5 h. Then, the ampoule was broken and its contents conditioned in a vacuum (5×10^{-5} Torr) at a temperature of 800 °C for an hour in order to remove the remaining C_{60}, which was followed by repeated weighing.

The type B samples were prepared by purification of a cloth-like material for 2 h using a 15% aqueous solution of H_2O_2 at a temperature of 125 °C and then conditioning in HCl for 20 min, which was followed by neutralization of the acid and filtration. Filling the samples with fullerenes was performed at temperatures of 350, 450, 550, 650, and 750 °C for 64.5 h. If C_{60} molecules fill single-walled nanotubes of (10, 10) chirality in a close 1D packing, with the intermolecular spacing being 1 nm, the mass ratio for C_{60}/SWNT is $(m_f/m_t)_{max} = 3/8$. For this reason, the degree of nanotube filling was characterized by the parameter $\eta = 8(m_f/m_t)_{exp}/3$, where $(m_f/m_t)_{exp}$ is the measured relative gain in the mass of a sample.

Measurements show virtually linear dependence of the filling degree on the filling temperature for samples of single-walled CNTs of type B, reaching about 90% at a filling temperature of 750 °C. The filling degree of type A samples passes a maximum (about 25%) at a filling temperature of 450 °C, which is somewhat lower (30%) than that for a sample of type B at the same temperature. The filling degrees measured on the basis of mass change determination are in correlation with TEM observations which clearly show the presence of C_{60} molecules inside single-walled nanotubes. These observations indicate that the distance between the centers of adjacent C_{60} molecules amounts to 0.998 nm, which corresponds to the known magnitude (1.004 nm) of the lattice parameter in C_{60} crystals. It can also be seen that the samples of type B contain much less contamination than those of type A, which can be attributed to the high chemical activity of OH radicals that form due to the decomposition of H_2O_2. It should be emphasized that the degree of filling peapods with fullerene C_{60} molecules was also examined in detail in Ref. [106] using Raman scattering and electron energy loss spectroscopy. The measurements taken by these two methods are in good agreement and imply the filling degree in some samples exceeding 70%.

An important distinctive feature of peapods derives from enhanced chemical stability of fullerene molecules enclosed inside the graphite shell of CNTs. The very wall of a nanotube can thereby be considered a protective envelope, preventing the destruction of encapsulated substance due to outer chemical action. This feature has been demonstrated in Ref. [98], where the stability of peapods with respect to oxygen was studied. Samples of single-walled nanotubes produced by the laser ablation method were purified by a 70% aqueous solution of HNO_3 at $T = 400$ K for 8 h. A sample washed with water and dried was subjected to oxygen processing at a pressure of 250 Torr and a temperature of 700 K for 20 min, which promoted the opening of the nanotubes. Then, the sample was sealed off together with a solid C_{60} and conditioned at a temperature of 670 K for 24 h, which resulted in the formation of peapods. TEM observations showed that the yield of peapods reached 70%. The samples produced in parallel with those not containing C_{60} were subjected to the thermal gravimetry procedure in an argon atmosphere with an admixture of 1% oxygen at a rate of temperature enhancement of 5 K min^{-1} from room temperature up to $T = 1270$ K. The measurements reveal that the decomposition of both pure single-walled CNTs and peapods is observed in a temperature range between 900 and 1200 K. However, the maximum rate of decomposition of pure CNTs occurs at 1110 K, while for peapods it corresponds to $T = 1070$ K. The maximum decomposition rate of C_{60} is reached at 960 K. Thorough TEM observations show that the action of oxygen at $T = 1070$ K results in the partial destruction of walls of single-walled nanotubes, while the C_{60} molecules encapsulated in these structures remain practically damage-free. Therefore, the C_{60} molecules encapsulated in single-walled nanotubes are less susceptible to the action of oxygen at elevated temperatures than a pure sample of C_{60}. Hence, the graphite surface of a nanotube can be considered an envelope protecting its interior from outer chemical action.

Single-walled nanotubes can be filled not only with fullerene C_{60} molecules, but also with C_{70} molecules which have not a spherical but an elongated structure, like a Rugby ball [3]. The C_{70} molecule has two different sizes, longitudinal and transverse, which suggests the possibility of the existence of two different peapod structures distinguished by the character of the orientation ordering of the C_{70} molecules inside the peapods. This idea has been confirmed recently in

Ref. [100], the authors of which studied peapods filled with C_{70} by the X-ray diffraction method. Single-walled CNTs 1.37 nm in diameter, bound into bundles, were produced by laser ablation of graphite using an Ni/Cr catalyst. Two types of peapods were found as a result of filling the nanotubes with C_{70} molecules using the standard method. These peapod types differ from each other in the average distance between the centers of adjacent molecules (1.0 ± 0.01 and 1.1 ± 0.01 nm), which corresponds to 'transverse' and 'longitudinal' alignments of C_{70} molecules in peapods. Analysis of measured results shows that the ratio of the number of CNTs with a longitudinal alignment to that of a transverse alignment comprises 7 : 3. It is assumed that the longitudinal alignment is inherent to nanotubes of smaller diameter than for the case of transverse one. In addition, the thermal expansion coefficient for the lattice parameter of a 1D crystal formed by C_{70} molecules encapsulated in a nanotube was measured. It was found that in the case of longitudinal alignment this coefficient is equal to 11×10^{-5} K^{-1} within the temperature range of 300 – 1000 K, which exceeds considerably the relevant magnitude for the interlayer distance in graphite (2.6×10^{-5} K^{-1}), the intermolecular distance in solid C_{60} fullerenes (5.4×10^{-5} K^{-1}), as well as the distance between single-walled nanotubes in a bundle (4.2×10^{-5} K^{-1}). This result demonstrates a disordering of longitudinally oriented C_{70} molecules in peapods under heating. The measurements provide an estimate of 39 meV for the disordering phase transition energy.

Parameters characterizing the mutual arrangement of graphite surfaces in peapods are similar to those in other structures studied before. Thus, the distance between the graphite surface of a single-walled nanotube and that of a fullerene molecule encapsulated in a peapod is very close to a magnitude of 0.335 nm, which characterizes the interlayer distance in crystalline graphite and the distance between surfaces of adjacent fullerene molecules in a crystal fullerite. This follows from X-ray diffraction measurements and electron microscopy observations which were confirmed with calculations. Thus, one should mention Ref. [104] where the interaction energy of fullerene molecules of spherical or ellipsoidal structure with the inner walls of a carbon nanotube was calculated, using the known interaction potential for carbon atoms. In addition, the interaction energy of a single-walled nanotube with another nanotube of lesser diameter encapsulated in it has also been calculated. The computation is based on the summation of van der Waals interaction energies for C – C atoms. It has been shown that in all cases (inner CNT, spherical and ellipsoidal fullerenes) the optimal distance between the surface of the encapsulated molecule and the outer CNT is close to the relevant magnitude for graphite (0.335 nm), with the deviations not exceeding 0.005 nm. The smallest equilibrium distance between the adjacent surfaces is found in a spherical fullerene molecule, which is explicable in terms of inter-atomic interactions.

The fullerene molecules resided inside a carbon nanotube form a 1D periodical structure that can be considered as a 1D crystalline fullerene (fullerite). The intermolecular distance in such a structure is about 0.97 nm, which is approximately 3% less than that in a 3D fullerite crystal [104]. Such compression of a 1D crystal compared to a 3D one is caused by the interaction of fullerene C_{60} molecules with the inner wall of the nanotube, which, apparently, promotes some breaking of the spherical symmetry of the molecule.

Interesting features in filling nanotubes with fullerene molecules were found in Ref. [111] where two-layer, but not single-layer, nanotubes were studied. This was made possible by the development of the CVD method, which has opened the way to the production of two-layer nanotubes in macroscopic quantities. In such a structure, the inner and outer layers are always spaced 0.335 nm apart, independent of the outer diameter. This offers the possibility of studying the formation of the fullerite structure in two-layer nanotubes of various diameters. A sample of nanotubes with an inner diameter ranging between 1.0 and 2.6 nm was conditioned in a 5M solution of nitric acid for 2 h in order to open the nanotubes. This was followed by washing with distilled water and drying at 700 K for 40 min. Filling the nanotubes with C_{60} fullerenes was performed in a vacuum at a temperature of 500 – 800 K for 48 h. Depending on the filling temperature, the yield of endohedral structures ranged between 20 and 50%. Moreover, high-resolution transmission electron microscope observations point to a notable dependence of the degree of nanotube filling and the degree of ordering of encapsulated fullerene molecules on the filling temperature. Thus, at a filling temperature of about 500 K one can observe partially filled nanotubes with a rather low degree of ordering. At a filling temperature of about 800 K, the filling degree is close to 100%. In this case, the degree of ordering of fullerite crystals reaches its maximum.

As the observations imply, the character of filling a nanotube with fullerene molecules is determined by its inner diameter. Figure 8 presents various endohedral structures formed in filling two-layer CNTs. Thus, in the case of an inner diameter of less than 1.5 nm, fullerene C_{60} molecules form practically a homogeneous linear chain. As distinct from single-walled nanotubes, which can be filled with fullerene C_{60} molecules only if their diameter exceeds 1.25 nm, the threshold magnitude of the inner diameter for filling two-layer nanotubes is as low as 1.1 nm. This can be explained by the influence of the outer layer of two-layer nanotubes, which enhances the van der Waals attraction of a fullerene molecule to the inner wall of the nanotube. In the case of nanotubes with an inner diameter higher than 1.45 nm, C_{60} molecules are packed in a '*zigzag*' manner (Fig. 8a). The centers of the fullerene molecules are located in a common plane and form a saw-like line. A further increase in the inner diameter of a

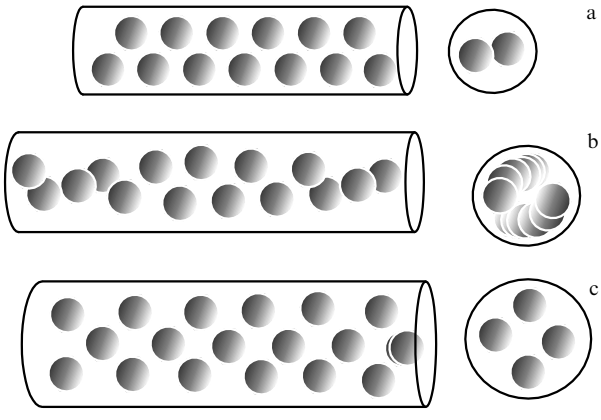

Figure 8. High-resolution transmission electron microscope images of the patterns of filling two-layer nanotubes of various diameters with fullerene C_{60} molecules [111]. (a) '*zigzag*' type arrangement; (b) screw structure, and (c) bimolecular structure.

nanotube gives rise to a more sophisticated inner structure of the fullerite crystal. Therewith, the position of the centers of the molecules is displaced in relation to the nanotube axis, so that they form a spiral structure inside the nanotube, the pitch of which depends on the inner diameter of a nanotube (Fig. 8b). Finally, nanotubes with inner diameter of about 2.6 nm and higher are able to house up to four fullerene molecules inside the transverse plane (Fig. 8c).

3.4.2 Transformation of a peapod into a two-layer nanotube. Filling single-walled nanotubes with fullerene molecules, resulting in the formation of peapods, usually occurs at an elevated temperature (typically about 500 °C). Therefore, it can be assumed that heating a peapod up to this or some higher temperature should result in the fullerene molecule evolution. However, in reality heating a peapod under vacuum conditions up to 800 °C or higher results in the joining of the encapsulated fullerene C_{60} molecules, which eventually finishes in the transformation of a 1D chain of these molecules into a single-walled nanotube of a smaller diameter [108 – 110]. In doing so, a single-walled nanotube intercalated with fullerenes transforms into a two-layer one. This follows from direct high-resolution electron microscope observations, as well as from the measured Raman spectra of samples. It is interesting to note that the interlayer distance in such a two-layer nanotube comprises 0.36 ± 0.03 nm, which is close to the magnitude of 0.335 nm inherent to multilayer graphite structures. Therewith, the above-indicated magnitude does not depend on an interrelation between the diameters of the initial nanotube and the fullerene molecule. Hence it follows that during the process of transforming a 1D chain of fullerenes into a nanotube the structure of the latter is rearranged in such a manner so as to provide the optimal interlayer spacing in the two-layer nanotube being formed.

The dynamics of the transformation of a peapod into a two-layer nanotube are studied in detail in Ref. [110] using high-resolution electron microscopy. Microphotos obtained show clearly that in the first stage of the transformation 2 – 3 fullerene molecules are joined into short nanotubes. These nanotubes have narrow spots connecting adjacent fullerene molecules. A further increase in the temperature or duration of conditioning the sample results in a smoothing of the narrow spots, so that short nanotubes resembling peanuts in shape are formed. Thereafter, these short nanotubes are joined into more elongated structures. The higher the temperature, the shorter the transformation time.

Along with electron microscopy, X-ray diffractometry is also an effective tool for studying the dynamics of the transformation of peapods into two-layer nanotubes [109]. The initial samples containing single-walled nanotubes bound into bundles were synthesized by the laser ablation method at an oven temperature of about 1500 K using Ni or Co as a catalyst. The transformation of the peapods occurred as a result of vacuum heating the samples at a temperature of 1523 K for 10 h. X-ray diffractometry of the samples revealed that the average degree of filling of the peapods amounted to about 80%. Defects (i.e., regions not filled with fullerene molecules) are therewith distributed in a random manner along the length of the nanotube. The transformation of the peapods results in lowering the filling degree down to 60 – 65%, which is explained in terms of keeping the distance between the inner and external nanotube walls at a level of 0.36 nm. An important distinctive feature of the peapod transformation phenomenon is that the transformation of peapods does not decompose bundles made up of nanotubes.

One more interesting feature of two-layer nanotubes formed as a result of the transformation of peapods is exhibited in Raman spectra of samples [106]. In these measurements, single-walled CNTs with a mean diameter of 1.39 ± 0.1 nm were used, being filled with fullerene C_{60} molecules up to a filling degree close to 100%. The transformation of peapods into two-layer nanotubes proceeded at a temperature of up to 1300 °C for 12 h. Raman spectra of the samples contain discriminable peaks corresponding to the radial breathing modes of inner and outer nanotubes. According to expression (3), the positions of these peaks uniquely determine the diameter of the relevant nanotube, and its width is related to the occurrence and number of defects of the nanotube surface structure. Raman spectra of two-layer nanotubes obtained in Ref. [106] are distinguished by an extraordinarily low width of resonances related to the radial breathing modes of inner nanotubes. Thus, the width of the resonance corresponding to the inner nanotube is about an order of magnitude lower than that for an isolated nanotube with the same diameter. This implies a very low content of defects in the inner nanotube.

3.4.3 Peapods filled with endohedral metallofullerenes. Besides peapods filled with fullerene molecules, nanotubes filled with *endohedral* fullerene molecules, i.e., fullerene molecules containing one or several atoms inside their cage, also present an interesting object for investigation. The structures formed are symbolized at times as $M_k@C_n@SWNT$. (Methods of synthesizing and exploring endohedral fullerenes, as well as their physical and chemical properties, are described in detail in Ref. [9].) Paper [102] is devoted to the synthesis and investigation of peapods formed as a result of filling single-walled nanotubes of about 1.4 nm in diameter with endohedral fullerene $La_2@C_{80}$ molecules. A sample of material synthesized by the electrical arc method and containing single-walled nanotubes of about one microgram in mass was purified by the acid treatment. Then, the sample was moistened with a drop of solution of $La_2@C_{80}$ in toluene or CS_2. After evaporation of the solvent, the sample was annealed in a vacuum of 10^{-7} Torr at a temperature of 700 K for 7 h, which was followed by thermal conditioning at 900 K for 10 h. This processing resulted in the filling of a large quantity of nanotubes with $La_2@C_{80}$ molecules. The filled single-walled nanotubes are easily visible with TEM, whereby one can see that La atoms are displaced in relation to the center of the fullerene molecule. Observations reveal that the nanotubes are filled with one of three known isomers of the fullerene C_{80} molecule, which is the C isomer having a symmetry D_{2h}, diameter 0.8 nm, and the structure close to a spherical one.

One of the important results obtained in the above-described experiment is a change in the internal structure of an endohedral molecule encapsulated in the nanotube cavity. Thus, the measured equilibrium distance between La atoms in the $La_2@C_{80}$ molecule encapsulated in a nanotube (0.47 nm in diameter) notably exceeds the relevant magnitude for an isolated $La_2@C_{80}$ molecule. This discrepancy is ascribed to the action of the nanotube, the diameter of which is somewhat less than that of the $La_2@C_{80}$ molecule plus the optimal gap (2×0.34 nm). Therefore, a fullerene molecule is acted on by a compressing force from a nanotube surface, which promotes a change in the electronic structure of the molecule and,

specifically, a change in the equilibrium distance between La atoms.

The parameters of a 1D crystal formed by filling a single-walled nanotube with endohedral fullerene molecules can differ notably from those of an isolated 3D crystal. Such a difference is explained qualitatively by taking into account the real behavior of the metal atom encapsulated in the fullerene molecule. Indeed, as follows from a large body of experimental and theoretical studies [9], the valence electrons belonging to the outer shell of such an atom are transferred fully or partly to the external surface of a fullerene molecule. Therefore, the atomic core enclosed inside the fullerene cage possesses a positive charge interacting with the charged fullerene surface and another core (if it exists). This interaction determines a specific localization of the atom inside the fullerene cage. The position of the atomic core is essentially displaced, as a rule, in relation to the center of the fullerene molecule. If the cage contains more than one atomic core, those being acted on by Coulomb repulsive forces are spaced apart by a considerable distance.

An off-center displacement of the position of a charged atomic core in an endohedral fullerene molecule brings about the existence of the appreciable electric dipole moment in such a molecule [9]. This promotes the formation of an ordered 1D crystal structure, where the elementary dipole moments of endohedral molecules are aligned in a similar manner, inside a nanotube filled with endohedral fullerene molecules. Such a structure was observed, in particular, in Ref. [103] devoted to the synthesis and investigation of $Gd@C_{82}$@SWNT peapods. Soot containing $Gd@C_{82}$ and other metallofullerenes was synthesized in a dc arc discharge (500 A, 21 V) in an He flow at a pressure of 55–65 Torr using as an anode rectangular graphite rods $15 \times 15 \times 300$ mm^3 in sizes with an admixture of powdered Gd (0.8 at.%). Fullerene molecules were extracted from the soot by the SOXHLET method for 60 h using CS_2 as a solvent, which was followed by the selection of $Gd@C_{82}$ molecules from the extract by repeated chromatographic separation. The resulting purity of the material reached 99.9%, which was confirmed by mass-spectrometry measurements. Single-walled CNTs bound into bundles 1.4–1.5 nm in diameter were produced by laser ablation of a graphite rod with an admixture of Fe/Ni catalyst (0.6–1.6 at.%). The nanotubes were then purified in flowing nitric acid at 160 °C for 8 h and annealed in dry air at 700 K for 20 min, which was necessary for their opening.

The nanotubes were filled with metallofullerene molecules in a sealed-off glass ampoule at 500 °C for 24 h. TEM observations revealed the resulting degree of filling of the nanotubes with metallofullerene molecules exceeding 60%. After holding for 100 h, the filling degree approached 100%. TEM images of the filled nanotubes evidence an off-center displacement of the Gd atom inside the C_{82} molecule. Observing the position of a Gd atom inside a fullerene molecule points to its fixed location in the molecule even at room temperature. Observations show the mean distance between $Gd@C_{82}$ molecules inside a nanotube to be 1.10 ± 0.03 nm, which is somewhat less than the relevant magnitude for the 3D molecular crystal $Sc@C_{82}$ (1.124 nm). A decrease in the intermolecular distance in a 1D crystal vs. that in a 3D one can be caused by the transfer of a part of the electronic charge of the metal atom from the outer surface of the fullerene molecule to the external surface of the CNT. The temperature dependences of the electrical resistance R of thin films $Gd@C_{82}$@SWNT, C_{60}@SWNT, and empty nanotubes

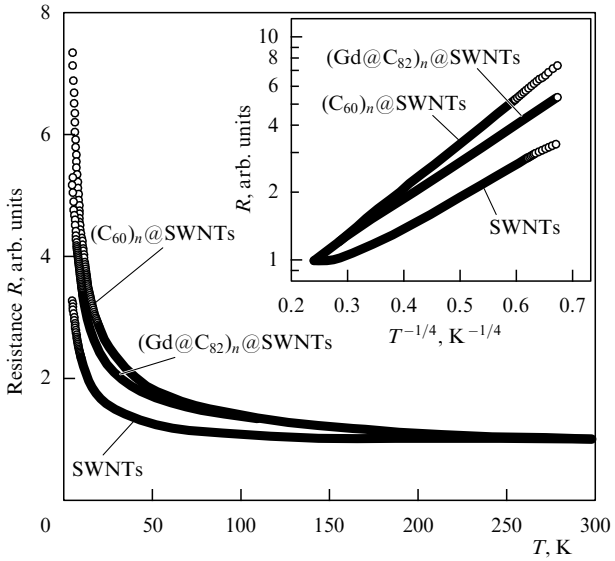

Figure 9. Relative temperature dependences of electrical resistance of films of nonfilled single-walled nanotubes (SWNT), nanotubes filled with fullerene C_{60} molecules, and endohedral fullerene $Gd@C_{82}$ molecules [103]. The same dependences drawn in the semilogarithmic scale as a function of $T^{-1/4}$ are shown in the inset to the figure.

were measured in Ref. [103] through the four-probe method. The measured results are presented in Fig. 9. The linear shape of the dependences expressed at the semilogarithmic scale as a function of $T^{-1/4}$ implies a hopping mechanism of conductivity. The difference in dependences for various samples indicates the important role of the process of electron scattering from encapsulated fullerene molecules.

Alignment of endohedral $La@C_{82}$ and $Gd@C_{82}$ fullerenes enclosed in a single-walled nanotube was also studied in Ref. [105] through a high-resolution electron microscopy. Off-center displacement of atoms encapsulated inside the fullerene cage is clearly discernible on microphotos of isolated peapods obtained at atomic resolution using computer processing. In this case, the predominantly longitudinal (along the nanotube axis) orientation of dipole moments of endohedral molecules is observed.

The extraordinary electronic properties of peapods filled with endohedral fullerenes relate to the above-mentioned phenomenon of the charge transfer from valence electrons belonging to an atom enclosed inside the cage of an endohedral molecule onto its external surface, as well as onto the surface of the nanotube. In particular, this follows from the temperature dependences of electrical conductivity of the $Dy@C_{82}$@SWNT peapod measured in Ref. [107]. The initial sample containing single-walled CNTs 3–6 μm in length was synthesized by the standard electrical arc method and purified in the conventional manner using hydrochloric acid at an elevated temperature. The nanotubes were filled with endohedral fullerene $Dy@C_{82}$ molecules in a deep vacuum at a temperature of 500 °C for 2 days. The samples obtained were ultrasonicated in order to separate individual peapods. This resulted in shortening the nanotubes down to 0.5–2 μm. The electrical conductivity of individual peapods was measured using the standard two-probe method at a distance of 150 nm between electrodes. The measurement data obtained at various temperatures imply a rather complicated electronic structure of peapods containing

endohedral fullerene molecules. This relates to the above-mentioned phenomenon of transfer of valence electrons from the encapsulated atom to the external surfaces of the fullerene and nanotube. At some temperature, whose magnitude depends on both the nanotube diameter and the filling degree, the conductivity was changed from type p to n. The quantity of the charge transferred depends on the temperature, the interrelation between the diameter of the fullerene molecule and the nanotube, as well as the filling degree; therefore, the magnitude of the critical temperature was changed from one sample to another.

4. Filling carbon nanostructures with gaseous substances

4.1 Molecular hydrogen

4.1.1 The hydrogen storage problem. Carbon nanotubes having extraordinarily high porosity are considered a prospective material for resolving the problem of storing and transporting gaseous hydrogen. This problem arises in connection with the necessity of developing ecologically clean motor transport. Using molecular hydrogen as a fuel in car engines allows practically complete elimination of pollution of the environment with harmful contaminations, since the only by-product of the hydrogen oxidation is water vapor. Therewith, it is assumed that the problem of producing hydrogen from water or natural gas can be resolved, in particular, by using nuclear power during a period of reduced loading. However, this is accompanied by problems related to the safe reversible storage and compact transportation of gaseous hydrogen, the effective solution of which will determine whether ecologically safe motor transport can be developed.

The possibility of using carbon nanostructures for storing hydrogen and other gases arises due to many circumstances. First, the objects under consideration have a mere surface structure. Allowing their consideration as the most appropriate object for filling with a gaseous substance through physical sorption. Thereby, the quantity of the adsorbed substance is proportional not to the volume but to the surface of the structure under consideration, and the highest sorption ability is inherent to those structures with the maximum specific surface. Second, carbon nanostructures possess generally good electrical conductivity, which in combination with high specific surface permits their use as the basis of electrochemical devices. In this case, the material is filled with a gaseous substance as the result of proceeding a surface electrochemical reaction. Finally, one should note that such carbon nanostructures as nanotubes, nanospheres, and nanofibers possess internal cavities which, under the proper conditions, can be filled in a reversible manner with a gaseous substance. Here, it is not only surface sorption that occurs but also volumetric filling of the cavity, so that the degree of filling the material with a gaseous substance can, generally speaking, considerably exceed that reached in the case of surface physical sorption.

4.1.2 Promising results of the first experiments. Interest in the usage of carbon nanostructures for hydrogen storage has particularly risen in the past few years as a result of the appearance of a set of experimental publications communicating on a high degree of filling of carbon nanostructures with molecular hydrogen. Thus, the widely known publication by Dillon et al. [112] reports on filling single-walled CNTs of about 1.2 nm in diameter, synthesized with the use of a Co catalyst, with molecular hydrogen. The nanotubes were bound into bundles consisting of 7 – 14 nanotubes. The surface of the nanotubes was decorated with amorphous carbon particles and Co nanoparticles enclosed in a graphite envelope and ranging between 5 and 50 nm in diameter. The content of Co is estimated as 20 wt.%. Filling the nanotubes and, for comparison, activated charcoal with hydrogen was studied with programmed thermal desorption spectroscopy. A sample was filled with hydrogen at room temperature and a hydrogen pressure of 0.5 bar for 10 min. The chamber containing the sample was cooled down to 130 K and pumped out, followed by further cooling down to 90 K. Then, the sample was heated at the rate of 1 K s^{-1}, and the desorbed hydrogen was detected by a mass spectrometer (thermal desorption spectroscopy). Results of the thermal desorption analysis are displayed in Fig. 10. The peak of the desorption intensity, observed at 150 K (curves *1*, *2* in Fig. 10a), corresponds to the hydrogen sorption on a porous surface of amorphous carbon which occurs in both raw nanotubes (*1*) and activated charcoal (*2*). Vacuum heating of the sample containing the nanotubes up to 970 K, followed by its filling with hydrogen, results in the appearance of an additional peak in the desorption curve (*3*) at 288 K. This peak relates to sections of the surface of the sample with an enhanced binding energy, which are attributed to the surface of single-walled nanotubes. The position T_m of this peak is displaced as the coverage of the surface increases (Fig. 10b), which depends on the hydrogen pressure and interrelates to the rate of desorption β. A linear character of the dependence $\ln(T_m^2/\beta)$ vs. $1/T_m$ (Fig. 10c) points to the first-order desorption mechanism and provides the magnitude of the activation energy for desorption, $E_d = 0.2$ eV. It should be noted that the high-temperature desorption peak (about 300 K) is not observable for samples of activated charcoal, pure polycrystalline cobalt, or multiwalled nanotubes produced in an arc discharge without the use of catalysts. The quantity of hydrogen adsorbed was measured as 0.01 wt.%. However, since the sample under investigation contained only a handful of single-walled CNTs (0.1 – 0.2 wt.%), the quantity of hydrogen absorbed by the nanotubes was estimated taking into account this content as 5 – 10 wt.%.

Publication of the above-cited work [112] has stimulated a real boom in studies of sorption properties of CNTs with respect to molecular hydrogen. The first results of these studies have already shown even higher sorption abilities of nanotubes. Thus, one can note Ref. [113], the authors of which elaborated a method for opening nanotubes, aiming to enhance the hydrogen sorption ability of single-walled CNTs. This method consists of oxidation of a sample preliminarily degassed in a vacuum at 970 K. Water vapor heated up to 375 – 975 K was used as an oxidizer. It has been stated that opening the nanotubes results in about a threefold enhancement of the standard desorption peak within the temperature range 250 – 300 K. The quantity of adsorbed hydrogen, taking into account the real content of CNTs in the sample (0.05%), is estimated as 10 wt.%.

Equally promising results have been obtained in work [114] performed with the participation of R Smalley, the Nobel Prize Laureate in Chemistry 1996. As distinct from the above-cited works [112, 113], the authors of Ref. [114] used a sample with a relatively high content of CNTs. For this reason, their conclusions are not based on the recalculation of

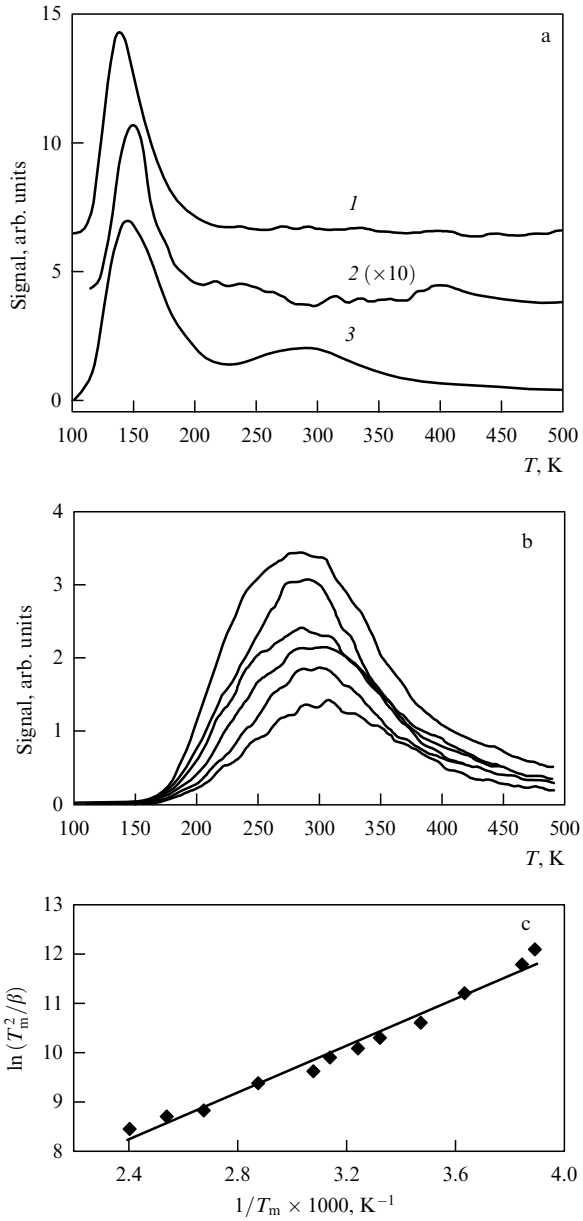

Figure 10. Sorption ability of single-walled nanotubes measured through temperature-programmed thermal desorption [112]: (a) *1* — thermal desorption spectrum of the raw sample of single-walled CNTs conditioned in the standard manner in a hydrogen atmosphere; *2* — thermal desorption spectrum of activated charcoal (tenfold magnification), and *3* — thermal desorption spectrum of the raw sample of single-walled CNTs heated in a vacuum up to $T = 970$ K before filling with hydrogen; (b) thermal desorption spectra of samples conditioned in a hydrogen atmosphere at $T = 273$ K for 10 min; the curves were drawn at various initial hydrogen pressures ranging between 25 and 300 Torr and relating to the coverage of the surface from 0.3 to 1, and (c) the dependence $\ln(T_m^2/\beta)$ vs. $1/T_m$ measured at various rates β of heating of a sample (T_m is the temperature corresponding to the maximum in the desorption rate). The rectilinear shape of the dependence demonstrates the physical sorption and provides the magnitude of desorption activation energy as $E_d = 19.6$ kJ mol^{-1} (about 0.2 eV).

the sorptive capacity of the material, taking into account the low content of CNTs in the sample, and therefore are not so conventional. The material containing single-walled nanotubes bound into bundles was produced by the laser ablation method. A 0.2 g sample of this material was inserted into dimethylformamide (0.1 g ml^{-1}) where it was ultrasonicated for 10 h until suspension formed. This promoted loosening of the bundles and probably the opening of the nanotubes. The material was then extracted by the vacuum filtration method using a ceramic filter. Transmission electron microscope observations revealed single-walled nanotubes of about 1.3 nm in diameter, bound into bundles 6–12 nm in diameter. After vacuum pumping out at 220 °C for 10 h, the sample was exposed to hydrogen for 15 h at $T = 300$ K and a pressure of 160 bar, and at $T = 80$ K and pressures of 130, 70, 4.5, or 0.5 bar. The specific surface of a sample of raw material, measured using nitrogen, amounted to 285 ± 5 m^2 g^{-1}. This magnitude is much lower than that for an individual nanotube (1300 m^2 g^{-1}), which is caused by the existence of the bundles. The content of hydrogen in single-walled nanotube bundles with a specific surface of 285 m^2 g^{-1} has been compared to that in porous carbon (saran) which is formed in the pyrolysis of polyvinylchloride and has a specific surface of 1600 m^2 g^{-1}. Figure 11 presents the dependences of the equilibrium content of carbon materials on the hydrogen pressure, measured by the volumetric method at $T = 80$ K. The ratio H/C was measured at 80 K and 3.2 bar as 0.040 and 0.28, respectively. The ratio of these quantities (1 : 7) is close to the ratio of the specific surfaces of carbon materials (1 : 5.6). A similar relationship was also observed under different measurement conditions. Processing the temperature dependences of a quantity of adsorbed hydrogen for the saran material provides the sorption energy of a hydrogen molecule on a surface as 38 meV (3.7 kJ mol^{-1}). As is seen from the data presented in Fig. 11, for raw samples of single-walled CNTs the filling degree of 8.25 wt.%, corresponding to the ratio H/C $\sim$ 1, was reached in the first trial at a pressure of 70 bar and $T = 80$ K. For the CNT sample subjected to treatment, this filling degree is reached at a pressure of 110 bar. In subsequent runs, the filling degree was lowered

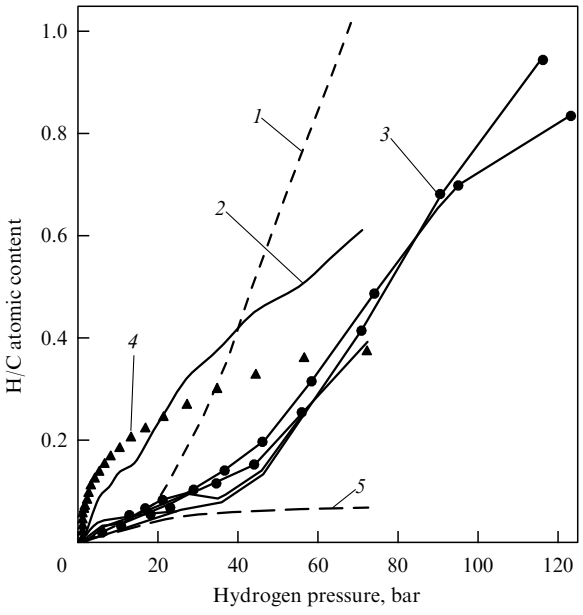

Figure 11. Relative amount of absorbed hydrogen measured in Ref. [114] as a function of the hydrogen pressure at $T = 80$ K for the (*1*) raw material containing single-walled nanotubes; (*2*) material subjected to the ultrasonication in dimethylformamide; (*3*) material noted in connection with curve (*2*) after repeated hydrogen filling and extraction cycles; (*4*) highly porous carbon material 'saran' having high specific surface, and (5) 'saran' material corrected by taking into account the ratio 3/16 of specific surfaces.

by about half. Processing the data obtained provides the magnitude of the energy of cohesion between nanotubes as 5 meV/C. This value is notably lower than those obtained in Ref. [115] (the cohesion energy is estimated as 17 meV/C) and Ref. [116] (35 meV/C). The origin of such a disagreement can be related to the absence of ordering in the arrangement of nanotubes, for which reason the contact area is much less than the area of the nanotube surface.

An even higher hydrogen sorption ability for nanotubes was observed in Ref. [117], where multiwalled nanotubes doped with Li and K were studied. Samples of multiwalled nanotubes ranging from 25 to 35 nm in diameter were produced as a result of thermal catalytic decomposition of CH_4. After purification by standard methods, the purity of the material reached 90%. The nanotubes had a conical structure. They were doped with Li and K using reactions with carbonates and nitrates of lithium and potassium. For the comparison, there had been prepared, using the same method, samples of powdered graphite 50 μm in average diameter, doped with Li and K. The specific surface of CNTs and graphite was measured as 130 and 8.6 $m^2\,g^{-1}$, respectively. The ratios Li : C and K : C in the nanotubes were measured by X-ray photoelectron spectroscopy and comprised about 1 : 15. The density of the sample of CNTs doped with Li was 0.9 g cm^{-3}, while that for graphite doped with Li amounted to 2 g cm^{-3}. The quantity of hydrogen adsorbed was measured by the thermal gravimetric analysis (TGA) procedure using hydrogen as a cleaning gas. The results obtained were verified by the thermal desorption method with a programmed rise in temperature (TPD).

The samples prepared for the experiments on hydrogen filling were conditioned in flowing purified hydrogen at 873 K for 1 h. The samples doped with Li were then cooled down to 300 K and heated again up to 873 K at the rate of 5 K min^{-1}. The hydrogen absorption started at 773 K and terminated at 423 K. The thermal gravimetry curves are shown in Fig. 12. As can be seen, for the sample doped with Li, the maximum hydrogen content (14.5 wt.%) is observed at $T = 673$, when the temperature is rising. Conditioning this sample at $T = 653$ K and the atmospheric pressure of hydrogen for 2 h resulted in the enhancement of the hydrogen content up to 20 wt.%. The samples doped with K were cooled from $T = 873$ K down to room temperature and conditioned under flowing hydrogen for 2 h. Then they were heated again up to 773 K at the rate of 5 K min^{-1}, which resulted in a slow rise in their mass. Subsequent conditioning of the samples at room temperature under flowing hydrogen for 2 h resulted in establishing the equilibrium (saturated) hydrogen content (14 wt.%). Exceeding room temperature promoted the desorption of the adsorbed hydrogen, the maximum intensity of which was observed between 300 and 423 K.

Similar results were obtained when filling graphite (doped with Li and K) with hydrogen. However, the filling degree for doped graphite amounted to 35 – 70% of that for CNTs. The filling degree for nondoped nanotubes does not exceed 0.4 wt.%. Spectral measurements indicate occurrence of the absorption band near the energy 1420 cm^{-1} in the conditions when the sample is saturated with hydrogen. This band matches the energy of the Li – H vibration quantum. Moreover, a week band within the range 2600 – 3350 cm^{-1}, corresponding to the C – H vibration, has also been observed. This band disappears upon heating the sample, which promotes hydrogen desorption. The above-described spectroscopic data point to the mechanism of dissociative

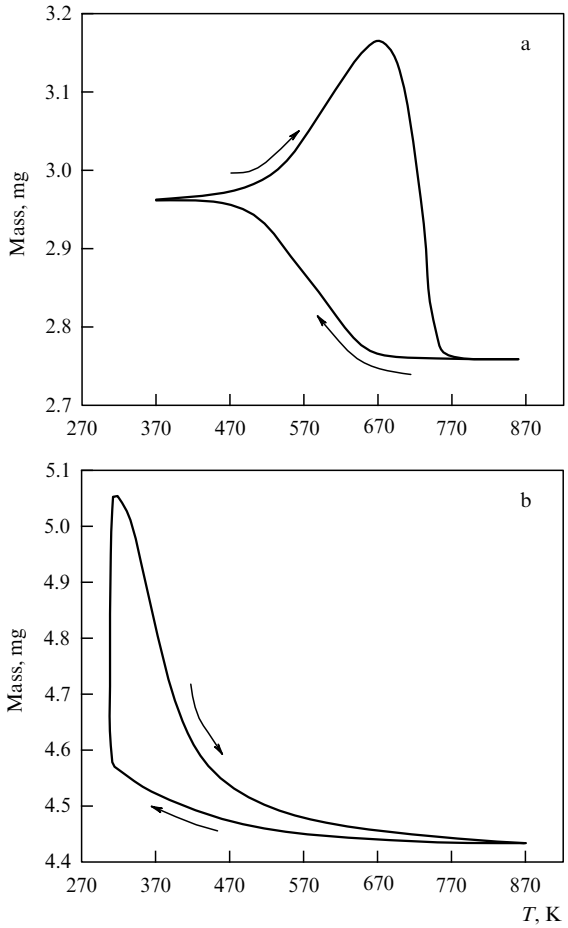

Figure 12. Thermogravimetric analysis curves characterizing reversible hydrogen sorption by samples containing multiwalled nanotubes doped with lithium (a) and potassium (b) [117]. The sample doped with Li was cooled down to 300 K, whereupon it was heated again up to 873 K; the sample doped with K was conditioned at room temperature for 2 h, whereupon it was heated up to 773 K.

hydrogenization of nanotubes and graphite. Since the 1420 cm^{-1} absorption band relating to the Li – H bond does not practically depend on the temperature, while the C – H-induced band within the range 2600 – 3350 cm^{-1} exists only at a high quantity of adsorbed hydrogen, it can be assumed that lithium atoms serve as a catalyst in the process of dissociative hydrogen sorption. It was shown that the doped samples can stand up to 20 sorption – desorption cycles with a loss in sorptive capacity of no more than 10%.

However, the conclusions of the above-cited work [117] were questioned in subsequent publications [118], whose authors have pointed to a role played by the degree of purity of examined hydrogen with respect to water vapor. Thus, in accordance with measurements [118], results [117] are reproducible only using wet hydrogen, while with dry hydrogen the filling degree amounts to as little as 1.8% (Li) and 2.5% (K).

Quite a high level of sorption ability was also observed in Ref. [119], the authors of which used as a sample a massif of spatially oriented multiwalled CNTs of diameter 50 – 100 nm and a surface density of $10^8 - 10^9$ mm^{-2}. The nanotubes were grown by plasma chemical deposition using methane as a carbon-containing substance on a stainless steel substrate 0.1 mm in thickness and 10×10 mm^2 in area. After 20 min of growth, the nanotube length reached 10 μm. After weighing

(with an accuracy of 0.01 mg), a sample containing the substrate coated with carbon nanotubes was inserted into a chamber designed for studying hydrogen filling. Then the sample was conditioned in hydrogen at a pressure ranging between 2 and 10 atm and a temperature increasing from room level up to 500 °C, which was followed by repeated weighing in order to determine the gain in weight. The release of hydrogen from the sample under heating was monitored using the thermal gravimetric analysis procedure, as well as a quadrupolar mass spectrometer. During the TGA procedure, the sample was heated from room temperature up to 300 °C at the rate of 5 °C min^{-1}. The measurements indicate a nonlinear dependence of the quantity of adsorbed hydrogen on the hydrogen pressure in the chamber. Thus, at a hydrogen pressure of 2 atm, the hydrogen adsorption was not observed even after conditioning for 24 h. Conditioning at a hydrogen pressure of 10 atm for 2 h resulted in a mass gain in the samples amounting to 5–7%. A notable enhancement in the sorption ability of CNTs for hydrogen was observed after treating the samples in 69% nitric acid for 3 min, followed by their washing in distilled water for 24 h. This effect is seemingly related to removing the catalyst particles from opened nanotube caps, which facilitates the hydrogen access into the nanotubes. The samples of nanotubes treated in such a manner increased in mass from 8.8 up to 13.8% due to hydrogen adsorption at room temperature at a pressure of 10 atm. Heating the samples filled with hydrogen up to a temperature of 300 °C in a vacuum of 10^{-6} Torr caused desorption of the hydrogen adsorbate, the rate of which increased with the temperature. The total quantity of hydrogen released due to vacuum heating of the sample did not exceed 80% of the mass of hydrogen adsorbate.

A record level of the degree of filling a graphite structure with hydrogen was observed in Ref. [120] (see also Refs [121–123]), where carbon nanofibers of the herring-bone type were used as an adsorbent. A typical structure of the nanofibers is illustrated in Fig. 13. In such a structure, the distance between plates comprises 0.337 nm, which is inherent to crystalline graphite and slightly exceeds the gas-kinetic size (0.29 nm) of the H_2 molecule. The material containing nanofibers was produced through the thermal catalytic decomposition of diverse hydrocarbons using variously sorted metal catalysts. This approach allows one to obtain fibers with various orientations of graphite planes about the fiber axis, depending on the conditions of synthesis and the sort of catalyst used. Longitudinal, transverse, and angular orientations correspond to the tubular, lamellar, and conical structures. The last is also called 'herring-bone'. Filling a sample of the material of about 0.2 g in mass with hydrogen was performed at room temperature and a hydrogen pressure up to 112 atm for 24 h in a steel chamber 22.66 ml in volume, the latter being connected to a high-pressure hydrogen chamber 75.31 ml in volume. The quantity of adsorbed hydrogen was determined by a decrease in the gas pressure inside the camera. A decrease in the hydrogen pressure down to normal promoted desorption of hydrogen from the samples, which was determined by the volume of the water being expelled. The desorption time was not longer than 10 min. It has been possible to extract the rest of the hydrogen adsorbate at an elevated temperature. For comparison, the quantity of hydrogen adsorbed by other adsorbents have been measured. The results of measurements are compiled in Table 3. The measured quantity of desorbed hydrogen is shown in parentheses. A difference between the masses of absorbed and desorbed hydrogen implies some contribution of the chemisorption to the absorption mechanism. It should be emphasized that the authors of experiment [120], the results of which have been reflected in Table 3, do not specify the sort of activated charcoal used. Since a large number of the activated charcoal types, which differ from one another in the porosity and in admixtures adsorbed on the surface of pores, are known, the values presented in the table have a rather qualitative, speculative character.

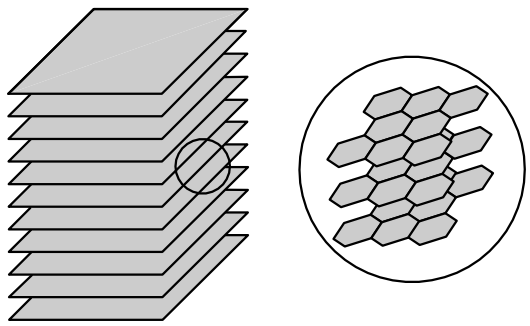

Figure 13. A schematic of the structure of graphite nanofibers produced as a result of thermocatalytic decomposition of gaseous hydrocarbons in the presence of metal catalysts [120]. The right picture presents an enlarged image of the region noted.

Table 3. Results of measurements of the sorptive capacity of various materials [120].

Sample	Mass, g	Quantity of adsorbed (desorbed) H_2, $l\,g^{-1}$	Quantity of adsorbed (desorbed) H_2, wt.%
Pd	0.223	0.24 (0.15)	2.07 (0.66)
$LaNi_5$	1.058	0.05 (0.03)	0.44 (0.13)
$MnNi_{4.5}Al_{0.5}$	0.742	0.38 (0.28)	3.33 (1.27)
Activated charcoal	0.898	0.18	1.63
Graphite	0.243	0.53	4.52
Nanofibers of tubular structure	0.121	1.42	11.3
Nanofibers of 'herring-bone' type	0.319	13.4	62±4.2
Nanofibers of lamellar structure	0.103	12.98	53.7±4

As can be seen, the experiment being considered demonstrates an extraordinarily high hydrogen sorptive capacity of carbon nanostructures. The samples containing nanofibers with a herring-bone structure can absorb more than 60 wt.% of hydrogen, so that about 2/3 of the hydrogen absorbate can be extracted in a reversible manner. Unfortunately, the above-described experimental results have not been confirmed in subsequent studies.

4.1.3 Analysis of sorption properties of carbon structures. An above short review of publications indicates a high hydrogen sorption ability of carbon nanostructures of various nature. However, the available experimental data in the field are characterized by a rather large scatter. Some of the above-cited publications were questioned critically in subsequent works [124–129]. Hence follows the necessity to analyze the limiting sorption characteristics of carbon nanostructures on the basis of the most general approach, independently of the

detailed peculiarities of a specific experiment. An attempt at such an approach is presented below.

Estimations of the hydrogen sorptive capacity of nanotubes are based on the concept of the physical sorption of molecules by a surface of carbon nanostructures. Only this kind of sorption provides the extraction of hydrogen absorbate at a reasonable temperature elevation. In doing so, as follows from numerous experimental results, the interaction energy of hydrogen molecules with a graphite surface does not exceed tenths of an electron-volt, which is much less than both the dissociation energy of the hydrogen molecule and the binding energy of carbon atoms in a nanotube. Therefore, one can hardly expect that the physical sorption of hydrogen molecules by the surface of a nanotube will result in a notable change in the molecular structure of each of these objects. For this reason, in estimating the limiting sorption characteristics of carbon nanostructures, the maximum reachable values of the surface and volumetric masses of hydrogen were set to those for liquid hydrogen. Such an approach can be applied equally to estimating the limiting sorption ability of any nanostructure, taking into account its real density and porosity.

First of all, we must estimate the limiting hydrogen sorption ability of a graphite layer on the assumption that the graphite surface is coated with a monomolecular hydrogen layer. In doing so, it would appear reasonable that the maximum surface density of hydrogen in the monolayer, $\sigma_H = 2.56 \times 10^{-9}$ g cm^{-2}, corresponds to the liquid hydrogen density $\rho_H \approx 0.07$ g cm^{-3}. These assumptions lead to the following expression for the maximum sorptive capacity of a graphite surface:

$$\eta_H = \frac{\sigma_H}{\sigma_C + \sigma_H} \approx 3.2 \text{ wt.\%}, \tag{9}$$

where the above-estimated relation (4) for the surface density of a plane graphite structure, $\sigma_C = 0.77 \times 10^{-7}$ g cm^{-2}, has been used. In the case of two-sided coating of a graphite surface with hydrogen monolayers, the maximum sorption ability reaches the doubled magnitude, $\eta_H \approx 6.4$ wt.%. However, it is well to bear in mind that the mean distance between neighboring layers in crystalline graphite (0.34 nm) is comparable to the gas-kinetic size of the hydrogen molecule (about 0.3 nm). For this reason, one can hardly expect a two-sided coverage of all the surfaces of such a structure with hydrogen monolayers, which cannot be placed between graphite layers. Therefore, the analysis performed implies that it is doubtful that the physical sorption of hydrogen by carbon surface structures would provide a hydrogen storage capacity notably exceeding 3 wt.%.

Now consider the possibility of volumetric filling of a surface carbon structure with molecular hydrogen. In doing so, we should distinguish two types of such a structure, one being an inner cavity bounded by a graphite surface, and the other a multilayer system consisting of graphite surfaces. The most appropriate example of the structure of the first type is a single-walled carbon nanotube. The density of such a structure is expressed by the relation

$$\rho_t = \frac{4\sigma_C}{D} = \frac{30.4}{D} \text{ (g cm}^{-3}\text{)}, \tag{10}$$

where D is the diameter of the nanotube in units of 10^{-8} cm. Assuming as before that the maximum reachable density of hydrogen filling the cavity of the nanotube corresponds to that of liquid hydrogen, $\rho_H \approx 0.07$ g cm^{-3}, we arrive at the following expression for the maximum degree of filling of a single-walled nanotube with molecular hydrogen:

$$\eta_H = \frac{\rho_H}{\rho_H + \rho_t} \approx \frac{0.07}{0.07 + 30.4/D}. \tag{11}$$

As can be seen, the filling degree of single-walled nanotubes rises with their diameter. In synthesizing single-walled nanotubes by methods based on thermal catalytic decomposition of crystalline graphite under the action of an electrical arc discharge or laser irradiation, mainly nanotubes from 1.2 to 1.5 nm in diameter are formed [8–13]. This means, in accordance with relation (11), that the maximum degree of filling of such structures with hydrogen, η_H, ranges within 2.7–3.4 wt.%. The filling degree $\eta_H = 6.5$ wt.%, which is sufficient for applications of carbon nanotubes as the basis of hydrogen storage devices, is reached by using nanotubes no less than 3 nm in diameter.

Now consider a multilayer nanotube consisting of n layers ($n \gg 1$), with the standard interlayer spacing $d \approx 0.335$ nm. The outer diameter of such a nanotube is expressed by the equation $D = D_0 + 2d(n-1)$, where D_0 is the diameter of the smallest inner tube. The density of such a multilayer nanotube is given by the relation

$$\rho_C = \frac{4n\sigma_C\left[D_0 + d(n-1)\right]}{\left[D_0 + 2(n-1)d\right]^2}, \tag{12}$$

which is reduced to that for an ideal graphite structure, $\rho_g = \sigma_C/d \approx 2.3$ g cm^{-3}, as $n \gg 1$. The maximum reachable mass content of hydrogen in such a structure, in accordance with relation (11), is equal to

$$\eta_H \approx 3 \text{ wt.\%}.$$

A modification of the multiwalled nanotube, where several inner layers are absent, deserves attention. It should be emphasized that such structures are sometimes observable in synthesis by using the chemical vapor deposition method [8]. The average density of such a 'defective' nanotube can turn out to be much lower than that in the case of the ideal structure. In accordance with relation (11), this gives rise to higher hydrogen sorption ability. Thus, if a multilayer nanotube consists of interstratified lacking and existing layers, the interlayer distance d in expression (12) comprises 0.67 nm but not 0.335 nm, which results in a density of such a nanotube, $\rho_C \approx 1.13$ g cm^{-3}, in the limiting case of $n \gg 1$. This is followed by the estimation of the sorption ability of such a defective nanotube: $\eta_H \approx 5.8$ wt.%, in accordance with equation (11). Generally speaking, the sorption ability of a defective multilayer nanotube depends on the number of lacking layers, their position inside the nanotube, and the overall size of the nanotube.

One more closed carbon structure that can be filled with molecular hydrogen constitutes a nanosphere made from a graphite surface [130]. Such nanostructures with diameters of several nm are produced, in particular, using plasma-assisted chemical vapor deposition with iron nanoparticles as a catalyst. Applying a similar approach, one obtains the estimate of the maximum hydrogen filling degree of a nanosphere with radius R:

$$\eta_H = \frac{\rho_H/3}{\rho_H/3 + \sigma_C/R}. \tag{13}$$

This expression implies that the liquid hydrogen filling degree of $\eta_H = 6.5$ wt.% is reached for a carbon nanosphere with a radius of not less than 2.3 nm.

Let us analyze one more approach to the problem of filling carbon nanostructures with molecular hydrogen. Considering a nanostructure as a porous media containing a large number of inner cavities (pores) accessible for the filling gas, one can estimate its sorption ability on the basis of the following speculative model. Suppose that a structure under consideration is immersed in liquid hydrogen that fills all the volume of the structure. Obviously, such a consideration provides an upper limiting estimate for the maximum sorption ability of the structure at hand. This estimate has the following form

$$\eta_H = \frac{\rho_H}{\rho_H + \rho_C} . \qquad (14)$$

Here, ρ_C is the density of the carbon structure under consideration. In the case of crystalline graphite one has $\rho_C \approx 2.25$ g cm^{-3}, so that inserting into formula (14) the magnitude $\rho_H = 0.07$ g cm^{-3}, corresponding to the density of liquid hydrogen, one finds $\eta_H \approx 0.03$ wt.%. This conclusion is in agreement with the above estimate (9) for the sorption ability of a graphite layer for hydrogen monomolecular coverage. As evidenced by the foregoing, a large difference in the densities of graphite structures and liquid hydrogen makes the possibility of obtaining a filling degree notably exceeding 3 wt.% rather problematic.

A similar estimation of the maximum filling degree for a bundle consisting of single-walled carbon nanotubes (Fig. 2) provides a more optimistic conclusion. This is caused by the lower density of such a material as compared to crystalline graphite. Such a bundle can be considered a specific modification of a carbon nanostructure. The density of a bundle made up of identical nanotubes of diameter D, spaced apart by a distance d, is expressed by the relation

$$\rho_C = \sigma_C \frac{2\pi D}{\sqrt{3}(d+D)^2} = 2.76 \times 10^{-7} \frac{D}{(d+D)^2} \ (\text{g cm}^{-3}) . \qquad (15)$$

The sorptive capacity of such a bundle is estimated through Eqn (14) taking into account Eqn (15):

$$\eta_H = \frac{\rho_H}{\rho_H + \rho_C} = \frac{\rho_H}{\rho_H + 2.76 \times 10^{-7} D/(d+D)^2} . \qquad (16)$$

This expression reaches its minimum at $D = d$, which is equal to

$$(\eta_H)_{min} = \frac{0.07}{0.07 + (0.69 \times 10^{-7})/d} . \qquad (17)$$

Equating the spacing between the surfaces of neighboring nanotubes in a bundle to the magnitude of $d = 0.335$ nm, which is inherent to multilayer graphite-like structures, we obtain from formula (17): $(\eta_H)_{min} \approx 3.3$ wt.%. It is pertinent to note that the smallest nanotube diameter observed amounts to about 0.35 nm [38], and the typical magnitude of this parameter ranges between 1.2 and 1.5 nm. Therefore, in accordance with expression (16), the sorption ability of a bundle of single-walled CNTs rises with their diameter (at a fixed spacing between the nanotubes in the bundle).

Table 4. The maximum hydrogen content in a bundle of single-walled nanotubes, determined on the basis of equation (16) for various nanotube diameters. The distance between the surfaces of neighboring nanotubes is $d = 0.335$ nm.

D, nm	0.4	0.6	0.8	1	1.5	2	3	4	5	6	8	10
η_H, %	3.3	3.56	3.9	4.4	5.4	6,5	8.6	10.6	12.6	14.5	18	21.3

Table 4 presents the dependence of the sorption ability of a bundle of single-walled nanotubes on their diameter, calculated on the basis of equation (16). In accordance with this dependence, the sorption ability of a bundle consisting of nanotubes 1–1.5 nm in diameter ranges within $\eta_H = 4.4–5.4$ wt.%. In the case of a bundle consisting of nanotubes 1.36 nm in diameter with the chirality indices (10, 10), which typically predominate in a material produced by thermal catalytic methods, the sorption ability reaches 5.2 wt.%. The sorption ability of $\eta_H = 6.5$ wt.% is gained in the case of a bundle consisting of nanotubes 2.1 nm in diameter.

Therefore, the above-made analysis implies that filling single-walled nanotubes synthesized by standard methods is hardly an effective way to solve the hydrogen storage problem. Therewith, filling not only nanotubes but also hollow intertube space does not provide any perceptible advantages either.

Results of the above analysis demonstrate that the main factor limiting the hydrogen-sorption ability of carbon nanostructures relates to the large difference (as much as about 30 times) in the densities of these structures and liquid hydrogen. Due to this difference, the maximum degree of filling of graphite structures with liquid hydrogen is about 3 wt.%. This conclusion has cast some doubt on the results of the above-cited publications [113, 114, 119, 120, etc.] reporting on observations of much higher sorption ability with respect to gaseous hydrogen, the density of which is dozens of times lower than that of liquid hydrogen. Nevertheless, the results mentioned require a comprehensive and noncontradictory explanation, which unfortunately is lacking at the moment. One such explanation [131] is based on a hypothesis according to which hydrogen absorbed between graphite planes comprises a metastable metal-like structure. In support of this hypothesis, the authors of Ref. [131] refer to paper [132], where an abnormally wide width and shift of NMR lines of absorbed hydrogen compared to the gaseous one are reported. However, this original hypothesis presenting a new point of view on the problem of production of metal hydrogen has not been confirmed in subsequent studies.

A notable increase in the hydrogen-sorption ability of graphite nanostructures can be expected in two cases: in filling hollow graphitic cavities with the minimum diameter higher than 2–3 nm, and in using chemical, but not physical, sorption of hydrogen molecules by graphite surfaces. In the latter case, the mean distance between hydrogen molecules can turn out to be much less than the relevant value for liquid hydrogen (0.37 nm). However, the characteristic magnitude of the chemical sorption energy is about an order magnitude higher than that for physical sorption. For this reason, reversible filling of carbon nanostructures through chemical sorption requires higher energy expenditures and produces thermal load. All these factors should be taken into account in analyzing the possibility of resolving the hydrogen storage problem by using carbon nanostructures. As can be seen, the solution of this problem requires nontrivial approaches to

both the technology of nanostructure production and the methods of filling them with molecular hydrogen.

4.1.4 Recent experiments on filling carbon nanostructures with hydrogen. The results of the above-made analysis have been qualitatively confirmed in recent publications. In accordance with these works, which were executed using purer samples and modern experimental equipment, the maximum degree of filling carbon nanostructures with hydrogen does not exceed 1–2 wt.%. Thus, a distinctive feature of Ref. [133], which examined a sample of single-walled nanotubes with a purity of about 90%, is the saturation effect for the dependence of the quantity of absorbed hydrogen on the hydrogen pressure. This effect implies that the quantity of hydrogen absorbate is close to the maximum possible for the specific sample.

The sample under investigation contained, in addition to about 90% single-walled nanotubes, iron particles 3–4 nm in diameter, used as a catalyst. The nanotubes were bound into bundles consisting of 10–100 individual nanotubes. The CNTs were filled with molecular hydrogen in a high-pressure chamber 34 ml in volume. The sample examined was inserted into the chamber, which was filled with hydrogen. The quantity of hydrogen absorbed by the sample depending on the hydrogen pressure was determined by processing measured pressures in the chamber taking into account the equation of the gas state. This dependence becomes saturated at a hydrogen pressure of about 200 atm, which corresponds to the maximum quantity of absorbed hydrogen equal to 0.91 wt.%. Comparing this magnitude with that of activated charcoal gives rise to the conclusion that the sorption ability of CNTs is somewhat higher (about 50%), taking into account the difference in the specific surface of these materials. The authors attribute this distinction to a difference in electronic structures of plane graphite surfaces and those rolled into a cylinder. In the latter case, the contribution of p-bonds between adjacent carbon atoms is higher, which promotes more effective surface sorption of molecules.

In order to fill the inner cavity of CNTs with hydrogen or other substances, it is necessary to open them, otherwise the absorption of hydrogen occurs by filling a space between nanotubes in the bundle, as well as the sorption on the external surface of the nanotubes. Such a possibility has been demonstrated, in particular, in Ref. [134], the authors of which studied hydrogen absorption by well-purified bundles in a space between single-walled CNTs. Nanotubes of about 1.38 nm in diameter were produced by laser ablation of graphite, using an Ni/Co catalyst. The samples were treated with H_2O_2 and HCl, followed by washing with a solution of NaOH, which provided a content of opened nanotubes in the material at a level of 90–95 wt.%. The samples were saturated with hydrogen at room temperature and a pressure of up to 90 atm. Hydrogen desorption was studied using the temperature-programmed desorption method which allowed the determination of the hydrogen activation energy in relation to sorption as 0.21 eV, thus indicating the physical sorption mechanism. The quantity of absorbed hydrogen rises approximately linearly with pressure, reaching 0.3 wt.% at a pressure of 90 atm. This corresponds to a coverage of the external surface of single-walled nanotubes at a level of about 40%. Thermodynamic analysis of the data obtained shows that hydrogen is absorbed in pores between tubes 0.2–0.3 nm in transverse size, but not inside the nanotubes.

Paper [135] can be considered an example of a thorough study of the sorption ability of single-walled nanotubes. Three methods were used for opening the nanotubes to ensure access for hydrogen: ball milling, powdering, and ultrasonication in the presence of diamond microcrystals. Material containing CNTs 1.4 nm in mean diameter was produced in an electrical arc discharge using an Ni/Y catalyst. The nanotubes were bound into bundles from 5 to 20 nm in diameter. A sample of 150 mg in mass was heated in a vacuum at a temperature of 920 K for 12 h, followed by ball milling. Another sample of the same mass was inserted into a water suspension containing diamond microcrystals 0.2 μm in size and was ultrasonicated using a standard titanium alloy-based ultrasound source. Then, the sample was washed and dried in air. The third sample was flooded with ethanol until a homogeneous suspension was obtained and was subjected to grinding in the presence of diamond microparticles 0.1 μm in size until the ethanol fully evaporated. The sorption ability of the samples was studied employing a thermal desorption spectroscope equipped with a mass spectrometer. Samples 10–20 mg in mass, subjected to either vacuum purification or heating in air at a temperature of 720 K for an hour, were conditioned in a deuterium atmosphere at room temperature and a pressure of 0.8 atm for 15 min. The thermal desorption curves obtained with two types of samples are shown in Fig. 14. The desorption peak at $T = 400$ K is observed for a raw sample, as well as for samples obtained by grinding and ball milling. The sample subjected to ultrasonication exhibits the desorption peaks at 465 and 630 K. The sorptive capacity of the raw material and the sample subjected to grinding is estimated as 0.001 wt.%. Ball milling for 30 min enhances this magnitude up to 0.05 wt.%. Ultrasonication for 10 h results in about the same sorption ability (0.065 wt.%). One should note that the samples not subjected to preliminary vacuum heating do not absorb hydrogen at all. From Raman spectral measurements it is inferred that by increasing the grinding time the content of single-walled nanotubes in the sample is lowered. Therefore, a rise in the sorption ability of a sample subjected to grinding is caused not by single-walled nanotubes but, seemingly, by fragments of their decomposition. By contrast, ultrasonication does not promote a notable decomposition of nanotubes. The authors attribute the enhanced sorptive capacity of the samples subjected to ultrasonication to the presence of Ti which effectively forms hydride compounds.

It is of interest here to compare the results of measurements concerning the hydrogen sorptive capacity of materials

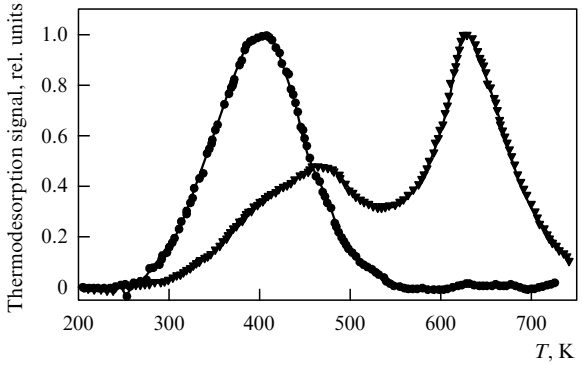

Figure 14. Thermal desorption curves of samples produced by ultrasonication (▼) and ball milling (●) of soot containing single-walled CNTs [135].

containing carbon nanotubes with the relevant data for nanostructured graphite (NSG). This comparison has been made in Ref. [136] where NSG produced from an artificial graphite powder of 99.997% purity and 2.25 g cm^{-3} in density with particle sizes up to 200 μm was used. In order to remove admixtures of water and functional groups, the powder was heated in a vacuum at 770 K for 3h. Then a sample of the powder 1.1 g in mass, destined for studies in terms of repeated adsorption/desorption of hydrogen, was subjected to ball milling in an argon atmosphere at room temperature for 50 h. Before carrying out sorption measurements, the sample was heated in a vacuum at 670 K for an hour. The specimen was saturated with hydrogen at a pressure of 60 atm at room temperature. During desorption the pressure in the chamber did not exceed 0.01 Torr. The measurements showed the hydrogen sorptive capacity of NSG in repeated cycles at the level of 0.2–0.25 wt.%, which is up to 10 times higher compared to raw graphite powder. The result obtained is in good agreement with the above-given estimates (14) of the sorption ability of a graphite nanostructure. Indeed, substituting into this expression the magnitude of the density for gaseous hydrogen at a pressure of 80 atm, $\rho_H = 0.0072$ g cm^{-3}, and for the nanostructured graphite, $\rho_C = 2.25$ g cm^{-3}, one obtains the magnitude of $\eta_H = 0.32$ wt.%, which is close to that observed in the experiment. Thereby, the above assumption on the volumetric, but not surface, filling of porous nanostructures with molecular hydrogen has been confirmed.

The dependence of the quantity M_H of absorbed hydrogen on the conditioning time t is well described by the function

$$M_H = A + B \ln t,$$

where the factor B rises sharply with the hydrogen pressure and takes the values of 9.0×10^{-3}, 4.2×10^{-2}, and 2.2×10^{-1} wt.%/ln (h) at pressures of 30, 57, and 80 atm, respectively. This is in agreement with the known sorption model, according to which hydrogen penetrates large-sized pores comparatively quickly, followed by a slow penetration through small-sized pores. To validate this model, the pore size distribution was determined using the results of standard measurements of the adsorption isotherms of nitrogen at 77 K. These measurements imply that crumbling a carbon powder results in an increase in the specific surface of a sample from 7 up to 780 m^2 g^{-1}, while the specific volume of nanopores rises from 0.002 up to 0.249 ml g^{-1}. The sample of NSG under investigation also contained pores of less than 1 nm in diameter. Therefore, crumbling the graphite powder promotes a considerable rise in its hydrogen-sorption ability, which is related to an increase in its specific surface and a decrease in pore size.

Most experiments on filling carbon nanostructures with molecular hydrogen are performed at high and superhigh gas pressures. This is necessary to provide for the penetration of hydrogen molecules into the smallest pores and cavities in the carbon structures, the size of which is comparable to that of a hydrogen molecule. An alternative approach to solving this problem is based on using electrochemical processes for filling the carbon nanostructures with hydrogen. In this case, the penetration of molecules into the pores comes about as a result of action of the electric field on a charged particle, whose interaction with the surface of a conducting electrode results in the formation of a hydrogen molecule or atom in the vicinity of this surface. An appropriate example of this approach is provided by recently published work [137], where the reversible filling of the multiwalled CNTs with atomic hydrogen as a result of the water electrolysis process has been demonstrated. The samples of multiwalled nanotubes were produced through the chemical vapor deposition method by decomposition of acetylene at a temperature of 650 °C in the presence of molecular hydrogen and an Fe–Al_2O_3 catalyst. The samples were purified in 37% HCl at a temperature of 140 °C for 6 h, which was followed by a distilled water treatment. The specimens produced contained multiwalled nanotubes 10–20 nm in outer diameter, 5–7 nm in inner diameter, and 0.34 nm in spacing between walls.

The three-electrode configuration of the electrochemical cell is presented in Fig. 15. A platinum grid was used as a counter-electrode, and a calomel saturating electrode was used as a base electrode. A sample containing 5 mg of multiwalled nanotubes was employed as an operating electrode. This sample comprised a finely dispersed powder impressed onto a gold disk. The iron particles, which were not fully removed by the above-described purification procedure and incorporated into the powder, were used for supporting the sample inside the cell by a permanent magnet. Galvanostatic measurements of the electrochemical capacity of samples containing multiwalled nanotubes were performed using as an electrolyte 6M KOH and 0.3M H_2SO_4 solutions and a charge/discharge current of 20 mA g^{-1}. The charging process was not terminated until the operating electrode potential reached its stable magnitude and the emission of gaseous hydrogen was clearly observed. The quantity of absorbed hydrogen was estimated through the quantity of charge passed through the electrode during the charging process.

From the galvanostatic measurements it is inferred that by using KOH solution as an electrolyte the charging current is saturated at a 1.3-V potential at the operating electrode. In this case, the charging capacity of the sample reached the magnitude of 10 mA-h g^{-1}, and the degree of filling of the sample with hydrogen amounted to 0.036 wt.%. These results are in satisfactory agreement with earlier experiments [125, 138]. A considerably higher hydrogen absorption degree was

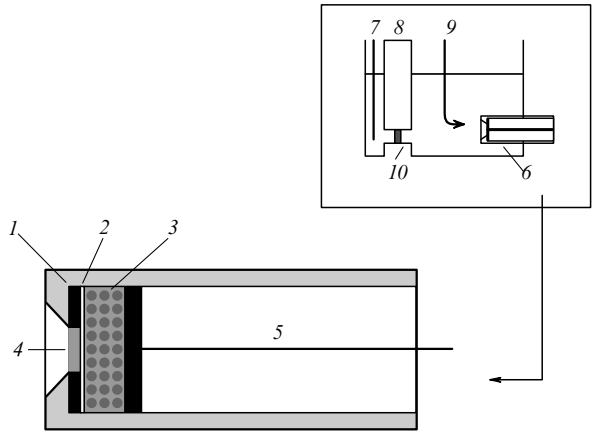

Figure 15. A schematic of a three-electrode cell for the electrochemical filling of multiwalled nanotubes with hydrogen [137]: *1* — sealing ring; *2* — gold foil; *3* — permanent magnet; *4* — sample containing nanotubes; *5* — current supply; *6* — nanotube sample holder; *7* — platinum grid; *8* — hole; *9* — calomel saturating electrode; *10* — glass substrate.

reached using an additional purification of nanotube samples through ultrasonication in 63 wt.% aqueous solution of HNO_3 for an hour, which was followed by mechanical stirring at a temperature of 70 °C for 6 h. In doing so, the charging capacity of the sample in the first charging cycle was 36 mA-h g^{-1}, which corresponded to the hydrogen-sorption ability of 0.1 wt.%. Therewith, a high degree of reproducibility of shape of charging – discharging curves obtained in repeated experiments was noted. While the above-indicated magnitude of the sorption ability of samples seems to be rather low, one can note the considerable positive role of acid treatment of samples in enhancing their sorptive capacity.

A further increase in the sorption ability of the samples (up to 0.27 wt.%) was reached as a result of opening the nanotube caps by the electrochemical oxidation reaction. However, experiments have shown that about 40% of the hydrogen absorbed in such a manner leaves the sample spontaneously during a short time. Therefore, opening CNTs facilitates the penetration of hydrogen into the nanotubes but does not promote its long-term storage.

As was noted above, in analyzing the hydrogen-sorption ability of carbon nanostructures one should discriminate between the surface sorption and volumetric filling of a ramified porous structure. A very limited number of experiments are known, where the mentioned discrimination was taken into account. In this connection, Ref. [139] is of interest, the authors of which have presented evidence of purely volumetric hydrogen filling of bundles consisting of single-walled CNTs. As a subject of investigation, samples of single-walled nanotubes bound into bundles, which were synthesized in an arc discharge in the presence of hydrogen (150 Torr) and argon (50 Torr), were used. The nanotubes were about 1.7 nm in diameter, while the diameter of the bundles reached 10 μm at lengths up to 100 μm. Sharpened graphite rods 10 mm in diameter were employed as a cathode. A disc 150 mm in diameter and 20 mm in height, manufactured by the pressing method at a pressure of 7.5×10^6 atm from graphite powder with the addition of finely dispersed Ni and Co in quantities of 2.5 and 1.0 at.%, respectively, as catalysts, was used as an anode. Besides that, the anode material contained 0.8 at.% of sulfur that stimulated the nanotube growth. The electrode axes were oriented at an angle of 30° – 50°, which also stimulated the effective growth of the nanotubes. The samples under investigation contained about 60% CNTs. They formed pellets 0.5 – 0.8 g in mass and 1.7 g cm^{-3} in density, which were produced from the raw CNTs by the hot pressing method without the usage of any binders. The sorption ability of the samples was measured at a pressure of 110 atm and room temperature. The quantity of absorbed hydrogen was determined by a decrease in pressure in the chamber containing the sample with CNTs. The maximum quantity of absorbed hydrogen (4 wt.%, which corresponds to the density of 68 kg m^{-3}, close to that of liquid hydrogen) was observed when the sample was subjected to thermal treatment under flowing heated argon at $T = 1473$ K for 2 h before the measurement. This result is in agreement with the above estimates of the sorptive capacity of the bundle of single-walled CNTs presented in Table 4. In accordance with those data, the limiting sorption ability of a bundle consisting of single-walled CNTs 1.7 nm in diameter is about 6 wt.%.

Measurements of the sorption ability of the samples were supplemented with measurements of their specific surface, which is the main parameter determining the sorption properties of a material. This parameter was measured using nitrogen absorption data at cryogenic temperatures. The quantity of adsorbed hydrogen that is released due to heating CNT samples was measured by the volume of water expelled. Experiments showed that at room temperature intense hydrogen desorption occurs when the pressure in the chamber is lowered below 40 atm. In vacuum conditions more than 70% of the hydrogen stored in the samples is released. The specific surface of samples was also measured and it reached about 110 m^2 g^{-1}. It is easy to see that the measured quantity of absorbed hydrogen [139] is as high as ten times that of surface hydrogen sorption, taking into account the measured magnitude of the specific surface of the sample. Therefore, the above-cited work provides experimental evidence of the volumetric mechanism of filling the CNT bundles with hydrogen.

4.2 Filling carbon nanostructures with other gases

4.2.1 Rare gases. As distinguished to sorption properties of carbon nanostructures with respect to hydrogen, which are of great practical significance, peculiarities of rare gas sorption by such structures are mainly of scientific interest. The characteristic size of a cavity formed by such structures is about 0.3 – 0.4 nm, which is comparable to that of most atoms. Therefore, both physical surface sorption of atoms and volumetric filling of a cavity with gaseous media are possible in the absorption of atoms by a carbon surface structure with nanometer-sized pores. These two mechanisms can be discerned in any particular case through a specially arranged experiment.

One of the first experiments of such a kind was reported in Ref. [140], the authors of which studied the filling of multiwalled CNTs with helium, xenon, and molecular nitrogen. The nanotubes were produced through the thermocatalytic decomposition of acetylene on a zeolite substrate in the presence of a metal catalyst. Under optimal conditions and for the total mass of the catalyst with a substrate of 3.5 g, the synthesis temperature was 600 °C, the rate of supply of acetylene was 10 ml min^{-1} and that of nitrogen was 110 ml min^{-1}, and the reaction time reached 60 min. In this case, the deposit produced amounted to 600 mg in mass. The zeolite substrate was fully removed by etching in an HF solution. Carbon particles were removed by either oxygen in air at 773 K or by a $KMnO_4$ solution at 343 K. Such purification resulted in an increase in multiwalled nanotube content up to 27 and 40%, respectively. Oxidation caused the appearance of defects in the form of –COOH (0.38 mmol g^{-1}), –OH (0.75 mmol g^{-1}), and –CO groups. Usage of potassium permanganate promoted the addition of 0.19 mmol g^{-1} of –COOH, 0.79 mmol g^{-1} of –OH, and 0.76 mmol g^{-1} of –CO. The nanotubes purified by both methods were 16 nm in outer diameter and 6 nm in inner diameter and consisted of about 15 graphite layers. The samples that were 0.05 g in mass were dried in a hot nitrogen flow at $T = 673$ K for 2.5 h, after which a cell was filled with a mixture of N_2 (2.24 %), Xe (8.9%), and He (88.86%) at a total pressure ranging between 1.4 and 5.2 atmospheres. In addition, one more sample of mass 0.018 g, purified by air oxygen, was sealed off in an atmosphere of pure Xe at a pressure of about 22 atm. The filling of the nanotubes was monitored by NMR spectra of ^{13}C and ^{129}Xe. The mass content of xenon in the sample was estimated as 90%, which corresponds to the ratio $N_{Xe}/N_C = 0.3$, where N is the coverage of the nanotube surface.

Further development of investigation in the field was stimulated by experiments [141–145] performed at Rice University (Texas, USA) that demonstrated the importance of the procedure of opening nanotubes before filling them with a rare gas. In accordance with these experiments, various radicals (–COOH, –OH, –CO, etc.) attached to the external surface of CNTs can be fully or partially removed by thermal treatment. This is accompanied by the formation of holes in nanotube walls and makes them accessible for filling with various gases.

A special feature of the experiment staged in Ref. [144] is the practically homogeneous samples of single-walled nanotubes in use, with a diameter of about 1.36 nm and chirality indices close to (10, 10). These samples were produced by laser sputtering of graphite in the presence of a metal catalyst. Before performing the experiment, the CNTs were purified through a chemical treatment with nitric and sulfuric acids, as well as hydrogen peroxide, which was followed by ultrasonication for separating them from each other. A sample of CNTs 46 μg in mass prepared in such a manner was heated in an ultrahigh vacuum up to a temperature of 1100 K at the rate of 1 K s^{-1}. When the temperature exceeded 600 K, the emission of molecules CO, CO_2, CH_4, and H_2 was observed, the intensity of which sharply increased with the rise in temperature. Experiments on filling the thermally treated CNTs with xenon were performed at $T = 90$ K. The experimental results showed a rise in the quantity of absorbed Xe as the treatment temperature increased. The maximum quantity of Xe inside the CNTs was reached at a treatment temperature of 1073 K and comprised about 5% carbon atoms. This quantity is as much as triple that when a 1D chain of Xe atoms spaced by the van der Waals minimum is inserted into a CNT 1.36 nm in diameter. The geometry indicates that this corresponds to the most dense filling of a CNT with Xe atoms. The temperature rise in the quantity of the gas absorbed is explained in terms of the possibility of opening holes in a nanotube surface by removing added functional groups. Therefore, an approach to a directional change in the CNT structure has been demonstrated with the intent of filling them as densely as possible.

The above-described approach has been further developed in the work of the same team [145], where as the subject of investigation the single-walled nanotubes of chirality (10, 10) were also used. As opposed to the above-cited Ref. [144], in this case the purification and opening of the nanotubes were performed by combining the thermal treatment and chemical processing by ozone. The samples were produced through the laser ablation method and purified by HNO_3/H_2SO_4 mixture. The nanotubes were bound into bundles 0.1–1 μm in length and terminated with closed caps. 22.8 μg of purified single-walled nanotubes were applied onto a tantalum foil plated with a layer of gold. Before the procedure of filling with Xe, each sample was repeatedly treated with ozone at 300 K, whereupon it was heated up to 973 K. The filling degree was measured in a chamber evacuated down to a pressure of 10^{-10} Torr and filled with Xe at a pressure of 7.4×10^{-7} Torr and a temperature of 95 K. During the ozone treatment of the sample, a dosed flux of ozone (containing 3% oxygen) into the vacuum chamber amounted to 2.9×10^{14} cm^{-2} s^{-1}. The quantity of absorbed Xe was determined by temperature-controlled desorption. The measurements show a considerable increase in the sorption ability of the sample after the ozone treatment. A low-temperature desorption peak at 110 K was observed in the absence of treatment. A desorption peak at 140 K appeared after ozone treatment. It was also found that the sorption ability of the sample increases much more if the ozone treatment is followed by thermal conditioning at 973 K for 20 min. The authors believe that such a treatment promotes the removal of functional groups CO and CO_2. At the initial stage of the ozone treatment, when the diameter of holes in the CNTs does not exceed 0.5–0.7 nm, a linear dependence between the time of ozone treatment, which determines the quantity and the size of holes, and the rate of Xe absorption at a fixed gas flow into the absorption chamber has been observed. This dependence goes to saturation as a result of further ozone treatment. It can probably be explained in terms of closing the holes with radicals COOH– and COR–, which have a considerable dipole moment and prevent access of Xe atoms to the interior of CNTs.

4.2.2 Nitrogen and oxygen. Nitrogen, being chemically inert and the most available of the known gases, is the most widely used in experiments on filling carbon nanostructures. Therewith, nitrogen can be considered a reference gas for establishing sorption characteristics for all the gases in common. Particularly, the standard procedure for determining the specific surface of porous substances is based on the measurement of their nitrogen-sorption ability [146]. Work [147] is an example of such a measurement, whose authors studied single-walled nanotubes with diameters ranging between 0.93 and 1.35 nm, produced through the thermocatalytic decomposition of CO at 1000 °C in the presence of iron particles (HiPCO process). As an initial material, gaseous iron pentacarbonyl $Fe(CO)_5$ was used, which decomposed in plasma forming carbon monoxide and iron nanoclusters. The samples of nanotubes 100 mg in mass were subjected to a thorough multistage purification procedure involving a lengthy ultrasonication of the bundles in dimethylformamide, followed by double centrifugation in methanol for separating the individual nanotubes, and hydrochloric acid treatment followed by oxidation at 500 K in humid air in order to remove metal and carbon particles and open the pores. The degree of purity of the samples was determined by a high-resolution electron microscopy and through the thermal gravimetry procedure. Measurements show that the above-described purification procedure results in a decrease in iron content from 22 down to 0.4 wt.%.

The specific surface of the samples was determined on the basis of processing absorption isotherms measured under liquid nitrogen (77 K). Measurements implied that the above-described procedure of purification of the samples results in about a threefold increase in their specific surface from 577 m^2 g^{-1} up to 1587 m^2 g^{-1}. One should note that the indicated magnitude of the specific surface can be considered a record achievement obtained as a result of efforts directed toward purification of nanotubes and opening their caps. Since, in accordance with the above estimates (4), (4a), the specific area of a graphite surface in the case of one-sided filling does not exceed 1300 m^2 g^{-1}, one can believe that in this case a partial two-sided filling of the surface with molecular nitrogen occurs.

Measurements of the nitrogen-sorption ability of CNTs, performed at various temperatures, can provide important thermodynamic data on the heat of adsorption of a nitrogen molecule on a distorted graphite surface. These data are of basic interest as they shed light on the problem of the

dependence of the adsorption heat of a molecule on the degree of curvature of the graphite surface. An experiment of this kind was performed in Ref. [148], the authors of which studied single-walled nanotubes 1.2 nm in mean diameter, produced through the laser ablation of graphite. Before the experiment, samples of soot containing CNTs were inserted into a copper chamber and conditioned in a vacuum at a temperature of 350 K for 24 h. Adsorption isotherms were measured at temperatures of 81.2, 83.3, 86.4, 88.45, and 93.72 K. Comparison of the obtained adsorption isotherms with those for graphite (Fig. 16) implies a considerably (as much as three times) higher nitrogen-sorption ability of nanotubes compared to graphite. Processing the adsorption isotherms has provided the dependence of the adsorption heat, determined by the relation $q = kT^2(\partial \ln p/\partial T)_N$, on the coverage N of the nanotube surface with nitrogen molecules. This dependence is shown in Fig. 17 and has a monotonically decreasing shape, which is caused by the existence on a nanotube surface of sections which are characterized by various magnitudes of heat adsorption. The maximum magnitude of this parameter is inherent to a boundary between neighboring nanotubes inside a bundle, and next is the external surface of a nanotube. The material is filled with nitrogen in a sequence corresponding to a decrease in the adsorption heat, so that the mean value of this parameter decreases with a rise in the filling degree. The binding energy of a nitrogen molecule and a nanotube surface is estimated to be 0.086 eV, which is practically no different from that of graphite [149]. Therefore, the above-described work has provided experimental support for concluding the independence of the heat of adsorption of a nitrogen molecule by a graphite surface from the curvature of this surface.

Carbon nanostructures are able to absorb gases through both their inner and outer surfaces (see Fig. 18). This matter has been studied quantitatively in Ref. [150] (see also Ref. [151]), whose authors studied single-walled nanotubes obtained by the electrical arc method using finely dispersed Ni and Y inserted into a graphite rod as a catalyst. Nanotubes of about 1.4 nm in diameter were terminated in closed caps and

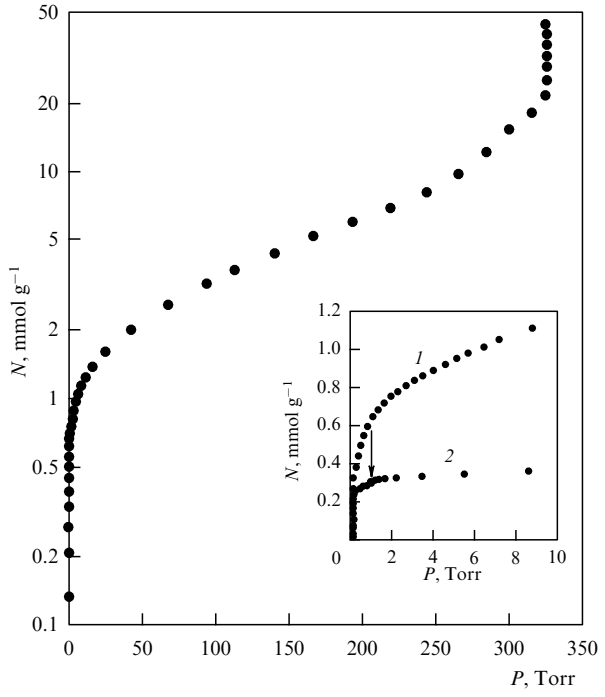

Figure 16. The adsorption isotherm of nitrogen by a sample containing single-walled nanotubes, measured at a temperature of 71 K [148]. In the inset to the figure this isotherm is compared with that for graphite: *1* — nanotubes, *2* — graphite.

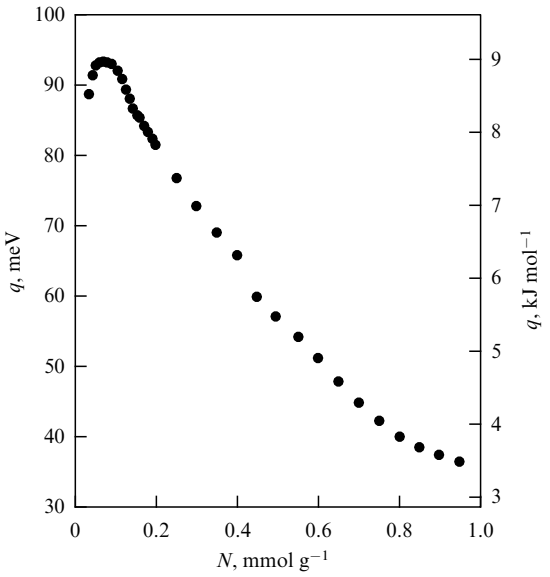

Figure 17. Dependence of the heat of adsorption of nitrogen by a material containing single-walled CNTs on the surface coverage [148].

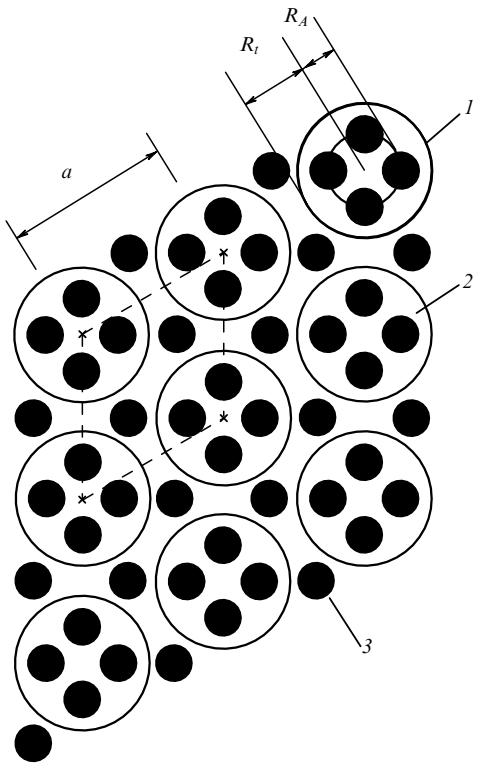

Figure 18. The cross section view of a bundle of single-walled nanotubes containing adsorbed gaseous molecules [150]. Molecules can be adsorbed by both outer (*1*) and inner (*2*) nanotube surfaces. One should furthermore discriminate the location of molecules in the narrow trench formed by adjacent nanotubes (*3*). Here, a is the distance between the CNT centers, R_t is the CNT radius, and R_A is the radius of an atomic particle.

bound into bundles 5–20 nm in diameter. The absorption of molecular nitrogen and oxygen by nanotube bundles was studied through the analysis of adsorption isotherms and using X-ray diffractometry. Some of the samples were subjected to thermal conditioning in air at 350 °C for an hour. This promoted the removal of some contaminations and the opening of the caps of the CNTs. Both raw and treated samples 15–25 mg in mass were studied in terms of gas absorption. The measurements were performed at $T = 77.3$ K, in accordance with the saturation vapor pressure of N_2 and O_2, 760 and 156 Torr, respectively. The measurements showed an increase in the quantity of gas absorbed as the gas pressure in the chamber raised. Besides that, it is stated that the thermal treatment increases by roughly twofold the quantity of gas absorbed in the case of both N_2 and O_2. This conclusion implies the existence of two sites where absorbed gases are accumulated: inside the nanotubes, and inside the bundles between the nanotubes. The first of these regions is unattainable for a gas in the case of raw nanotubes, because they have closed caps. In the case of treated nanotubes, both the regions are similarly attainable. As follows from the experimental data, these regions have approximately equal gas-sorption capacity. The analysis of X-ray diffractograms shows that molecular gases adsorbed by bundles of raw nanotubes, coat the outer surface of CNTs with a monolayer. The molar ratio of adsorbed molecules is estimated at 0.04. For the treated nanotubes, the magnitude of this parameter reaches 0.1, so that the components corresponding to the outer and inner surfaces of the nanotube make about equal contributions. Therefore, it was found that the raw nanotubes adsorb gases only through their outer surfaces, while for treated nanotubes filling their inner cavity is followed by filling the innertube space in the bundles.

Investigations point to considerable distinctions in the character of interaction of a nitrogen molecule with the inner and outer surfaces of a nanotube. Thus, Ref. [152], where the character of nitrogen absorption by open and closed end caps is compared, a notable difference in the relevant magnitudes of the heat of sorption is found. Nanotubes 1.2 nm in mean diameter were produced by the laser ablation of graphite. In order to open the nanotube end caps, the samples were ultrasonicated in a (3 : 1) mixture of $H_2SO_4 + HNO_3$ for 24 h, whereupon one part of the samples was annealed at 873 K for 12 h, while another one was annealed at 1073 K. Both types of samples were conditioned in a vacuum at 350 K for 24 h. The pressure dependences of the quantity of absorbed nitrogen measured at 71 K present monotonically increasing functions. Annealing CNTs at 873 K results in about a doubling of the quantity of absorbed nitrogen at any pressure. For CNTs annealed at 1073 K, the indicated gain factor is close to 3. Therewith, the maximum specific quantity of absorbed nitrogen for open-ended nanotubes amounts to about 10 wt.%, which notably exceeds the relevant magnitude estimated assuming a one-layer coverage of the graphite surface with nitrogen. Therefore, the experimental data obtained show a considerable increase in the sorption ability of CNTs due to their opening. Hence, it follows that the most effective sorption mechanism is related to filling the inner cavity of a CNT, which is possible only if the nanotube has an open end cap. Therewith, filling an open-end CNT starts from the inner cavity, while coating the outer surface occurs only after one-layer coating of the inner surface. Processing the absorption isotherms measured at various temperatures (between 117.25 and 129.95 K) provides the magnitudes of the heat of sorption of a nitrogen molecule by the surface of a CNT. The relevant magnitude for the inner surface of a CNT is 161.4 meV, which is about double the amount for closed-cap nanotubes (78.5 meV). Therefore, open-end CNTs are much more attractive material for gas storage than closed-end ones, because effective filling is reached for the former at considerably lower pressures and higher temperatures.

Experiments on the investigation of oxygen sorption properties of carbon nanostructures are not as easy to interpret as in the case of nitrogen. This is due to much higher chemical activity of molecular oxygen compared to that of nitrogen and, in particular, the possibility of a charge transfer from a graphite surface to a molecule. This possibility follows, for instance, from quantum chemical calculations [153–155], in accordance with which the sorption of molecular oxygen by a graphite surface is accompanied by the transfer of a charge, estimated at about 0.1 of the electron charge. However, this conclusion contradicts known experimental data [156], indicating that the sorption of oxygen by a graphite surface does not change the electron photoemission spectra of carbon. One more peculiarity of the sorption of molecular oxygen, distinguishing this case from that of nitrogen, relates to the rather low dissociation energy of this molecule (5.12 eV comparing to 9.76 eV for N_2). Due to this difference, the dissociative sorption of oxygen becomes more probable, which is accompanied by the dissociation of the molecule, followed by the release from the surface of one of the atoms formed.

The adsorption–desorption kinetics of oxygen by bundles of single-walled nanotubes in comparison with highly ordered pyrolytic graphite (HOPG) were studied in Ref. [157] with the purpose of clarifying the sorption mechanism and establishing the possibility of dissociative sorption. Samples of single-walled nanotubes 1.2 nm in mean diameter were purified through repeated heating up to 1200 K in a 10^{-10} Torr vacuum. A cloth-like layer of CNTs was coated onto a tantalum disc 1 cm in diameter. A sample of HOPG was attached to the opposite side of the disk and was used for comparison purposes. The disc was placed into a sealed-off cryostat whose temperature could reach 28 K. Then, the chamber was treated with a dosed flux of oxygen of about 10^{-11} mol s^{-1} cm^{-2} in intensity, which corresponds to a rate of coating the sample surface of about 0.01 monolayer s^{-1}. The character of oxygen thermodesorption was studied in the case of HOPG by increasing the temperature of the sample from 28 up to 44 K at a rate of 0.25–0.5 K s^{-1}, and in the case of CNTs by increasing the temperature from 28 up to 100 K. The measurement results provided the magnitude of the energy of sorption of O_2 molecules by an HOPG surface (11.8–12.3 kJ mol^{-1}, which corresponds roughly to 0.12 eV). For single-walled nanotubes, this parameter was measured at about 0.18 eV. Experimental data show the absence of both chemisorption and dissociative sorption of O_2 by a surface of nanotubes. The sorption of oxygen on a graphite surface is due to a purely van der Waals interaction. Therefore, the presence of absorbed oxygen on a surface of nanotubes has no influence on their electrical characteristics and cannot be used for the determination of oxygen content in the atmosphere. The equilibrium coverage of the surface of single-walled CNTs with oxygen at room temperature was determined to be about 10^{-5} molecules per carbon atom.

4.2.3 Sorption of polyatomic molecules. Investigation of the sorption of polyatomic molecules by carbon nanostructures is

of interest in connection with a practically important problem — the development of gaseous fuel storage facilities and sensors, the electronic characteristics of which are sensitive to the presence of some specific molecules adsorbed on the surface. In investigating the surface sorption of a polyatomic molecule one meets specific difficulties related to the intrinsic anisotropy of polyatomic molecules, due to which the sorption characteristics of a molecule depend not only on the temperature and the state of a surface, but also on the orientation of the molecule with respect to the surface of an adsorbent. An up-to-date experiment, as a rule, is not able to discriminate this dependence and, therefore, usually deals with orientationally averaged sorption characteristics.

Adsorption of CO_2 by a surface of single-walled CNTs 0.9 – 1.4 nm in diameter was studied in Ref. [158], whose authors produced the nanotubes using the above-described procedure of thermocatalytic decomposition of CO in the presence of an Fe catalyst [147]. As a result of the multistage purification procedure, which was also described above, the specific surface of the sample reached about 1600 $m^2\ g^{-1}$, and the specific pores volume 1.55 $cm^3\ g^{-1}$. The specific surface of a sample of activated charcoal, used for comparison, amounted to 1284 $m^2\ g^{-1}$. The adsorption isotherms of the samples related to CO_2 were measured at temperatures of 0, 35, 125, and 200 °C. Processing these isotherms provided the magnitude of the adsorption heat of the CO_2 molecule on the surface of the nanotube as 0.24 eV, which indicates the physical mechanism of sorption.

In analyzing experiments on investigation of adsorption of gases by bundles of single-walled CNTs one should take into account the nonhomogeneity of the sorption properties of the surface inside a bundle. First of all, it relates to inner and outer surfaces of a nanotube. In addition, the sorption characteristics of the narrow trench forming on the boundary between adjacent nanotubes in a bundle are undoubtedly distinguished from those of a free nanotube surface. Finally, one can suppose that the sorption characteristics of the boundary between two nanotubes of equal diameter should be different from those in the case of different diameters. Some attempts to answer quantitatively the above-formulated questions were undertaken in Refs [159 – 164], the authors of which combined the measurements of the quantity of CH_4 absorbed by CNT samples with model thermodynamic and quantum chemistry calculations. Thus, in Ref. [159] the measurements of the methane-sorption ability of CNT bundles through the neutron diffraction method were supplemented with quantum chemistry and thermodynamic calculations on the basis of semiempirical methods. Samples of single-walled nanotubes with diameters within the range 1.35 ± 0.2 nm, bound into bundles, which were produced in an electrical arc discharge using a Y/Ni catalyst, have been studied. The bundles involved 30 – 50 individual nanotubes. As an adsorbate the gaseous CD_4, which is an appropriate object for neutron diffraction measurements, was used. The authors have reached an important conclusion on the basis of the measurements performed, relating to the occurrence of deformations of nanotubes as a result of high-pressure gas filling. The nanotubes deformed in such a manner present a natural lock preventing spontaneous escape of adsorbed molecules out of the sample. In doing so, the problem of confinement of absorbed molecules inside carbon nanostructures finds its solution, and it offers an opportunity for fully reversible filling of such structures with gaseous substances. Calculations performed also indicate a higher sorptive capacity of bundles consisting of nanotubes of various diameters, compared to those having equal diameters.

One should note that the study of the methane-sorption properties of CNTs is of special interest, since methane contains a considerable quantity of hydrogen (25 wt.%) and can be used, like hydrogen, as an effective environmentally safe car fuel. The heat of sorption of methane on a surface of bundles of single-walled CNTs was determined in Ref. [160] for various coverages of a surface on the basis of treatment of adsorption isotherms. At a low coverage (about 10%), the heat of sorption was determined at 250 meV, which is in good agreement with the preceding measurements [161, 162]. The dependence of the adsorption heat on the coverage of the surface is shown in Fig. 19. One can see a lowering of the adsorption heat with increasing coverage of the surface, which can be determined by the action of two factors. First, when covering a homogeneous surface an increase in the coverage causes a rise in the contribution of intermolecular interaction to the energy of sorption. This contribution usually has a negative sign. The second factor, determining the dependence of the heat of sorption on the surface coverage, relates to the occurrence of various sections on the surface of nanotubes bound into bundles, which are characterized by various magnitudes of the heat of sorption. At a low coverage, the sections having the maximum heat of sorption are filled. The role of sections with a lower magnitude of the heat of sorption increases as the coverage rises, which is why the effective magnitude of the heat of sorption decreases.

The size of the methane molecule is larger than that of rare gas atoms and diatomic molecules. For this reason, the problem of penetration of a methane molecule into the inner cavity of a nanotube is a challenge for researchers. The simplest way to solve this problem was discovered by the authors of Ref. [164], who used ultrasonication in an attempt to cut the outer caps of nanotubes. Samples of single-walled CNTs bound into bundles about 12 nm in diameter were produced through the laser ablation method using either an Ni/Co or Rh/Pd catalyst. Therewith, the average diameter of the nanotubes amounted to either 1.4 or 0.85 nm, respectively. As a result of purification of the samples through

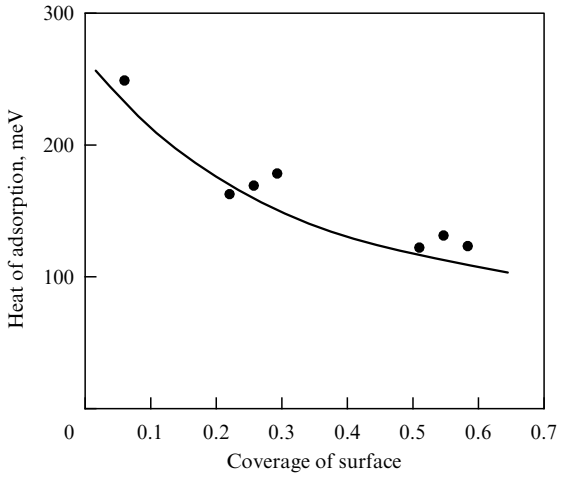

Figure 19. The dependence of the heat of adsorption of CH_4 molecule by a surface of single-walled nanotubes bound into bundles on the surface coverage, obtained through processing adsorption isotherms [160].

standard methods, the nanotube content reached 90%. The density of the samples was about 1.33 g cm^{-3}. Ultrasonication of the samples in a (3 : 1) mixture of H_2SO_4 and HNO_3 for 24 h resulted in shortening the average length of the nanotubes down to 0.5 μm.

The degree of filling of CNTs with methane (CH_4) or ethane (C_2H_6) was determined by measuring the hydrogen (H_2) content through the nuclear magnetic resonance (NMR) method. A sample of CNTs of about 15 mg in mass was preliminarily annealed in a vacuum at a temperature of 400 °C for one hour, and then placed in an NMR cell and acted on by methane or ethane at room temperature and a pressure of 0.45 atm. Processing the adsorption isotherms has provided the heat of sorption for a methane molecule on a CNT surface at 235 ± 2 meV, which notably exceeds that for a graphite surface (126 meV) and agrees well with the above-cited measurements [160–162]. The measured magnitude of the heat of sorption of an ethane molecule on the surface of a CNT bundle (303 ± 15 meV) is also notably higher than that for a graphite surface (170–190 meV [165]). Measurements show that the ultrasonication promotes about tenfold increase in the quantity of absorbed methane. This is probably caused by the possibility of penetration of methane molecules into CNTs due to their cutting.

The passage from the mechanism of physical sorption to that of chemical sorption, observed in the case of sorption of polyatomic molecules on a surface of nanotubes, can be considered as a striking manifestation of the already mentioned dependence of the energy of sorption of a polyatomic molecule on a graphite surface on its curvature. Such a passage was recently found in investigating the sorption of acetone molecules by a CNT surface [166]. Samples of single-walled CNTs 10 mg in mass, produced through the HiPCO method, were immersed in 300 ml of acetone and ultrasonicated for an hour, whereupon they were dried in air. The samples treated in such a manner, in parallel with raw samples, were saturated with acetone, the content of which was determined by the standard procedure of temperature-programmed desorption. In doing so, the temperature was increased from 300 up to 700 °C at the rate of 3 °C per minute. In addition, the oxygen content and the chemical state of carbon were determined through X-ray photoelectron spectroscopy. Measurements imply that the heat of sorption of an acetone molecule and fragments of its decomposition on a CNT surface ranges between 1 and 2.5 eV, which exceeds considerably that for the surface of graphite (0.33 eV [167]) and activated charcoal (0.4 eV [168]). This indicates that the physical sorption mechanism for acetone molecules is substituted with the chemical one, as a plane graphite surface is distorted.

4.2.4 Sorption sensors. The high sensitivity of electronic characteristics of carbon nanotubes to the occurrence of adsorption of molecules or radicals on their surfaces suggests the possibility of designing on their basis a highly sensitive and superminiature sensor which is able to detect the presence of tiny admixtures in the atmosphere. This possibility was studied, in particular, in Ref. [169], the authors of which used a slightly pressed layer of a cloth-like material $1 \times 2 \times 0.1$ mm^3 in size, containing CNTs bound into bundles. The material was produced through the electrical arc sputtering of graphite in the presence of a catalyst. The sample contained 50–70% nanotubes. The nanotubes were about 1.4 nm in mean diameter and formed bundles 15 nm in mean diameter. The occurrence of molecules adsorbed on the surface of CNTs was detected through the magnitude of the thermoelectric power of the sample, which was measured by the four-probe method at a temperature drop $\Delta T < 0.5$ K along the sample.

Room temperature measurements showed that the thermoelectric power of the raw sample purified from adsorbates by vacuum thermal treatment for 10 h ranged between -45 μV K^{-1} and -40 μV K^{-1}. The negative sign and the temperature dependence, close to linear, demonstrate the metallic origin of the conductivity of the sample, which is determined by nanotubes with metallic electron conductivity. Filling the sample with He at atmospheric pressure and $T = 500$ K results in enhancement of the thermoelectric power by about 12 μV K^{-1}. Therewith, the time necessary for establishing the stationary magnitude of the thermoelectric power (0.26 h) is about 3 times shorter than that for the recovery of this magnitude after beginning to pump out He (0.83 h). Similar measurements performed with H_2 showed that the relative increase in the mass of the sample under investigation due to adsorption of hydrogen reached 0.5%. Therewith, the thermoelectric power of the sample decreases linearly as the quantity of adsorbed hydrogen rises. A similar dependence of the thermoelectric power of the sample on the quantity of material absorbed is observed in the case of NH_3. By contrast, the thermoelectric power of samples containing nanotubes rises as the quantity of adsorbed O_2 or N_2 increases. The distinction in the above-indicated dependences suggests differences in the mechanism of influence of molecular sorption upon the electronic characteristics of CNTs. One can assume that in the case of increasing dependence the adsorbed molecules are electron acceptors, while in the case of a decreasing one they are donors.

Considerable distinctions in the dependences of the thermoelectric power on the content of adsorbed molecules, which have been observed for molecules of various types, offer the possibility to develop a quite simple and highly effective CNT-based sensor. Devices of such a type would find their application in prospecting minerals, in systems of emergency protecting large plants and, specifically, nuclear plants from gaseous emissions, in devices controlling the car exhaust, etc.

5. Conclusions

The discovery of carbon nanotubes is one of the most considerable achievements of modern science. This carbon modification is intermediate in structure between graphite and fullerenes. However, with respect to many properties carbon nanotubes have nothing in common with either graphite or fullerenes. This permits one to consider and study nanotubes as a proper material possessing unique physical and chemical characteristics.

One of the most interesting properties of carbon nanostructures, which is of importance from the viewpoint of both basic research and applied development, relates to their extraordinarily high specific surface. This, on the one hand, makes these structures an attractive subject for physical and chemical investigations of surface processes and phenomena on a nanometer scale. The occurrence of cavities of nanometer scale inside such structures offers an opportunity for investigating basic mechanisms of capillary phenomena, physical and chemical sorption, etc. on a size comparable to

the parameters of crystal structures. Thus, the appearance of carbon nanotubes made it possible to study the dependence of the heat of sorption of various molecules on the curvature of a graphite surface. Results of such studies are a source of invaluable information on mechanisms of interaction of atomic particles with surfaces. Filling the inner cavity of a nanotube with molecules whose size is comparable to the inner diameter of the nanotube results in the formation of a 1D crystal inside the nanotube. Such a crystal in its basic properties is quite different from those of 3D crystal structures. The experimental investigation of such crystals has been made possible only since the discovery of nanotubes.

On the other hand, an abnormally high specific surface of carbon nanostructures and occurrence of elongated closed cavities inside them make these structure very attractive tools for solving applied problems. Filling nanotubes with metals leads to the development of the most miniature wires, which can become elements of future nanoelectronic devices. The possibility of filling carbon nanotubes and other nanostructures with gases offers the prospect for developing effective gas storage devices which can be used, in particular, as a basis for environmentally safe types of transport. The dependence of the electronic characteristics of nanotubes on the occurrence of adsorbed molecules of various sorts on their surface offers the possibility to create on this basis superminiature sensor devices responding to the presence of undesirable or dangerous admixtures in atmosphere.

Researchers working in the field of carbon nanotubes have travelled a considerable way during the 15 years which have passed since their discovery. The following issues can be noted as important stages characterizing this progress: the discovery of multiwalled and, subsequently, single-walled nanotubes [7]; the discovery of the capillarity phenomenon and the ability to fill nanotubes with liquid substances [15]; the establishment of an interconnection between the structural and electronic characteristics of a single-walled nanotube [170]; elaboration of the method for producing CNTs on the basis of thermal catalytic decomposition of hydrocarbons [171]; discovery of the electron field emission from nanotubes [172, 173]; the elaboration of a method for the large-scale production of single-walled nanotubes with close structural and electronic characteristics [37]; the development of methods for the homogeneous filling of large patterned surfaces with similarly aligned nanotubes having close electronic characteristics [24]; the manufacture of a model sample of a flat panel display with a CNT-based cold cathode [172, 173], and the production of peapods constituting single-walled carbon nanotubes filled with fullerene molecules along their length [19]. The above-presented list of achievements in the field can be easily continued; however, it is already obvious that during a short period of time we have seen a passage from the description of elongated objects, formed as a result of the thermal decomposition of graphite, through the synthesis of nanotubes with given structural and electronic characteristics to the fabrication of reliably operating CNT-based devices. This example shows again the important fruitful role of basic research, which can result in the quick progress of applied technologies at the successful concurrence of circumstances.

The solution to the problem of the application of CNTs depends primarily on the production cost of nanotubes in a macroscopic amount. As of now, it considerably exceeds that of gold, which apparently excludes the possibility of large-scale applications of this material. Nevertheless, such nanotube properties as their extra tiny size, good electrical conduction, high emission characteristics, etc. allow one to hope even now for their effective application in such fields as chemical technology, hydrogen energy, nanoelectronics, and so forth, where their good sorption properties in combination with electroconductivity and mechanical characteristics are of high importance. The successful solution of these problems will become one more example of the effective influence of basic research on scientific and technological progress.

This work has been supported by grant ISTC 2484, grant CRDF in the framework of REC 'Plasma', and the Program supporting scientific schools of the RF.

References

1. Kroto H W et al. *Nature* **318** 162 (1985)
2. Krätschmer W et al. *Nature* **347** 354 (1990)
3. Eletskiĭ A V, Smirnov B M *Usp. Fiz. Nauk* **163** (2) 33 (1993); **165** 977 (1995) [*Phys. Usp.* **36** 202 (1993); **38** 935 (1995)]
4. Smalley R E *Rev. Mod. Phys.* **69** 723 (1997); *Usp. Fiz. Nauk* **168** 323 (1998)
5. Curl R F *Rev. Mod. Phys.* **69** 691 (1997); *Usp. Fiz. Nauk* **168** 331 (1998)
6. Kroto H W *Rev. Mod. Phys.* **69** 703 (1997); *Usp. Fiz. Nauk* **168** 343 (1998)
7. Iijima S *Nature* **354** 56 (1991)
8. Eletskiĭ A V *Usp. Fiz. Nauk* **167** 945 (1997); **172** 401 (2002) [*Phys. Usp.* **40** 899 (1997); **45** 369 (2002)]
9. Eletskiĭ A V *Usp. Fiz. Nauk* **170** 113 (2000) [*Phys. Usp.* **43** 111 (2000)]
10. Rakov E G *Usp. Khim.* **69** (1) 41 (2000) [*Russ. Chem. Rev.* **69** 35 (2000)]
11. Dresselhaus M S, Dresselhaus G, Eklund P C *Science of Fullerenes and Carbon Nanotubes* (San Diego: Academic Press, 1996)
12. Saito R, Dresselhaus G, Dresselhaus M S *Physical Properties of Carbon Nanotubes* (London: World Scientific Publ., 1998)
13. Ebbesen T W *Carbon Nanotubes*: *Preparation and Properties* (Boca Raton, Fl.: CRC Press, 1997)
14. Pederson M R, Broughton J Q *Phys. Rev. Lett.* **69** 2689 (1992)
15. Ajayan P M, Iijima S *Nature* **361** 333 (1993)
16. Ebbesen T W *Annu. Rev. Mater. Sci.* **24** 235 (1994)
17. Ebbesen T W *Phys. Today* **49** (6) 26 (1996)
18. Züttel A et al. *Int. J. Hydrogen Energy* **27** 203 (2002)
19. Smith B W, Monthioux M, Luzzi D E *Nature* **396** 323 (1998)
20. Burteaux B et al. *Chem. Phys. Lett.* **310** 21 (1999)
21. Hirahara K et al. *Phys. Rev. Lett.* **85** 5384 (2000)
22. Hamada N, Sawada S, Oshiyama A *Phys. Rev. Lett.* **68** 1579 (1992)
23. Iijima S, Ichihashi T *Nature* **363** 603 (1993)
24. Thess A et al. *Science* **273** 483 (1996)
25. Journet C et al. *Nature* **388** 756 (1997)
26. Lamy de la Chapelle M et al. *Carbon* **36** 705 (1998)
27. Journet C, Bernier P *Appl. Phys. A* **67** 1 (1998)
28. Cowley J M et al. *Chem. Phys. Lett.* **265** 379 (1997)
29. Henrard L et al. *Eur. Phys. J. B* **13** 661 (2000)
30. Bernaerts D et al. *Solid State Commun.* **105** 145 (1998)
31. Qin L-C et al. *Chem. Phys. Lett.* **268** 101 (1997)
32. Venema L C et al. *Phys. Rev. B* **61** 2991 (2000)
33. Rao A M et al. *Science* **275** 187 (1997)
34. Liu B et al. *Chem. Phys. Lett.* **320** 365 (2000)
35. Saito R et al. *Phys. Rev. B* **57** 4145 (1998)
36. Jost O et al. *Appl. Phys. Lett.* **75** 2217 (1999)
37. Sawada S, Hamada N *Solid State Commun.* **83** 917 (1992)
38. Peng L-M et al. *Phys. Rev. Lett.* **85** 3249 (2000)
39. Sun L F et al. *Nature* **403** 384 (2000)
40. Qin L-C et al. *Nature* **408** 50 (2000)
41. Peng H Y et al. *Appl. Phys. Lett.* **77** 2831 (2000)
42. Wang N, Li G D, Tang Z K *Chem. Phys. Lett.* **339** 47 (2001)
43. Prinzbach H et al. *Nature* **407** 60 (2000)
44. Zettl A, Cummings J, in *Electronic Properties of Novel Materials — Molecular Nanostructures* (AIP Conf. Proc., Vol. 544, Eds H Kuzmany et al.) (Melville, NY: AIP, 2000) p. 526
45. Mordkovich V Z et al. *Carbon* **34** 1301 (1996)

46. Mordkovich V Z et al., in *New Horizons of π-Electron Materials* (Berlin: Springer-Verlag, 1997)
47. Yudasaka M et al. *Appl. Phys. Lett.* **67** 2477 (1995)
48. Ruoff R S et al. *Nature* **364** 514 (1993)
49. Zhou O et al. *Science* **263** 1744 (1994)
50. Liu M, Cowley J M *Carbon* **32** 393 (1994)
51. Liu M, Cowley J M *Ultramicroscopy* **53** 333 (1994)
52. Kosaka M et al. *Chem. Phys. Lett.* **233** 47 (1995)
53. Huira H et al. *Nature* **367** 148 (1994)
54. Bursill L A, Peng J-L, Fan X-D *Philos. Mag. A* **71** 1161 (1995)
55. Zhang X B et al. *Europhys. Lett.* **27** 141 (1994)
56. Ivanov V et al. *Chem. Phys. Lett.* **223** 329 (1994); *Carbon* **33** 1727 (1995)
57. Amelinckx S et al. *Science* **265** 635 (1994); Bernaerts D et al. *Philos. Mag. A* **71** 605 (1995)
58. Biró L P et al. *Phys. Rev. B* **56** 12490 (1997); *Appl. Phys. Lett.* **73** 3680 (1998)
59. Bernaerts D et al., in *Physics and Chemistry of Fullerenes and Derivatives*: *Proc. of the Intern. Winterschool on Electronic Properties of Novel Materials* (Eds H Kuzmany et al.) (Singapore: World Scientific, 1995) p. 551
60. Weldon D N, Blau W J, Zandbergen H W *Chem. Phys. Lett.* **241** 365 (1995)
61. Luo J Z et al. *Catal. Lett.* **66** 91 (2000)
62. Eswaramoorthy M, Sen R, Rao C N R *Chem. Phys. Lett.* **304** 207 (1999)
63. Yin Y F, Mays T, McEnaney B *Langmuir* **15** 8714 (1999)
64. Bacsa R R et al. *Chem. Phys. Lett.* **323** 566 (2000)
65. Nikolaev P et al. *Chem. Phys. Lett.* **313** 91 (1999)
66. Bronikowski M J et al. *J. Vac. Sci. Technol. A* **19** 1800 (2001)
67. Du W-F et al. *Nano Lett.* **2** 343 (2002)
68. Cinke M et al. *Chem. Phys. Lett.* **365** 69 (2002)
69. Webb P A, Orr C *Analytical Methods in Fine Particle Technology* (Norcross, GA: Micrometrics Instrument Corp., 1997)
70. Ebbesen T W *J. Phys. Chem. Solids* **57** 951 (1996)
71. Tsang S C et al. *Nature* **372** 159 (1994)
72. Tsang S C et al. *J. Chem. Soc. Chem. Commun.* (17) 1803 (1995)
73. Rao A M et al. *Nature* **388** 257 (1997)
74. Sloan J et al. *Chem. Commun.* (8) 699 (1999)
75. Sloan J et al. *Acc. Chem. Res.* **35** 1054 (2002)
76. Sloan J et al. *Chem. Phys. Lett.* **329** 61 (2000)
77. Meyer R R et al. *Science* **289** 1324 (2000)
78. Brown G et al. *Chem. Commun.* (9) 845 (2001)
79. Kondratyuk P, Yates J T (Jr.) *Chem. Phys. Lett.* **383** 314 (2004)
80. Suzuki S et al. *Phys. Rev. B* **67** 115418 (2003)
81. Ye J T et al. *Phys. Rev. B* **67** 113404 (2003)
82. Maurin G et al. *Nano Lett.* **1** 75 (2001)
83. Shimoda H et al. *Phys. Rev. Lett.* **88** 015502 (2002)
84. Jeong G-H et al. *Phys. Rev. B* **68** 075410 (2003)
85. Saito Y et al. *Chem. Phys. Lett.* **212** 379 (1993)
86. Yosida Y *Appl. Phys. Lett.* **64** 3048 (1994)
87. Zhang G L *J. Appl. Phys.* **80** 579 (1996)
88. Loiseau A *Fullerene Sci. Technol.* **4** 1263 (1996)
89. Guerret-Piecourt C et al. *Nature* **372** 761 (1994)
90. Demoncy N et al. *Eur. Phys. J. B* **4** 147 (1998)
91. Zhang G Y, Wang E G *Appl. Phys. Lett.* **82** 1926 (2003)
92. Gan B et al. *Chem. Phys. Lett.* **333** 23 (2001)
93. Tsai S H et al. *Carbon* **38** 1899 (2000)
94. Okuyama F, Hayashi T, Fujimoto Y *J. Appl. Phys.* **84** 1626 (1998)
95. Smith B W, Luzzi D E *Chem. Phys. Lett.* **321** 169 (2000)
96. Smith B W et al. *J. Appl. Phys.* **91** 9333 (2002)
97. Bandow S et al. *Chem. Phys. Lett.* **337** 48 (2001)
98. Zhang M et al. *Chem. Phys. Lett.* **369** 680 (2003)
99. Kataura H et al. *Synthetic Met.* **121** 1195 (2001)
100. Maniwa Y et al. *J. Phys. Soc. Jpn.* **72** 45 (2003)
101. Monthioux M *Carbon* **40** 1809 (2002)
102. Smith B W, Luzzi D E, Achiba Y *Chem. Phys. Lett.* **331** 137 (2000)
103. Kataura H et al., in *Electronic Properties of Synthetic Nanostructures* (AIP Conf. Proc., Vol. 723, Eds H Kuzmany et al.) (Melville, NY: AIP, 2004) p. 222
104. Hodak M, Girifalco L A *Chem. Phys. Lett.* **350** 405 (2001); Girifalco L A, Hodak M *Appl. Phys. A* **76** 487 (2003)
105. Suenaga K et al. *Appl. Phys. A* **76** 445 (2003)
106. Kuzmany H et al. *Appl. Phys. A* **76** 449 (2003); Pfeiffer R et al. *Phys. Rev. Lett.* **90** 225501 (2003); Pichler T et al. *Phys. Rev. B* **67** 125416 (2003)
107. Chiu P W et al. *Appl. Phys. A* **76** 463 (2003)
108. Bandow S et al. *Chem. Phys. Lett.* **337** 48 (2001)
109. Abe M et al. *Phys. Rev. B* **68** 041405(R) (2003)
110. Bandow S et al. *Chem. Phys. Lett.* **384** 320 (2004); *MRS Bull.* **29** (4) 260 (2004)
111. Khlobystov A N et al. *Phys. Rev. Lett.* **92** 245507 (2004)
112. Dillon A C et al. *Nature* **386** 377 (1997)
113. Dillon A C et al. *Fullerenes* **3** 716 (1999)
114. Ye Y et al. *Appl. Phys. Lett.* **74** 2307 (1999)
115. Tersoff J, Ruoff R S *Phys. Rev. Lett.* **73** 676 (1994)
116. Benedict L X et al. *Chem. Phys. Lett.* **286** 490 (1998)
117. Chen P et al. *Science* **285** 91 (1999)
118. Yang R T *Carbon* **38** 623 (2000); Pinkerton F et al., in *Hydrogen Millennium*: *Proc. of the 10th Canadian Hydrogen Conf., Québec City, Canada, May 28–31, 2000* (Eds T K Bose, P Bernard) (Québec: Canadian Hydrogen Association, 2000)
119. Chen Y et al. *Appl. Phys. Lett.* **78** 2128 (2001)
120. Chambers A et al. *J. Phys. Chem. B* **102** 4253 (1998)
121. Park C et al. *J. Phys. Chem. B* **103** 10572 (1999)
122. Rodriguez N M, in *MRS 1996 Fall Meeting* (Boston: Academic Press, 1996) p. D11.6
123. Rodriguez N M, in *Proc. of the 9th Canadian Hydrogen Conf., Vancouver, Canada, February 7–10, 1999* (Ed. P H Howard) (Vancouver, 1999)
124. Schlapbach L, Züttel A *Nature* **414** 353 (2001)
125. Schlapbach L et al., in *Electronic Properties of Molecular Nanostructures* (AIP Conf. Proc., Vol. 591, Eds H Kuzmany et al.) (Melville, NY: AIP, 2001) p. 609
126. Ogden J M *Phys. Today* **55** (4) 69 (2002)
127. Züttel A *Mater. Today* **6** (9) 24 (2003)
128. Züttel A *MRS Bull.* **27** (9) 705 (2002)
129. Darkrim L F, Malbrunot P, Tartaglia G P *Int. J. Hydrogen Energy* **27** 193 (2002)
130. Bai X D et al. *Appl. Phys. Lett.* **79** 1552 (2001)
131. Klebanov Yu D, Sumarokov V N *Poverkhnost'* (4) 9 (2001)
132. Schutz W, Klos H, in *Electronic Properties of Novel Materials*: *Progress in Molecular Nanostructures* (AIP Conf. Proc., Vol. 442, Eds H Kuzmany et al.) (Woodbury, NY: AIP, 1998) p. 485
133. Lawrence J, Xu Gu *Appl. Phys. Lett.* **84** 918 (2004)
134. Shiraishi M, Takenobu T, Ata M *Chem. Phys. Lett.* **367** 633 (2003)
135. Haluska M et al., in *Electronic Properties of Molecular Nanostructures* (AIP Conf. Proc., Vol. 591, Eds H Kuzmany et al.) (Melville, NY: AIP, 2001) p. 603
136. Kajiura H et al. *Appl. Phys. Lett.* **82** 1929 (2003)
137. Lombardi L et al. *Electrochem. Solid-State Lett.* **7** A115 (2004)
138. Nützenadel C et al. *Electrochem. Solid-State Lett.* **2** 30 (1999)
139. Liu C et al. *Appl. Phys. Lett.* **80** 2389 (2002)
140. Colomer J-F et al. *J. Chem. Soc. Faraday Trans.* **94** 3753 (1998)
141. Kuznetsova A et al. *J. Chem. Phys.* **112** 9590 (2000)
142. Mawhinney D B et al. *Chem. Phys. Lett.* **324** 213 (2000)
143. Mawhinney D B et al. *J. Am. Chem. Soc.* **122** 2383 (2000)
144. Kuznetsova A et al. *Chem. Phys. Lett.* **321** 292 (2000)
145. Kuznetsova A et al. *J. Chem. Phys.* **115** 6691 (2001)
146. Zhao M et al. *Phys. Rev. B* **66** 155403 (2002)
147. Ohba T, Kaneko K *J. Phys. Chem. B* **106** 7171 (2002)
148. Yoo D-H et al. *J. Phys. Chem. B* **106** 3371 (2002)
149. Inaba A, Chihara H *Can. J. Chem.* **66** 703 (1988)
150. Fujiwara A et al. *Chem. Phys. Lett.* **336** 205 (2001)
151. Inoue S et al. *J. Phys. Chem. B* **102** 4689 (1998)
152. Yoo D-H et al. *J. Phys. Chem. B* **107** 1540 (2003)
153. Sorescu D C, Jordan K D, Avouris P *J. Phys. Chem. B* **105** 11227 (2001)
154. Peng S, Cho K *Nanotechnology* **11** 57 (2000)
155. Jhi S-H, Louie S G, Cohen M L *Phys. Rev. Lett.* **85** 1710 (2000)
156. Nilsson A et al. *Phys. Rev. Lett.* **68** 982 (1992)
157. Ulbricht H, Moos G, Hertel T *Phys. Rev. B* **66** 075404 (2002)
158. Cinke M et al. *Chem. Phys. Lett.* **376** 761 (2003)
159. Johnson M R et al. *Chem. Phys.* **293** 217 (2003)
160. Talapatra S, Migone A D *Phys. Rev. B* **65** 045416 (2002)
161. Talapatra S et al. *Phys. Rev. Lett.* **85** 138 (2000)

162. Weber S E et al. *Phys. Rev. B* **61** 13150 (2000)
163. Cao D et al. *J. Phys. Chem. B* **107** 13286 (2003)
164. Kleinhammes A et al. *Phys. Rev. B* **68** 075418 (2003)
165. Vidali G et al. *Surf. Sci. Rep.* **12** 135 (1991)
166. Chakrapani N et al. *J. Phys. Chem. B* **107** 9308 (2003)
167. Elkington P A, Curthoys G *J. Phys. Chem.* **73** 2321 (1969)
168. Gales L, Mendes A, Costa C *Carbon* **38** 1083 (2000)
169. Adu C K W et al. *Chem. Phys. Lett.* **337** 31 (2001)
170. Saito R et al. *Appl. Phys. Lett.* **60** 2204 (1992)
171. José-Yacamán M et al. *Appl. Phys. Lett.* **62** 657 (1993)
172. de Heer W A, Châtelain A, Ugarte D *Science* **270** 1179 (1995)
173. Gulyaev Yu V et al., in *IVMC'94*: *7th Intern. Vacuum Microelectronics Conf., Grenoble 1994* (Technical Digest) (Piscataway, NJ: IEEE, 1994) p. 322; *J. Vacuum Sci. Technol. B* **13** 435 (1995); *Mikroelektronika* **26** (2) 84 (1997) [*Russ. Microelectronics* **26** (2) 66 (1997)]; Chernozatonskii L A et al., in *IVMC'95*: *8th Intern. Vacuum Microelectronics Conf., Portland, Oregon, July 30 – August 3, 1995* (Technical Digest) (Piscataway, NJ: IEEE, 1995) p. 363; *Chem. Phys. Lett.* **233** 63 (1995)